



*LIGO Laboratory / LIGO Scientific Collaboration*

LIGO-E080166-00-D

*LIGO*

14 April 2008

---

**HAM Crossbeam Redesign for Advanced LIGO:  
FEA Study**

---

Andy Stein, Stephany Foley, Ken Mason

Distribution of this document:  
LIGO Science Collaboration

This is an internal working note  
of the LIGO Project.

**California Institute of Technology**  
**LIGO Project – MS 18-34**  
**1200 E. California Blvd.**  
**Pasadena, CA 91125**  
Phone (626) 395-2129  
Fax (626) 304-9834  
E-mail: [info@ligo.caltech.edu](mailto:info@ligo.caltech.edu)

**Massachusetts Institute of Technology**  
**LIGO Project – NW22-295**  
**185 Albany St**  
**Cambridge, MA 02139**  
Phone (617) 253-4824  
Fax (617) 253-7014  
E-mail: [info@ligo.mit.edu](mailto:info@ligo.mit.edu)

**LIGO Hanford Observatory**  
**P.O. Box 1970**  
**Mail Stop S9-02**  
**Richland WA 99352**  
Phone 509-372-8106  
Fax 509-372-8137

**LIGO Livingston Observatory**  
**P.O. Box 940**  
**Livingston, LA 70754**  
Phone 225-686-3100  
Fax 225-686-7189

*Note: all CAD models are generated using SolidWorks 2007, SP3.1; all FEA is computed using COSMOSWorks 2007, SP3.0.*

## **Introduction**

This report describes some analyses of the mechanical characteristics of the existing HAM Support Structure and compares these characteristics to those of two competing concepts for use in the Advanced LIGO HAM systems.

### *Existing Crossbeam (a.k.a. Gullwing) Design*

In Figure 1, we see a SolidWorks CAD model of the existing Support Structure installed in a partially assembled HAM chamber. Here, we consider the Support Structure to include: 1) a Crossbeam on either side of the chamber, 2) a set of Support Tube Clamps, and 3) two Support Tubes, to which the ISI would be mounted.

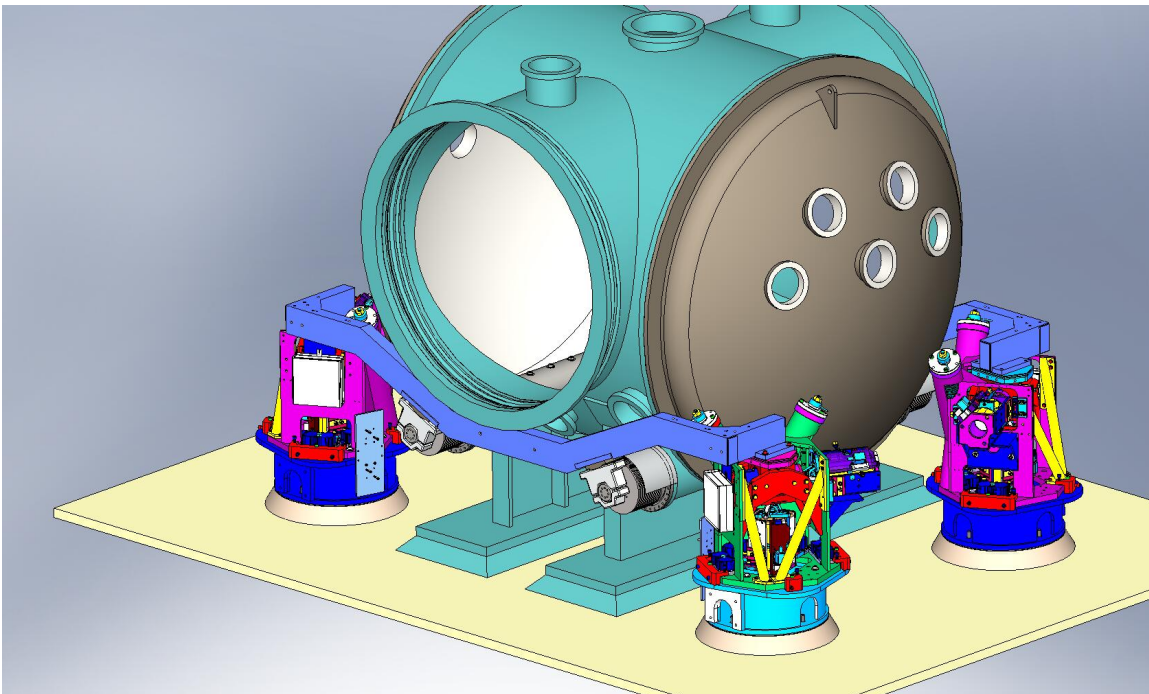


Figure 1. SolidWorks assembly, showing the existing Crossbeam Support Structure installed in the HAM chamber. Note the existing Crossbeams have the well-known “Gullwing” shape. Four HEPI systems support the four ends of the Support Structure.

### *New, Low Crossbeam Concept*

Figure 2 shows a new concept for the HAM Support Structure, which we refer to as the Low Crossbeam design. There are several significant differences between this concept and the existing Crossbeam assembly, which are intended to improve system performance:

- The Crossbeam is made from a round tube, instead of the Gullwing’s rectangular cross-section. This should allow for increased torsional stiffness, as well as better stiffness in the horizontal plane. The Gullwing is fairly narrow (only 3” wide, versus 6” tall), while the proposed round Crossbeam has a diameter of 5.5” (available from McMaster-Carr, P/N 7767T976). The tube’s stiffness may be

increased by welding sections of rectangular extrusions to the cross-section (see the orange block on the bottom of the middle of the tube, in Figure 2).

- The force loop is significantly shorter, allowing for increased overall stiffness. This is accomplished by shortening the path from the actuation point on HEPI – the Boot – to the Support Tube Clamps. This concept uses two sections of tube welded at an angle, which would bolt both to the side of the HEPI Boot and to the end of the Crossbeam. We refer to this component as the Connector Tube, below.
- The Support Tube Clamps are shorter, and mate differently to the Support Tube's ends. Instead of the end cylinders mating directly inside aluminum Vee blocks, we propose slipping an intermediate sleeve over the Tube end. This sleeve would have spherical surfaces on either side, which would mate inside a spherical cup cut into the Clamp. Though not shown here, there would be a spring-loaded preloading device bolted securely to the Clamp, which would provide a well controlled preload force to this new ball-type joint. See Figure 3.

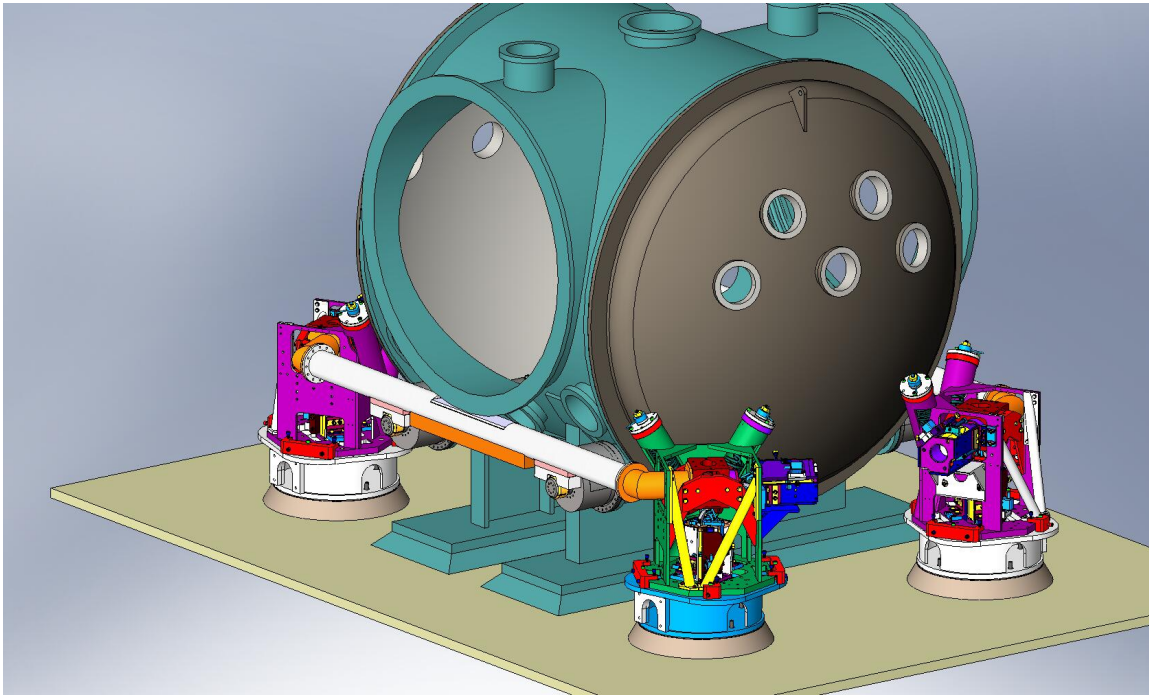


Figure 2. One of the concepts for the Support Structure to be used in the Advanced LIGO HAMs. This system will be referred to below as the Low Crossbeam design, because of its mounting position on HEPI.

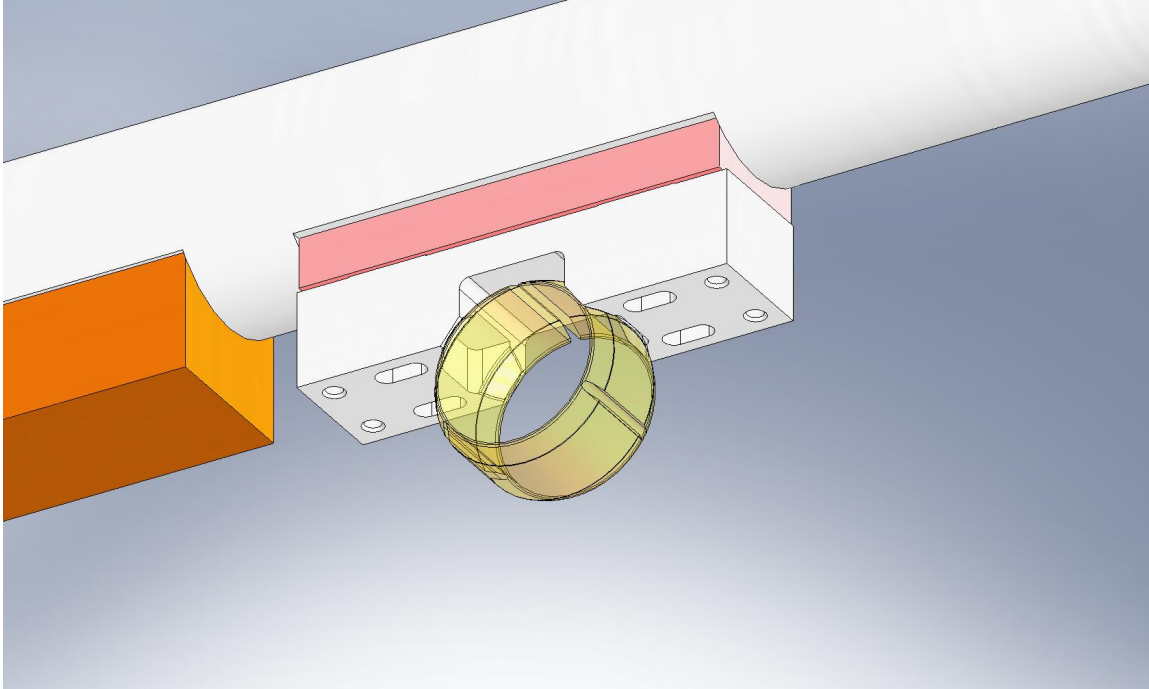


Figure 3. Detail of ball joint Clamp proposed for both new Crossbeam concepts. A Sleeve (shown transparent in this image) would first slip over the cylindrical end of the Support Tube. The Sleeve would have spherical surfaces cut on the outside, which would mate into four spherical pads of equal radius and common center, cut into the Clamp. Note, the Clamp is significantly shorter than the existing Crossbeam's Clamps, which should help improve the system's overall stiffness. Instead of making the Clamp from Aluminum (as the old Vee-style is), we would use a stiffer material (perhaps stainless steel).

There are some other important features of the Low Crossbeam concept, which should be considered before selecting the final design:

- In the existing HEPI system, a horizontal L4-C accelerometer is mounted to the side of the Boot, where the Connector Tube would attach. This means that either 1) the Connector Tube design must provide clearance for and access to the L4-C when installed on the Boot, or 2) the L4-C must be moved to a different part of the Boot (most likely its top surface).
- The existing HEPI system also has a set of Caging braces connected to the Housing, which surround the Boot. Some of this Caging may need to be redesigned, to allow access for the Connector Tube. Note this concern is not addressed further in this report.
- There are electronics mounted to the side of the HEPI Housing, covering the window through which the Connector Tube would pass (see Figure 4). This unit would need to be moved to another part of HEPI.
- The HEPI Piers would need to be shortened from their current nominal height of 9.92" to a height of 8.92". This may require significant additional work at LIGO Livingston, to pick the existing HEPI systems off of their Piers then remount them



to shorter Piers. This is not a concern for LIGO Hanford, since HEPI has not yet been installed there.

- To allow clearance between the Crossbeam and the HAM chamber's door flange, a section of the Crossbeam's tube is removed and replaced with a flat plate welded into the tube. See Figure 5. A quick analysis indicates minimal loss of stiffness from this change.
- Clearance is also tight between the Crossbeam and the Support Tube Bellows. To fit the Low Gullwing design, we remove "scalloped" sections of the Crossbeam tube, as shown in Figure 6.

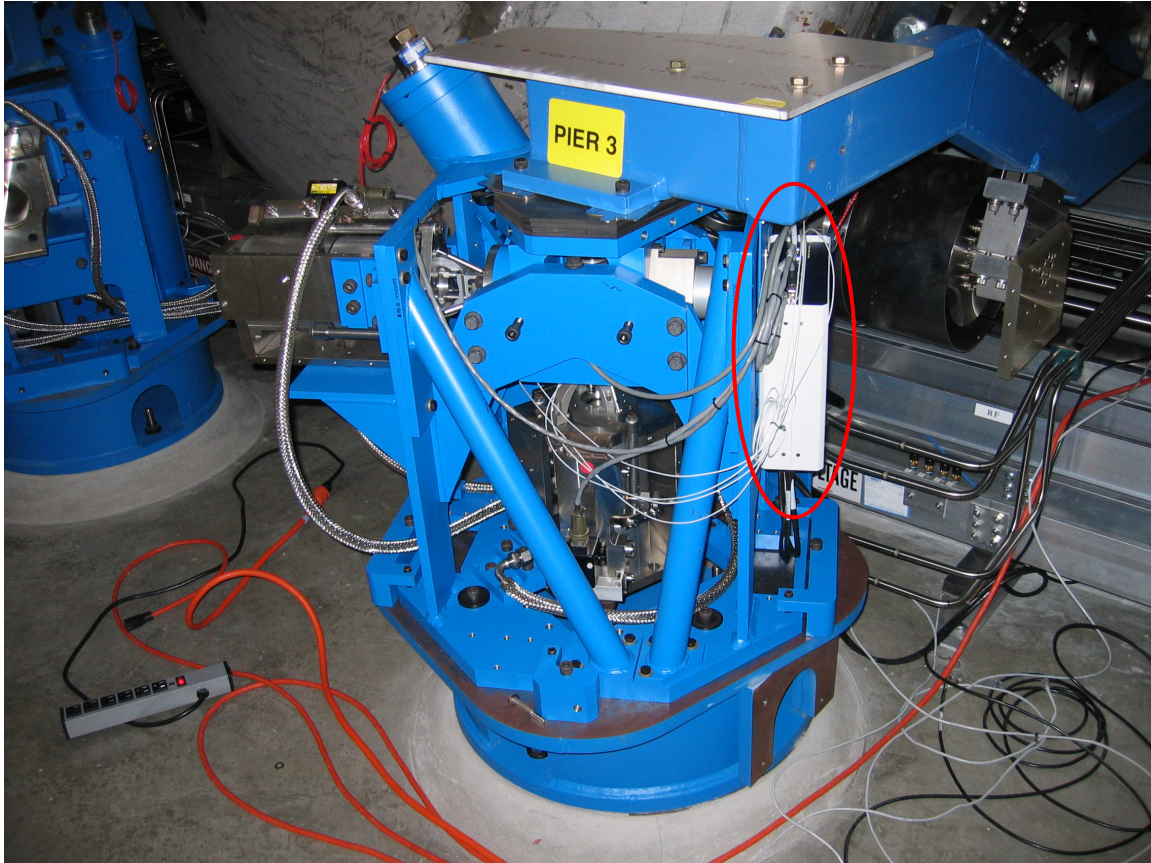


Figure 4. One of the HEPI systems installed at LIGO Livingston Observatory. We see an electronics unit mounted to the right side of the Housing, which would need to be moved for the Low Crossbeam concept.

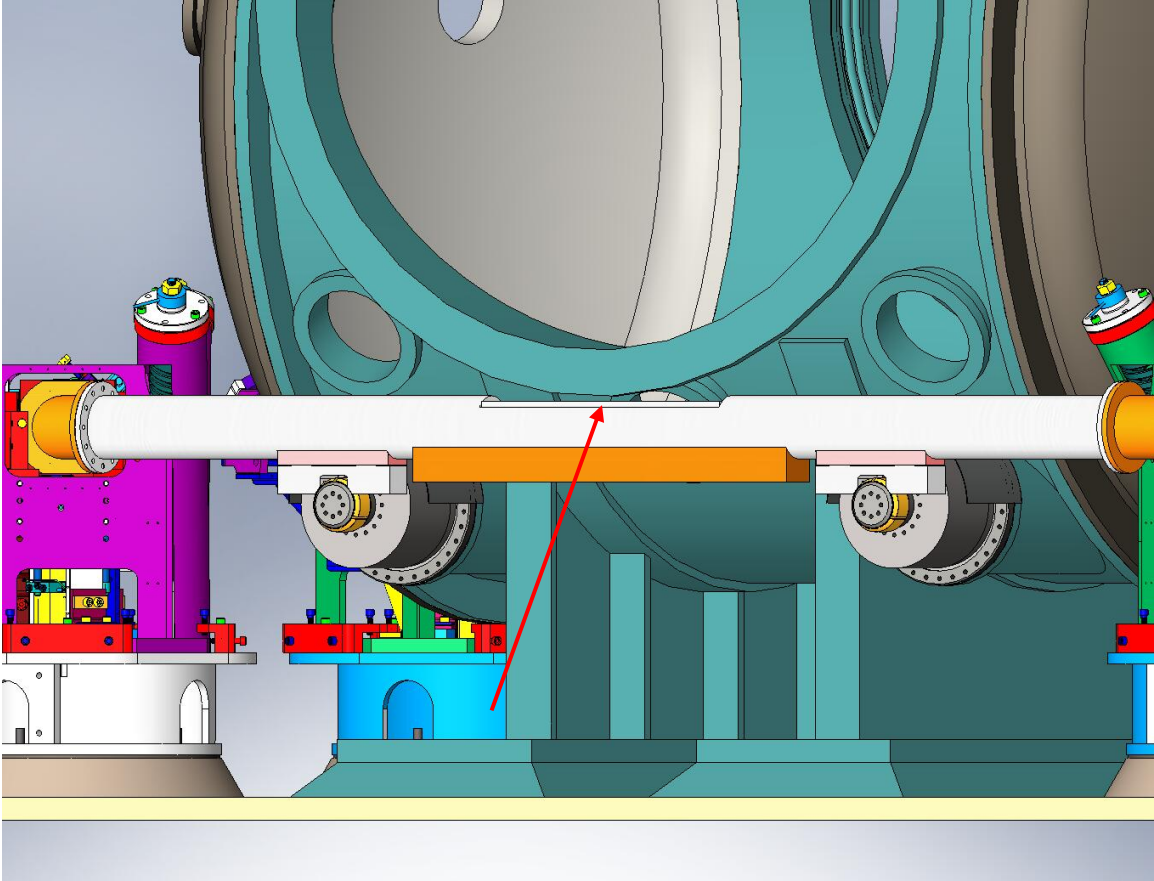


Figure 5. To allow clearance between the Low Crossbeam and the HAM chamber door, we remove the top side of the Crossbeam's tube near its center and replace with a flat plate.

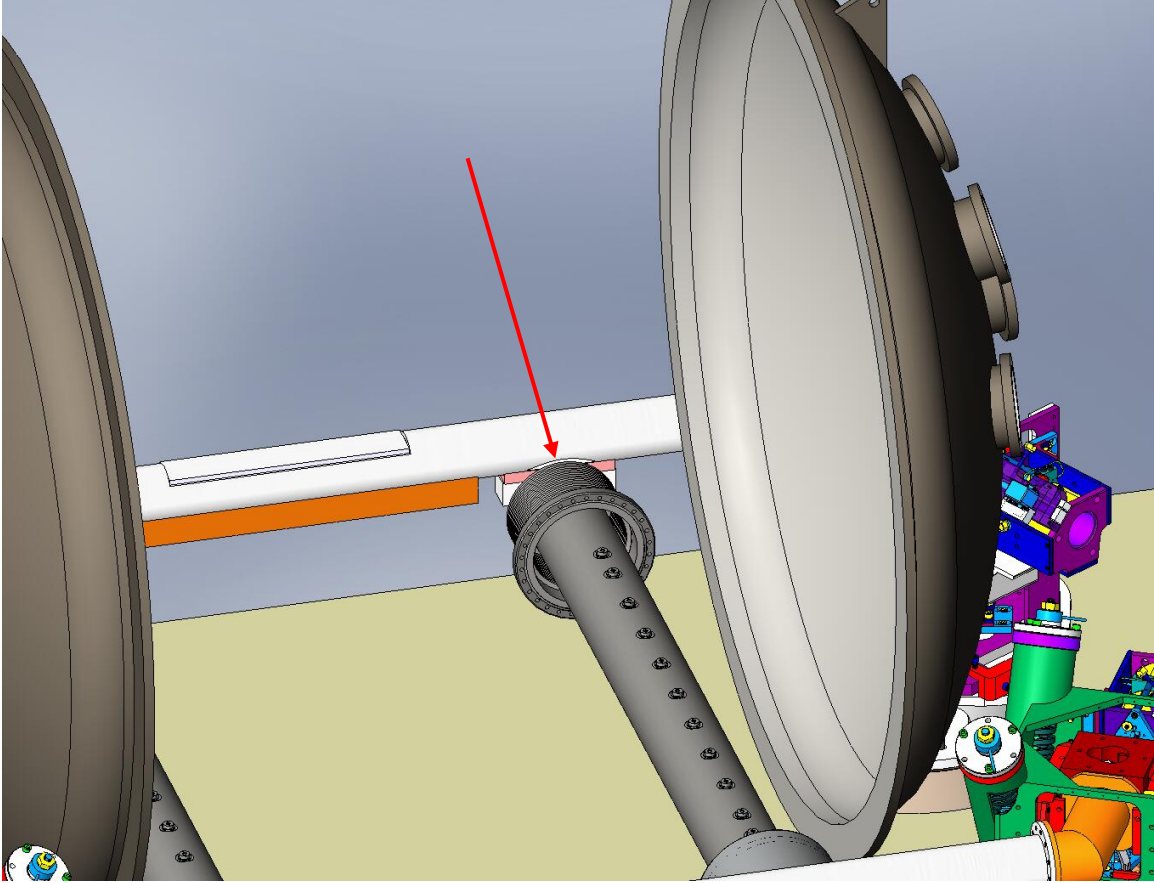


Figure 6. Scallop-shaped cuts are made in the Low Crossbeam tube, to allow clearance between the tube and the Bellows. (HAM chamber hidden from view.)

*New, High Crossbeam Concept*

To avoid interference with the horizontal L4-C on the HEPI Boot (as well as the Caging around the Boot), we have considered a slightly modified concept, shown in Figure 7. Both the Crossbeam and Clamp designs are identical to those used in the Low Crossbeam concept. However, the Connector Tube would bolt to the top of the HEPI Boot, instead of the side. This eliminates some of the packaging concerns raised for the Low Crossbeam design, at the cost of a slightly longer force loop (which presumably corresponds to a lower system stiffness).



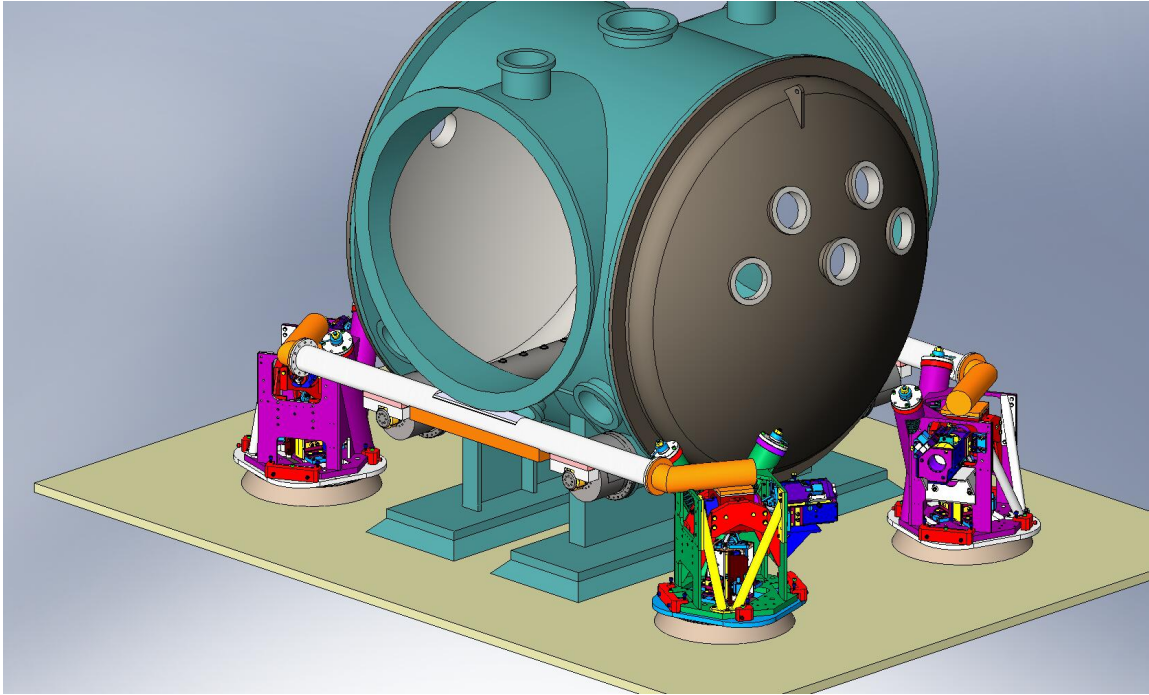


Figure 7. The High Crossbeam concept. Note the HEPI Piers are eliminated and replaced by much shorter spacers.

Some critical features of the High Crossbeam design include:

- To allow for a straight Crossbeam tube, we must lower the HEPIs significantly. Instead of the 8.92"-tall Pier used in the Low Crossbeam design, we propose using a 1.5"-thick Spacer. The Spacer would need to include all the holes necessary to fasten to the grout studs and to accept the mounting screws for the HEPI Housing. It is possible that the additional work required to lower the existing HEPI systems at LIGO Livingston would be substantially greater than what would be required for the Low Crossbeam retrofit – this issue has not been investigated thoroughly, however. It is also possible the Spacer does not provide enough clearance for HEPI's Vertical Actuator, though an initial review of the CAD indicates there would be more than 1" clearance left between the grout and the lowest point on the Actuator. Before selecting this design, however, we must check if it would be possible to install and service the Actuators with such a short Spacer.
- In an effort to minimize the force loop, the current design includes a Connector Tube which does not fully clear the top of the HEPI Housing. Instead, there is a pocket cut into the underside of the Tube to provide the needed clearance. See Figure 8. We expect some reduction in stiffness from this, though the effect does not appear to be too significant. This is similar to techniques proposed for packaging the Crossbeam tube around the HAM Bellows and the chamber door flange.
- Since the Crossbeam tube's diameter is greater than the existing Gullwing's width (5.5" to 3"), we must remove some material from the tube to fit around the HEPI Offload Spring. This is shown in Figure 9.

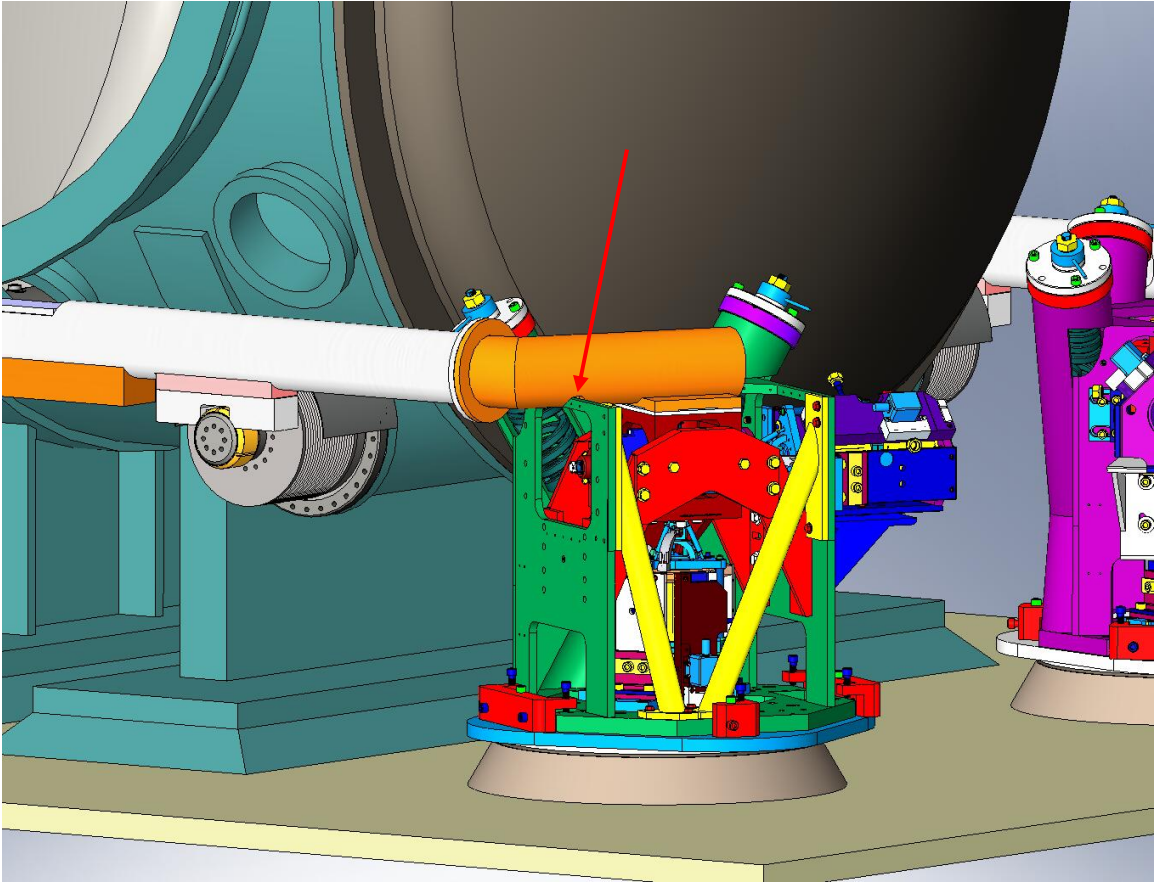


Figure 8. The arrow points to a notch cut into the High Crossbeam's Connector Tube. The notch provides clearance between the Tube and the HEPI Housing. This is a design detail that should be reconsidered if the High Crossbeam concept is chosen for Advanced LIGO.



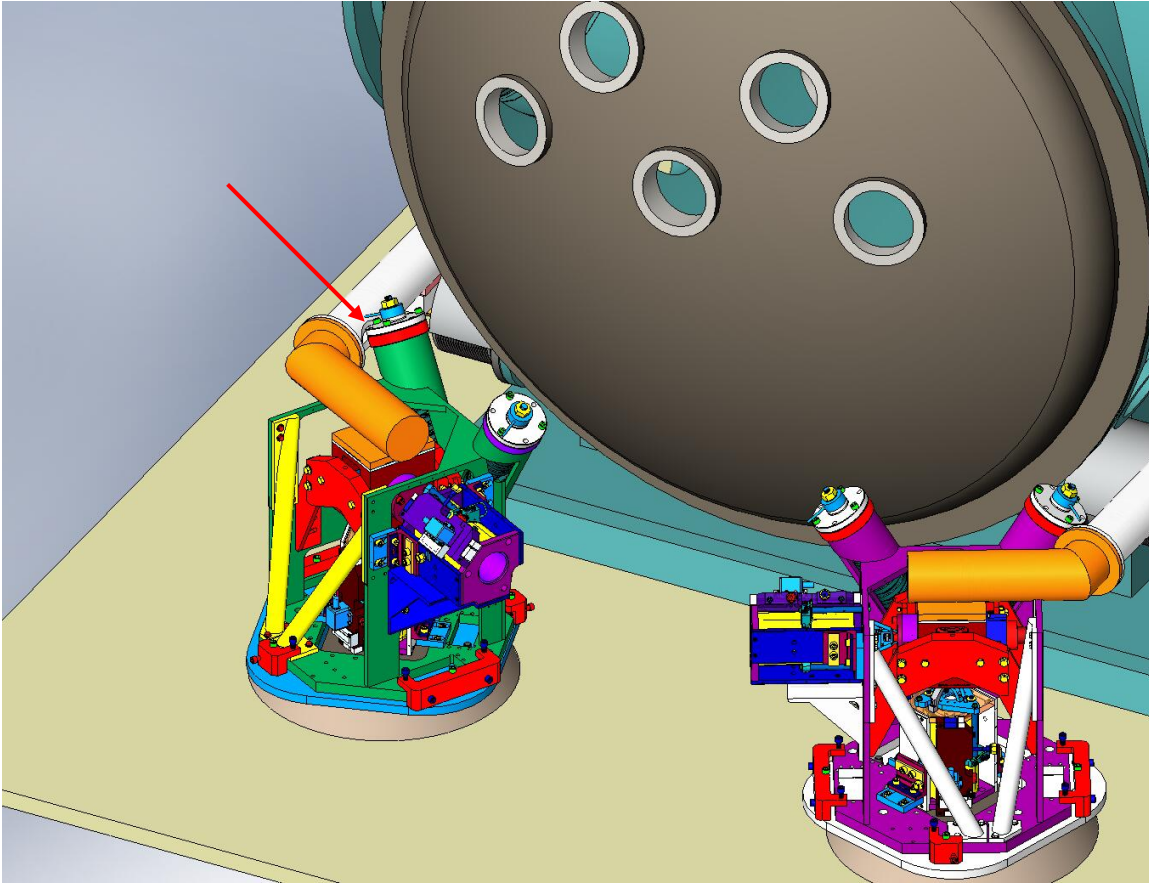


Figure 9. In another effort to package a new Crossbeam within the existing hardware, a cylindrical cut is made to the inside of the Crossbeam tube, to avoid the HEPI Offload Spring. Again, this detail would need to be revisited if the High Crossbeam were selected.

Fastener details are not considered at this stage of the design. Both the Low and High Crossbeam concepts would probably require some change to the bolt patterns on the HEPI Boot interfaces.

The next section of the report discusses static FEA results for the existing Crossbeam design, as compared to those for both the Low and High Crossbeam concepts.

### **Static Analysis – Model #1: Existing Crossbeam Assembly**

We first analyze the existing Crossbeam structure under static loading, to characterize its effective stiffnesses. We define the problem as follows: when one of the HEPI Actuators pushes on the HEPI Boot with a known force, how much does the Boot deflect? Also, how much does the Boot tilt, in the sensitive direction of the HEPI's Horizontal L4-C accelerometer?

#### Model Geometry

For this system, we consider the design space consisting of 1) the HEPI Boot, 2) the Crossbeam (and the hardware connecting it to the Boot), 3) the Clamp that couples the

end of the Support Tube to the Crossbeam, and 4) the end of the Support Tube itself. *Note: we are not considering a redesign of the Support Tube, but the coupling between the Tube and the Crossbeam is a critical part of the system's stiffness, and so the end of the Tube is included in the analyzed models.* To make the problem tractable, we use simplified geometry for all these components. Also, we choose to look at only one half of one Crossbeam assembly, as shown in Figure 10. By looking at similarly defined subsystems for all the analyzed designs, we should be able to draw strong conclusions about the stiffness of one design *relative* to another.

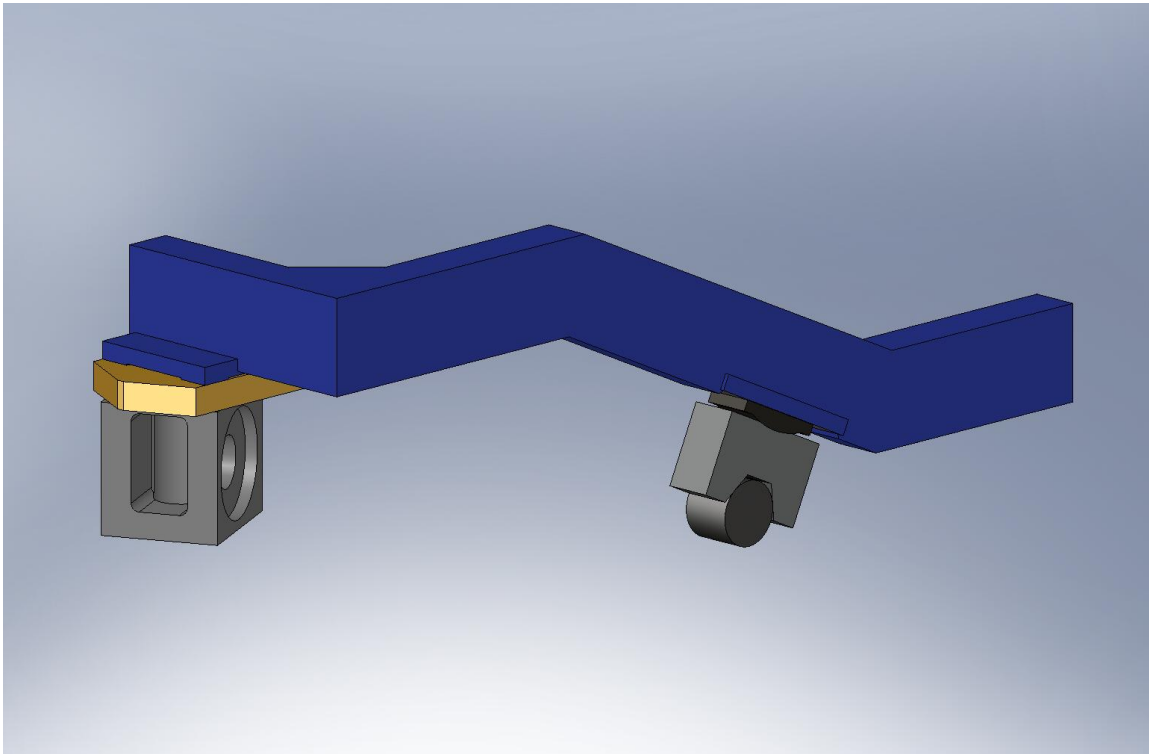


Figure 10. SolidWorks model used for static FEA of existing Crossbeam system. The system studied is one half of a Crossbeam, with HEPI Boot connected at the end and Support Tube “nub” clamped underneath.

#### *Model Geometry: HEPI Boot*

We ignore the Offload Springs which couple the HEPI Housing to the Boot (and nominally support the weight of the ISI and support structure). We assume the Springs' stiffness is much smaller than the effective stiffness of the remaining Crossbeam system, so its contribution to the predicted deflections should be negligible. We also eliminate several minor features of the Boot geometry which do not contribute significantly to the system stiffness, such as the bottom “tail” to which the Springs would mount.

For each of the static analyses, we assume one HEPI Actuator is driving the system, while the other Actuator is maintaining its position. In the simplest view of the “inactive” Actuator, it is preventing the system from translating in a direction parallel to its driving axis (infinite stiffness in 1-DoF), while allowing the system to rotate or translate in any other direction (infinite compliance in 5-DoF's). This loosely approximates the behavior

of the Actuator's Tripod and Blade Flexures. To model this effect simply in COSMOS, we must apply a 1-DoF constraint at a point on the Boot, at the center of the interface between the Actuator and the Boot. Since the interface where the Vertical Actuator bolts to the Boot has a hole through its center, we add material to the SolidWorks Boot model. The constrained points (as well as the points where the Actuator forces are applied) are implied by a pair of triangular "Split Line" features in the SolidWorks model. The constrained/forced points are simply the peaks of these two triangles, as shown in Figure 11.

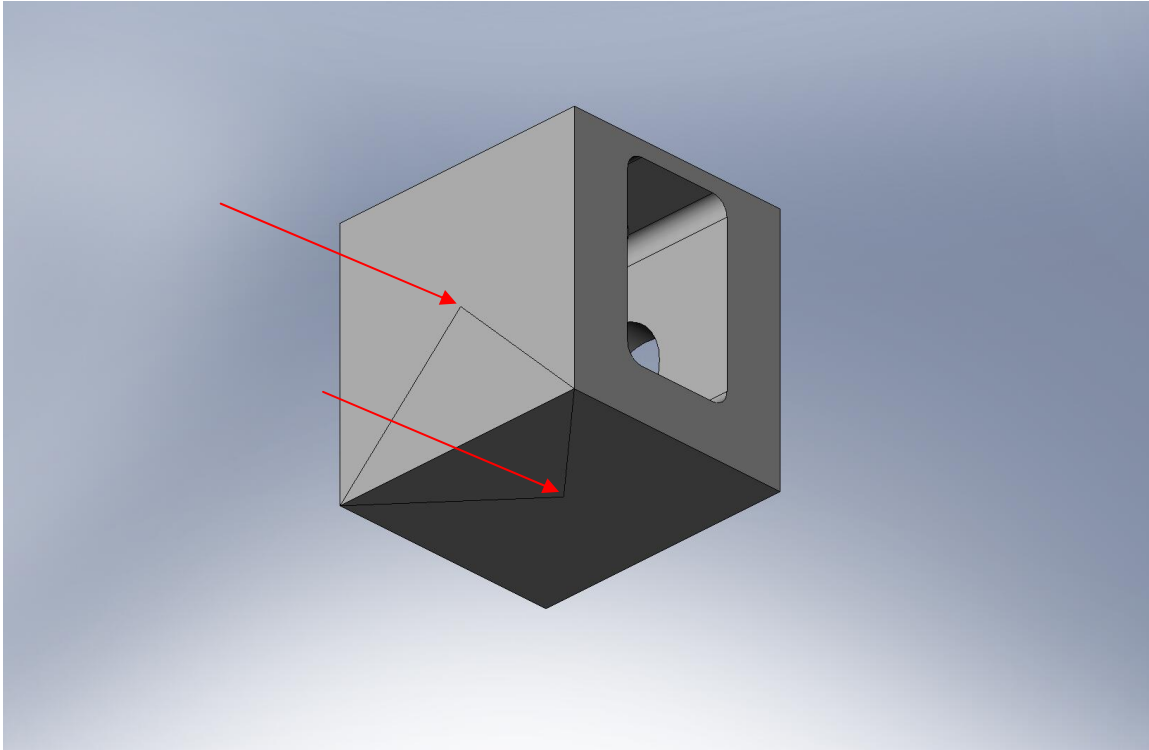


Figure 11. Simplified geometry used for HEPI Boot. Note the two triangular shapes added to the faces to which the two Actuators attach. The peaks of the triangles are picked out in the COSMOS models, to specify where constraints or forces are applied to the Boot.

Clearly the real axial stiffness of the Actuators is not infinite, nor is the compliance in the other 5 DoF's really infinite. However, the resulting analysis should produce reasonable results assuming 1) the axial stiffness of an Actuator is much greater than the effective stiffness of the modeled Crossbeam system, and 2) the Actuator stiffnesses in the other 5 DoF's are much smaller than the effective stiffness of the modeled system.

*Model Geometry: HEPI Shim Stack*

A stack of steel Shims is used as a spacer, for bolting the existing Crossbeam to each HEPI Boot. For this FEA, we assume the stack is solid, and we remove most of the tapped and thru holes.

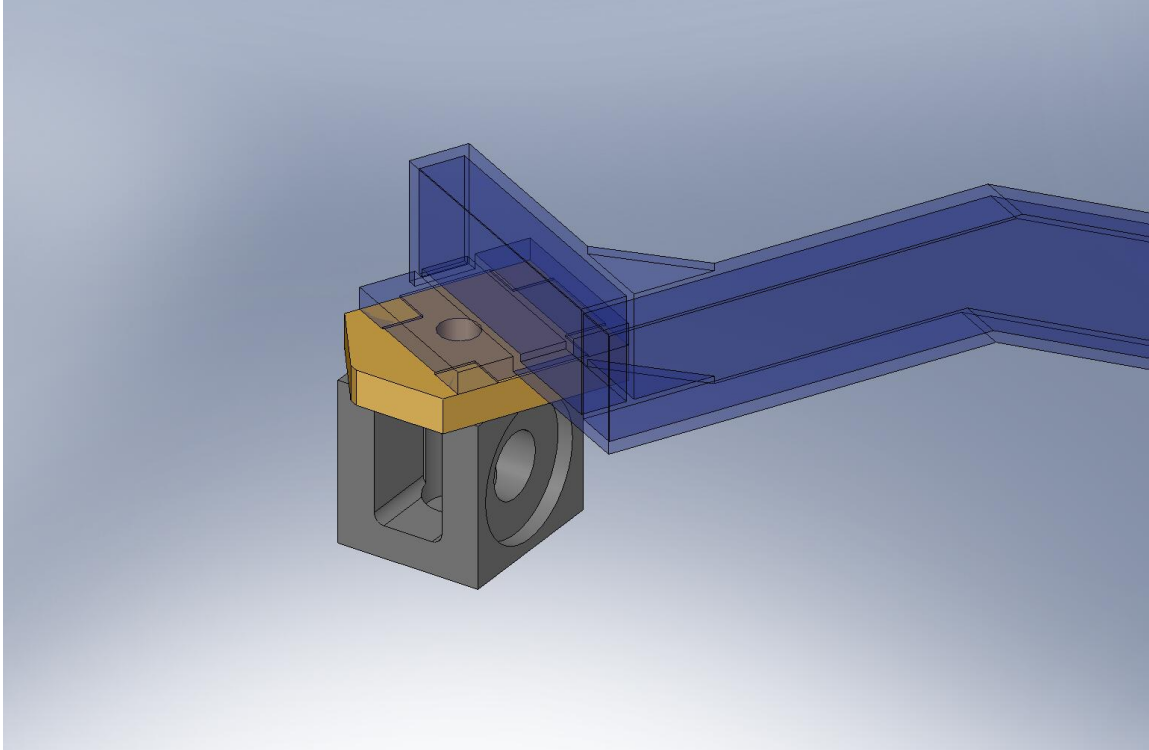


Figure 12. The gold-colored block attached to the top of the HEPI Boot represents a stacked set of Shims. The Crossbeam is shown transparent in this view. We can see four pads on the bottom of the Crossbeam's attachment plate in contact with the top of the Shim stack.

*Model Geometry: Crossbeam*

The basic geometry for the existing Crossbeam is taken from the model D972612-D. To simplify the calculations, we remove several minor features, such as tapped and thru holes. However, the wall thicknesses, welded plate sizes, and all the other critical dimensions are taken directly from the nominal design. As described above, the model is cut off at the Crossbeam mid-plane. Also, there are four rectangular pads on the bottom of the end plate, where the Crossbeam connects to the HEPI Shim Stack. These pads are located around the attachment bolt holes that preload the Crossbeam/Shim Stack interface – we expect the stiffness of this connection to be dominated by interface areas directly around these bolts.

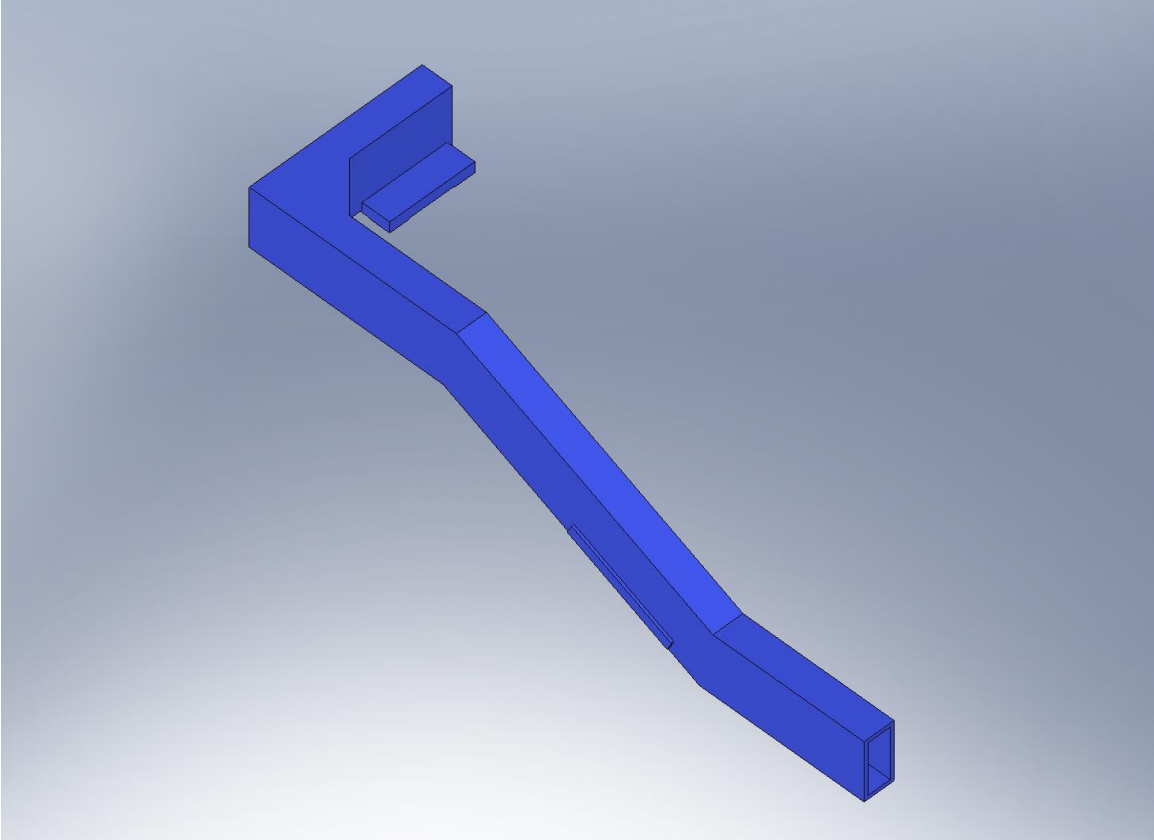


Figure 13. Simplified model of existing Crossbeam, used for static FEA.

*Model Geometry: Clamp Spherical Bearing*

We use the nominal geometry of the Clamp Spherical Bearing (D972615-B), except for the removal of four thru holes. Note the resulting predicted stiffness of the joint formed between the Bearing and the Clamp Mounting Base (see next section) may be unrealistically high. The FEA assumes a “bonded” joint everywhere these two components touch (this is true of mating components in these FEA studies, generally). However, the bearing surface is fairly large, and may be difficult to preload while maintaining good contact everywhere.



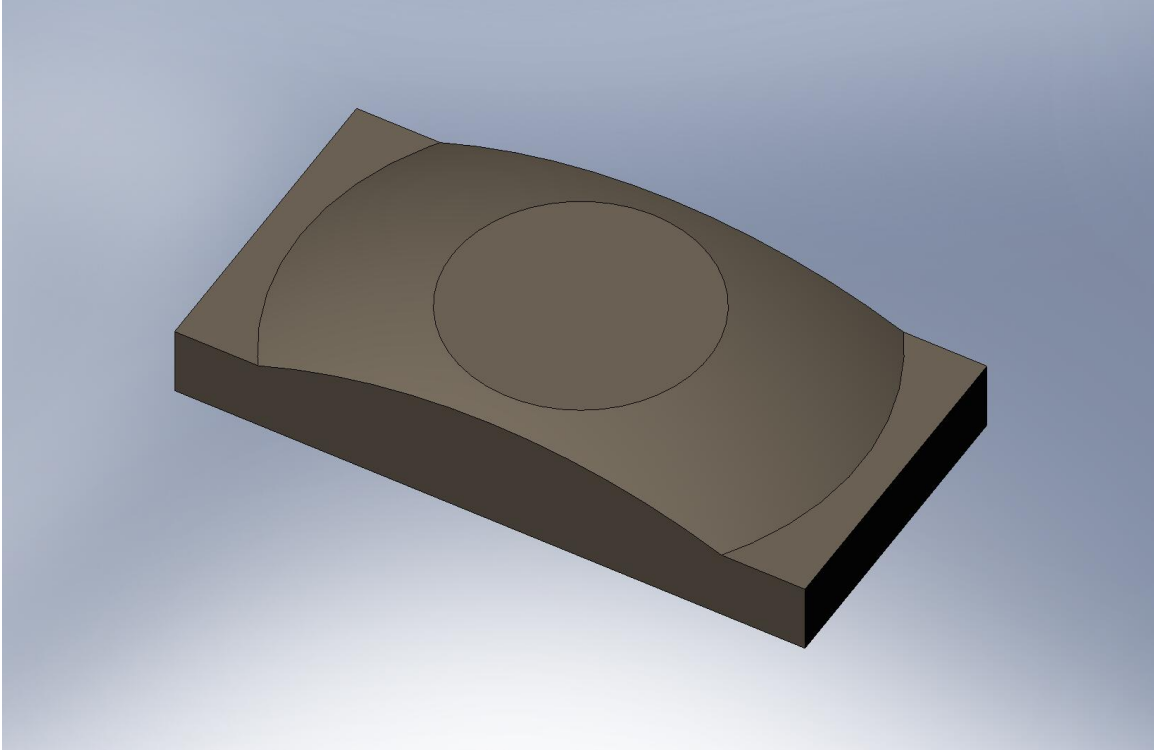


Figure 14. Simplified model of existing Clamp Spherical Bearing.

*Model Geometry: Clamp Mounting Base*

The geometry for the Clamp Mounting Base (D972613-C) is greatly simplified. The tabs on either side of the Base are removed, since they do not contribute to the assembly's stiffness. Also, the holes and radiused edges are removed, to allow for fewer mesh elements. As mentioned above, we assume "bonded" joints everywhere – including the joint between the end of the Support Tube and the Base's Vee.

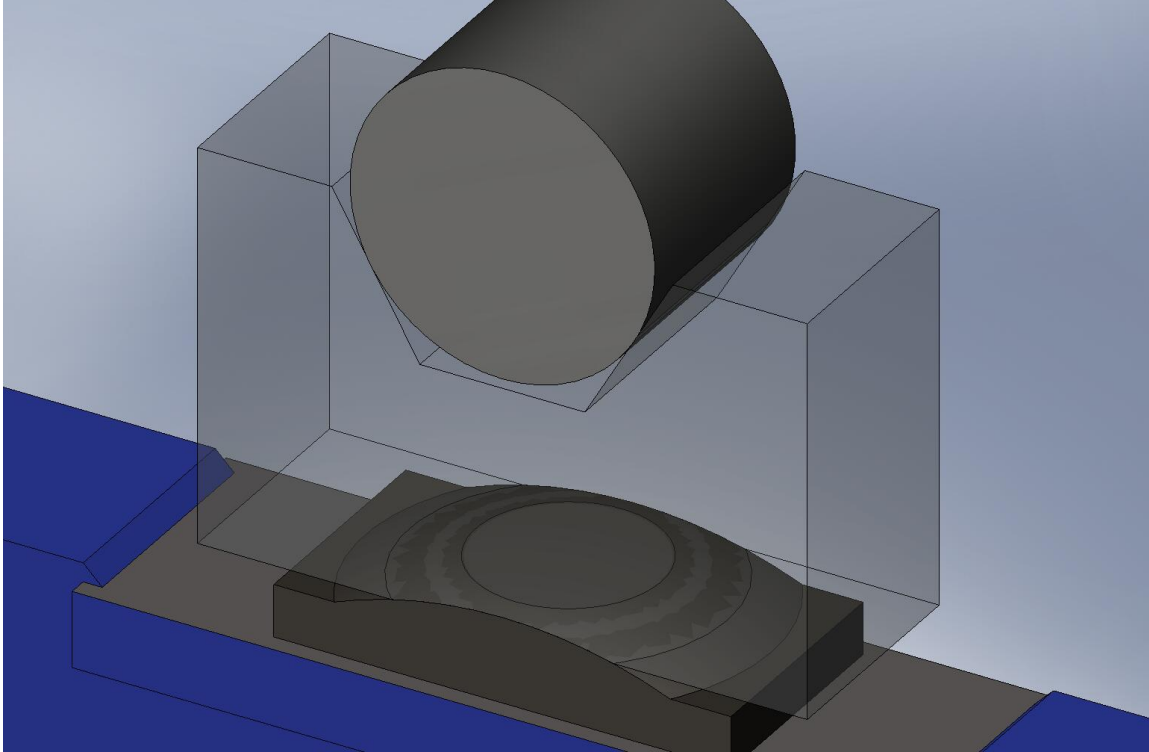


Figure 15. Transparent view of Clamp Mounting Base, coupling the Support Tube to the Crossbeam (via the Spherical Bearing).

*Model Geometry: Support Tube “Nub”*

We add a pair of flat surfaces to the end of the Support Tube (Figure 16), which mates flat to the two angled faces within the Clamp Mounting Base’s Vee. This feature allows the COSMOS FEA solver to find a solution in this interface. This should provide a conservative approximation for the stiffness of the cylinder-on-flat Hertzian contact problem. In reality, the contact patches will be smaller, resulting in lower real stiffness.

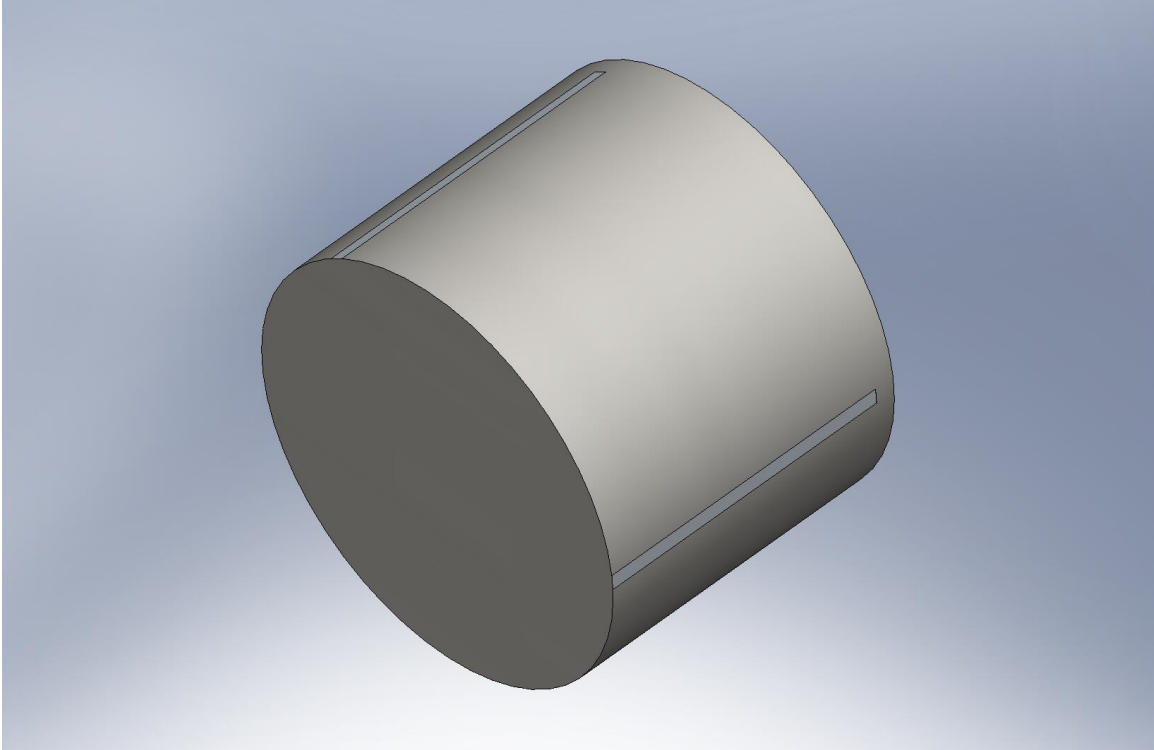


Figure 16. Rectangular flats cut into the cylindrical outer surface of the Support Tube's end.

#### Mesh Details

In general, the higher the mesh density, the more accurate the analysis will be. Computing power sets a practical limit on how dense we can make the mesh, however. Generally, if the mesh is too sparse, the modeled system will appear stiffer than the physical system (assuming the rest of the model is accurate).

When defining the mesh, we specify a higher element density in areas where we expect the largest strains. For the existing Crossbeam model, we specify higher mesh densities on 1) the flats on the Support Tube, and 2) the spherical surface on the Spherical Bearing (Figure 17).

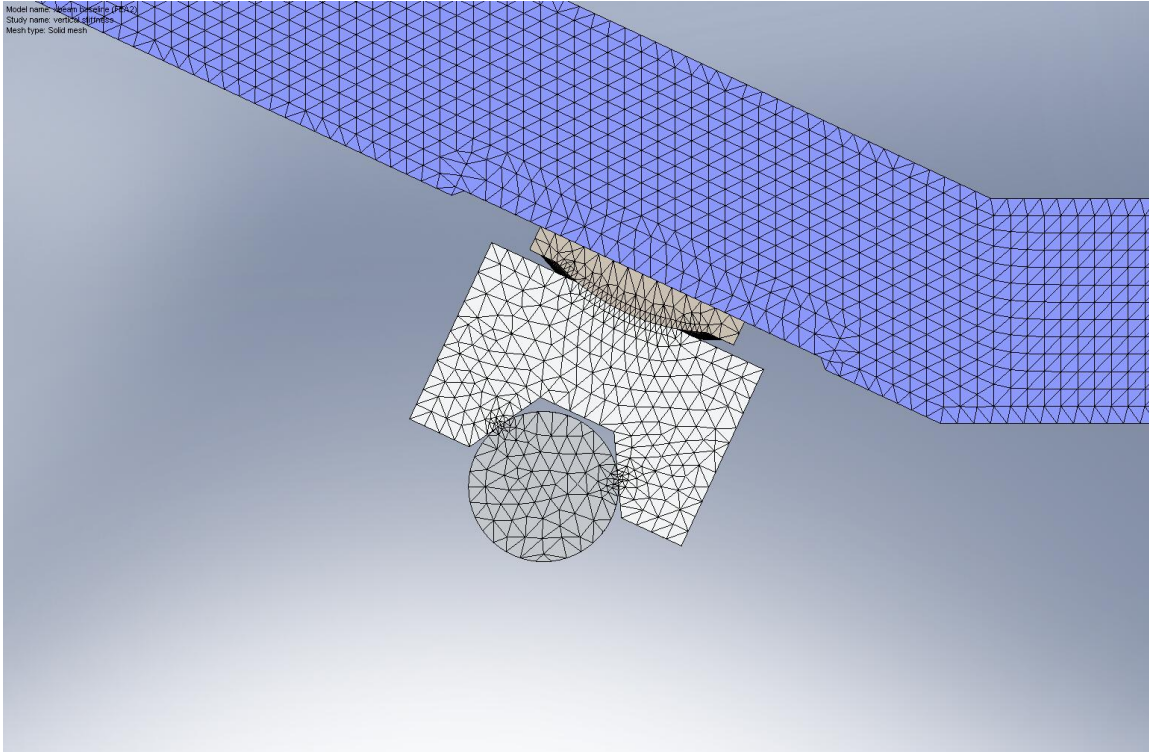


Figure 17. Mesh is more dense where the Support Tube contacts the Mounting Base and where the Mounting Base contacts the Spherical Bearing. We expect these to be regions of relatively high strain, therefore requiring more accurate modeling.

We use the COSMOS mesher to build the meshed model. The resulting model is shown in Figure 18, and has the following characteristics:

- mesh controls – 1) 2 flats on Support Tube end: 0.075"; 2) spherical surface on Spherical Bearing: 0.150"
- element size=0.45"
- total nodes=196,979
- total elements=118,643
- % elements with aspect ratio < 3=99
- % elements with aspect ratio > 10=0.003
- % distorted elements=0.0008

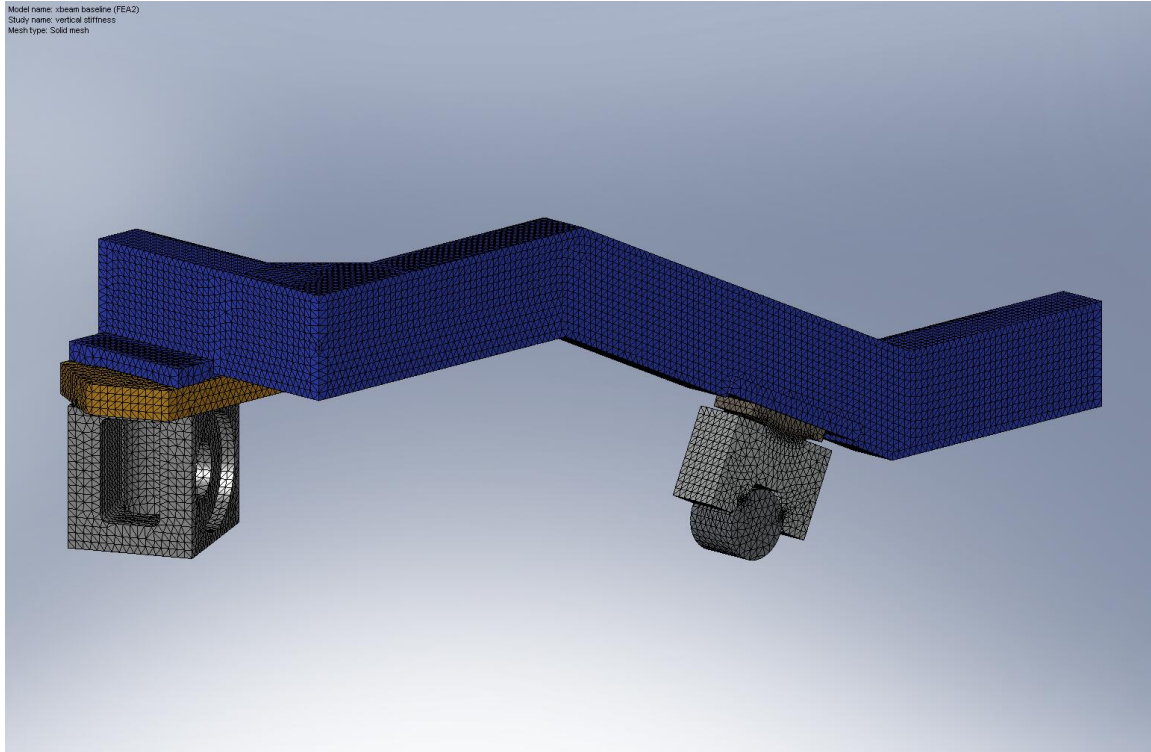


Figure 18. FEA model of the existing Crossbeam assembly, after meshing.

### Materials

The components of this FEA model are assigned the following material properties, which should be representative of the materials that compose the physical parts:

- *HEPI Boot*: Plain Carbon Steel –  $E_x=210$  GPa,  $\nu=.28$ ,  $G_{xy}=79$  GPa
- *HEPI Shim Stack*: Plain Carbon Steel – ...
- *Crossbeam*: Plain Carbon Steel – ...
- *Clamp Spherical Bearing*: Plain Carbon Steel – ...
- *Clamp Mounting Base*: Aluminum AA356.0-F –  $E_x=72$  GPa,  $\nu=.33$ ,  $G_{xy}=27$  GPa
- *Support Tube*: AISI 304 –  $E_x=190$  GPa,  $\nu=.29$ ,  $G_{xy}=75$  GPa

### Boundary Conditions

#### *Study #1: vertical stiffness*

We define a vertical force of 1,000 N, acting upward (positive Z-direction) on the actuation point on the bottom of the HEPI Boot.

There are three constraints acting on the system:

- 1) the exposed face on the Support Tube “nub” is *fixed* – none of the elements on this face may translate or rotate;
- 2) the exposed cross-section face on the Crossbeam must obey a *symmetry* constraint – none of the elements on this face may move out of plane. This constraint generally works if the mirrored half of the system is identically defined in terms of geometry, material, and boundary conditions. Though this is not generally true for the physical Crossbeam system (e.g., forces applied on one side may not be identical to those applied on the other), this constraint should not influence the



results in a way that is biased toward one design or another, and therefore should be sufficient when used to compare relative stiffnesses;

- 3) actuation point on side surface of HEPI Boot cannot translate in a direction parallel to the Horizontal Actuator's axis.

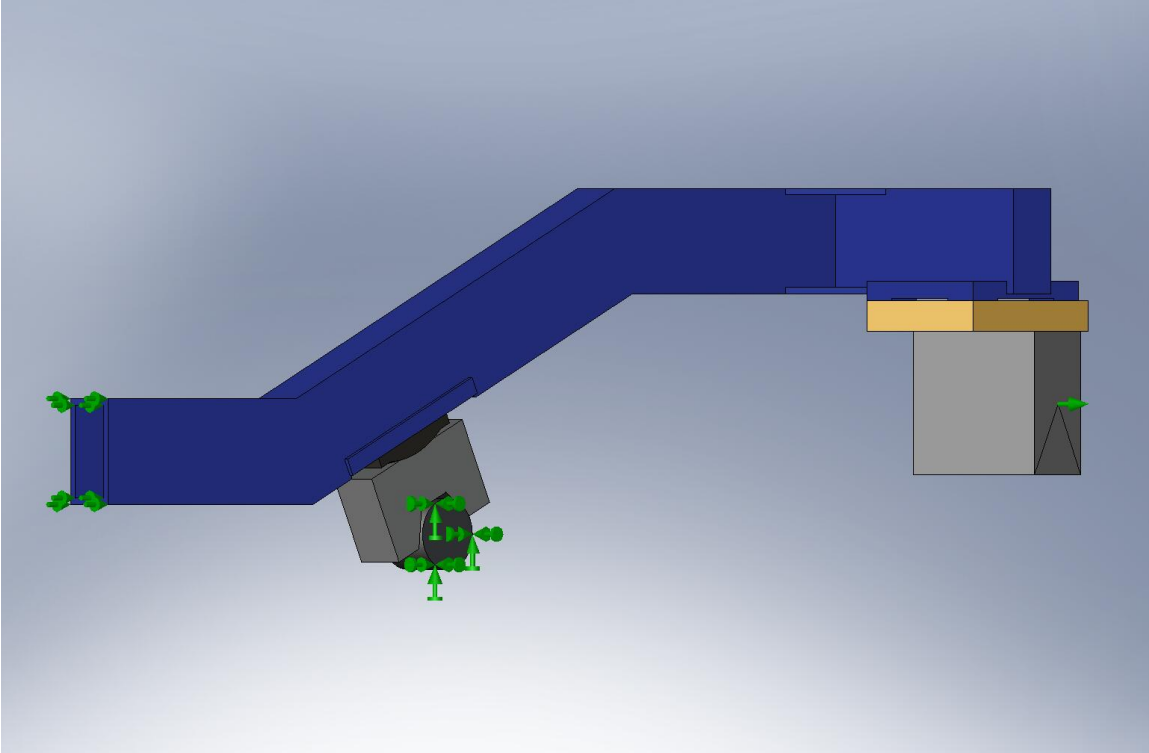


Figure 19. COSMOS snapshot, showing constraints defined for the existing Crossbeam system. Green arrows indicate constrained degrees of freedom. Though it cannot be seen in this image, there is also a purple arrow pointing upward, which is anchored to the actuation point on the bottom of the HEPI Boot. This arrow represents the vertical force applied to the system.

*Study #2: horizontal stiffness*

We define a horizontal force of 1,000 N, acting on the actuation point on the side of the HEPI Boot, in the direction of the Horizontal Actuator.

There are three constraints acting on the system:

- 1) the exposed face on the Support Tube “nub” is *fixed*;
- 2) the exposed cross-section face on the Crossbeam must obey a *symmetry* constraint;
- 3) actuation point on bottom surface of HEPI Boot cannot translate in a direction parallel to the Vertical Actuator's axis.

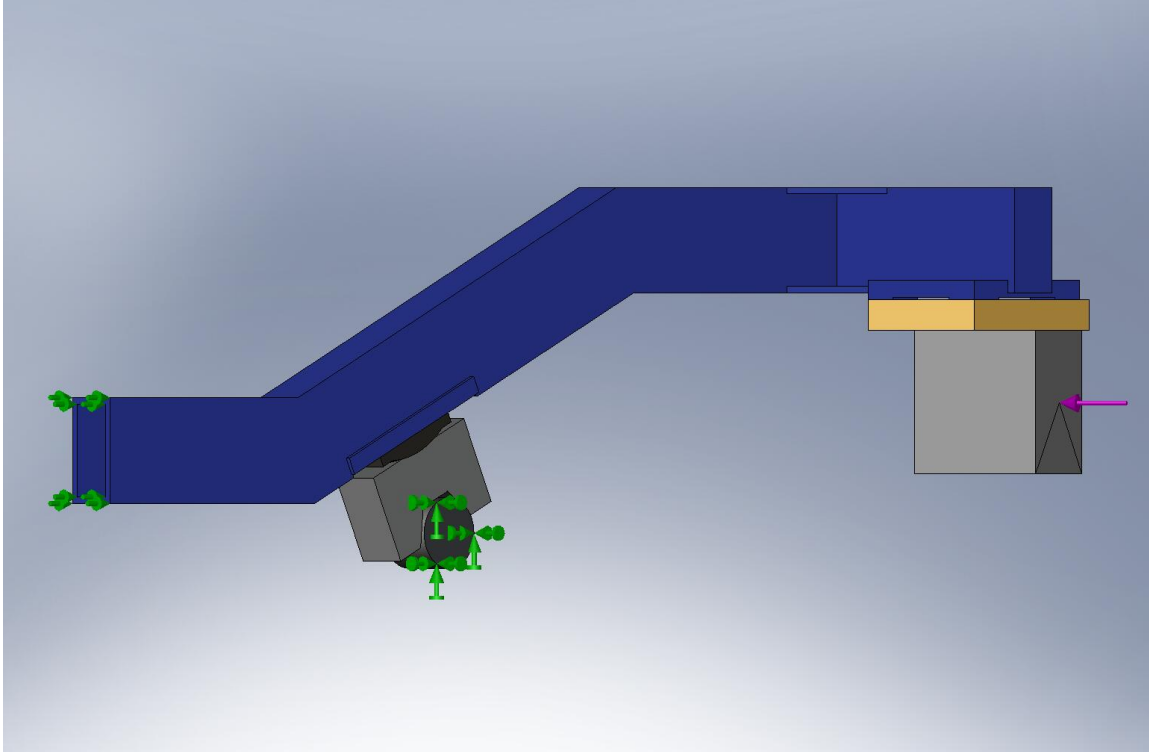


Figure 20. Boundary conditions for the horizontal stiffness study, for the existing Crossbeam system. Here, we see the purple arrow representing a horizontal force on the HEPI Boot. Also present, but not visible, is a 1-DoF constraint on the bottom face of the Boot.

### FEA Results

#### *Study #1: vertical stiffness*

For a 1,000 N vertical force, the FEA solver predicts a vertical displacement of 407  $\mu\text{m}$  at the point of actuation. So, we have:

$$\mathbf{K}_{\text{gullwing,vert-}\delta} = 2.5 \text{ N}/\mu\text{m},$$

where  $\mathbf{K}_{\text{gullwing,vert-}\delta}$  is the effective stiffness of the existing Crossbeam assembly as seen by the Vertical Actuator on HEPI.

In addition to the vertical deflection, we measure a rotation in the sensitive direction of the Horizontal L4-C of 701  $\mu\text{rad}$ . This corresponds to a parasitic rotational stiffness of:

$$\mathbf{K}_{\text{gullwing,vert-}\theta} = 1.4 \text{ N}/\mu\text{rad}$$

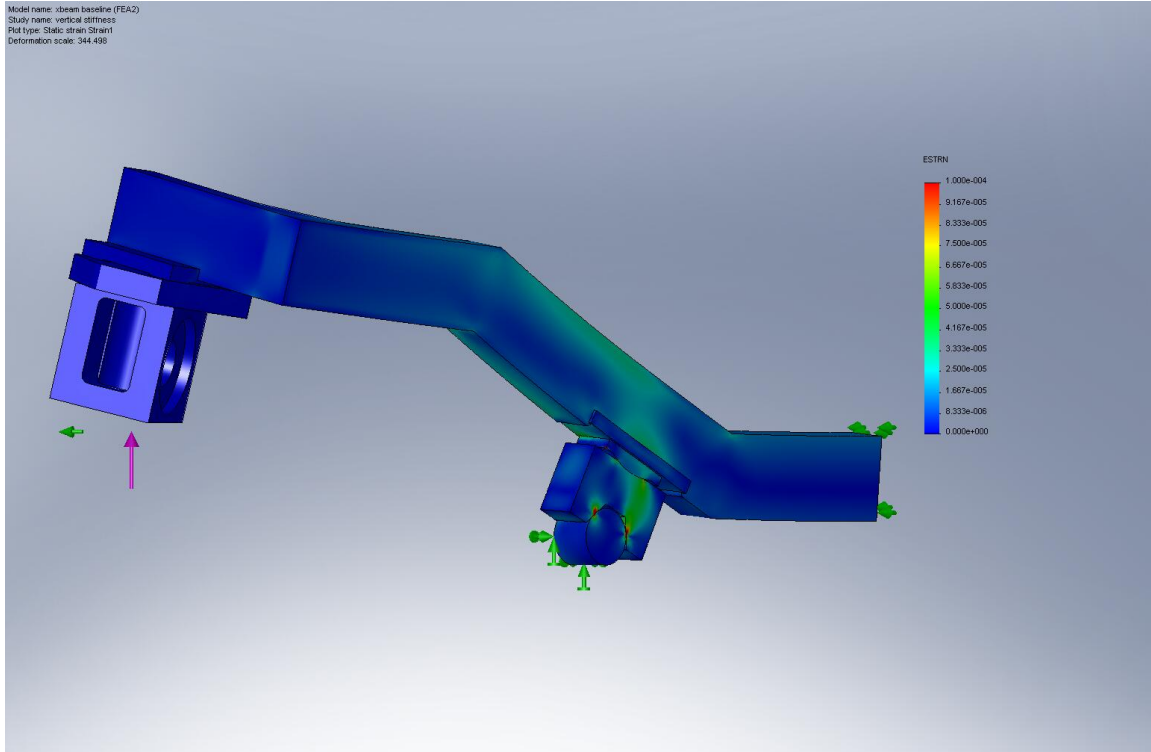


Figure 21. COSMOS strain plot, for vertical force applied to existing Crossbeam assembly. Red areas have strain  $\geq 10^{-4}$ . Deformation is exaggerated, by a factor of 344x.

*Study #2: horizontal stiffness*

For a 1,000 N horizontal force, the FEA solver predicts a horizontal displacement of 392  $\mu\text{m}$  at the point of actuation. So, we have:

$$\mathbf{K}_{\text{gullwing,horz-}\delta} = 2.6 \text{ N}/\mu\text{m},$$

where  $\mathbf{K}_{\text{gullwing,horz-}\delta}$  is the effective stiffness of the existing Crossbeam assembly as seen by the Horizontal Actuator on HEPI.

We also measure a rotation in the sensitive direction of the Horizontal L4-C of 104  $\mu\text{rad}$ . This corresponds to a parasitic rotational stiffness of:

$$\mathbf{K}_{\text{gullwing,horz-}\theta} = 9.6 \text{ N}/\mu\text{rad}$$

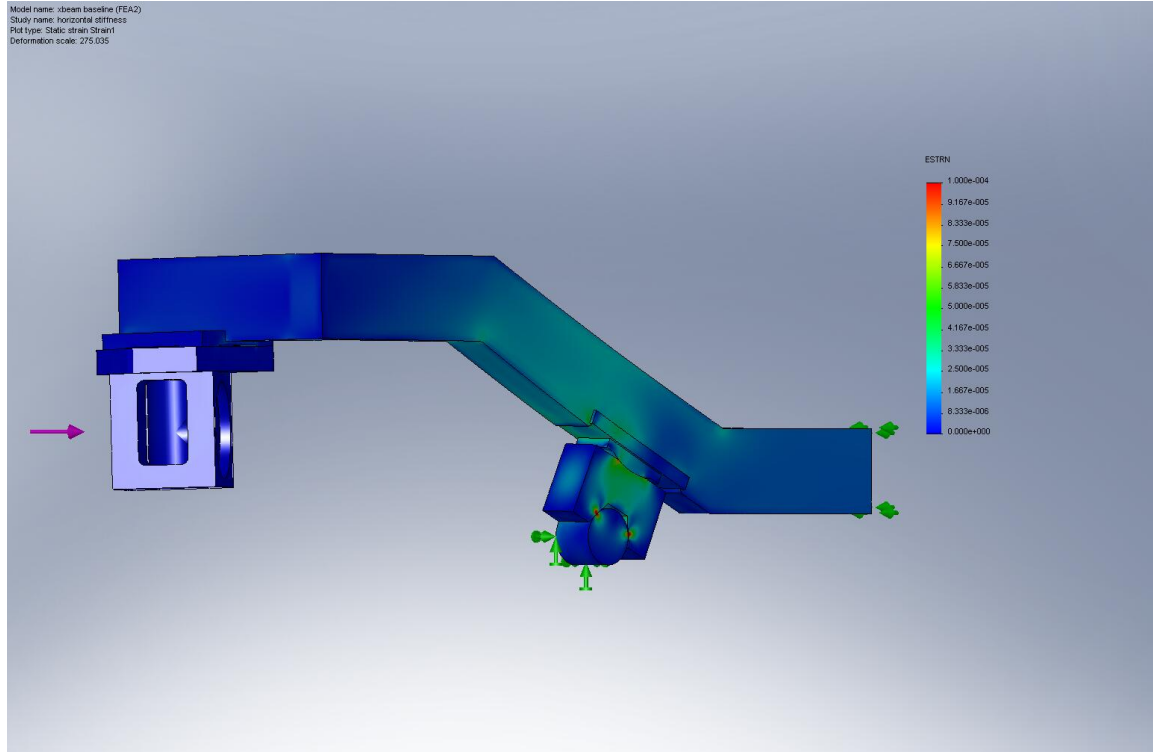


Figure 22. COSMOS strain plot, for horizontal force applied to existing Crossbeam assembly. Red areas have strain  $\geq 10^{-4}$ . Deformation is exaggerated, by a factor of 275x.

## Static Analysis – Model #2: Low Crossbeam Assembly Concept

### Model Geometry

The model of the HEPI Boot is identical to that shown in Figure 11. All the other components used in the Low Crossbeam assembly differ in some way, as described below:

#### *Model Geometry: Connector Tube*

The Low Crossbeam Connector Tube is simply two sections of 5.5” OD, 1/2”-thick tube “welded” together at an angle, with two flat bolt flanges welded onto either end (Figure 23). In the assembly, the square flange (with large-radius corners) is bonded to the side of the HEPI Boot, while the round flange is bonded to the end of the Crossbeam tube.

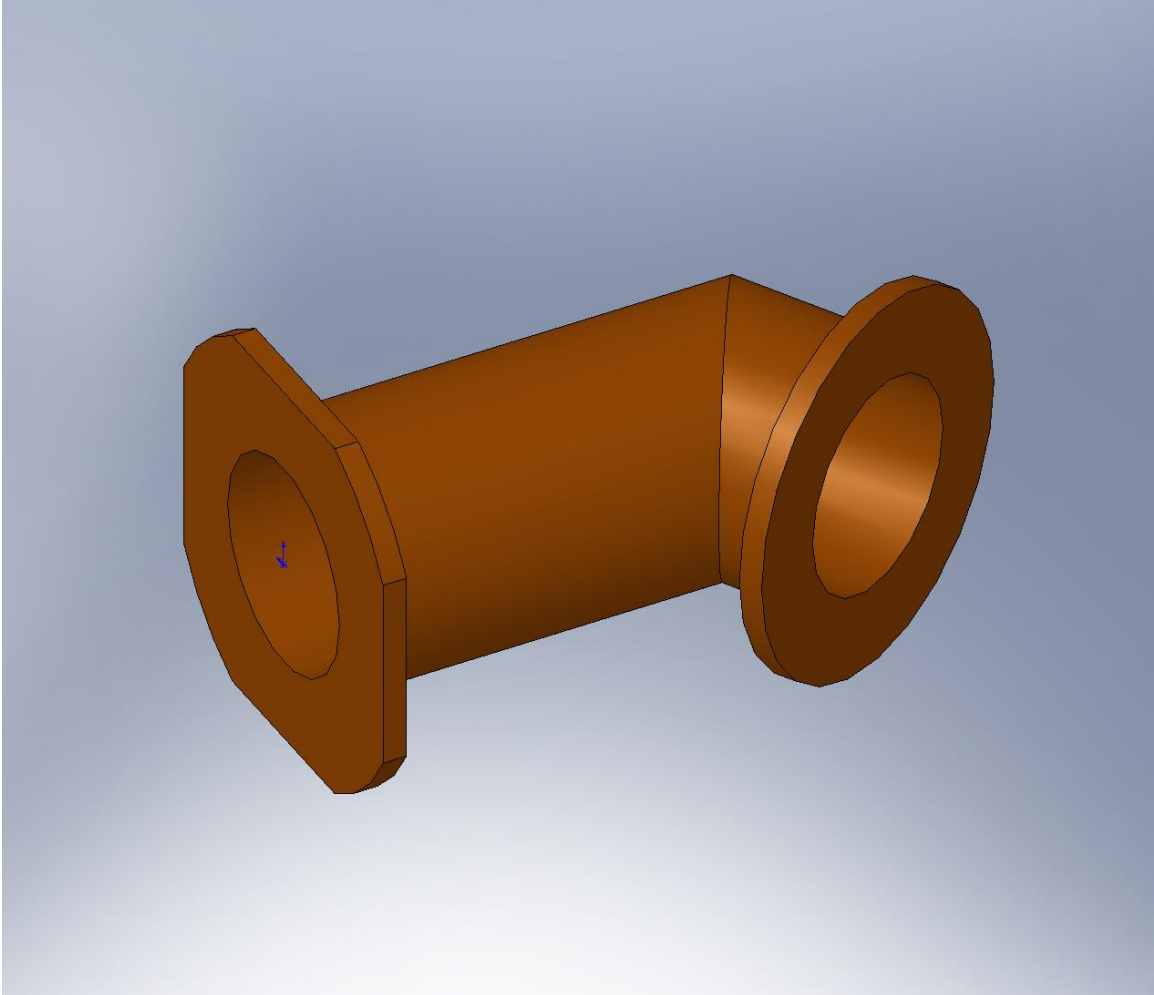


Figure 23. Model of Connector Tube for the Low Crossbeam FEA model.

*Model Geometry: Crossbeam*

The Crossbeam tube's FEA model is shown in Figure 24. The tube has an OD of 5.5" and a wall thickness of 1/2". A flange is welded to the end of the tube, for the interface to the Connector Tube. A flat plate and two rectangular extrusions are welded into the round tube, as shown in Figure 25 and Figure 26.



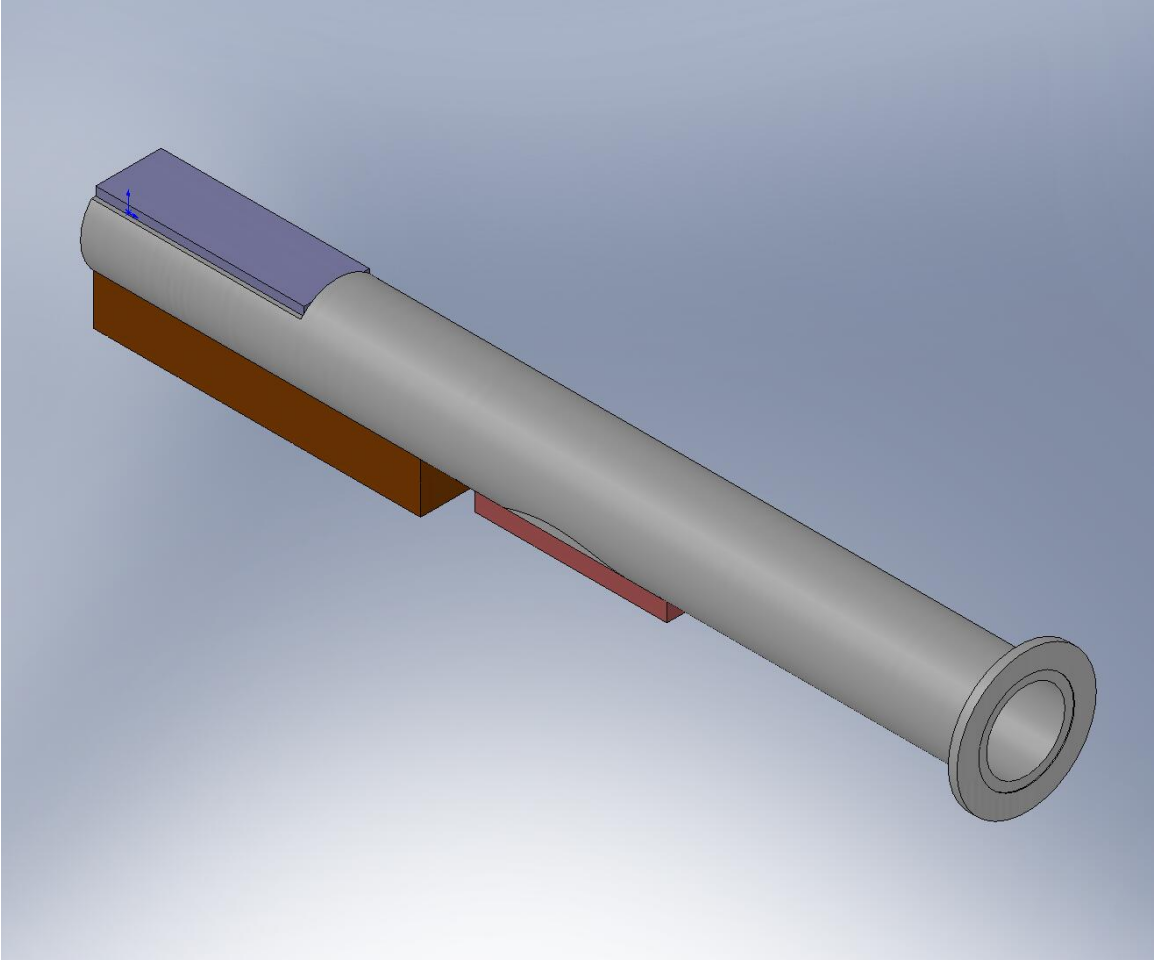


Figure 24. FEA model of proposed Crossbeam tube. Refer to Figure 25 and Figure 26 for details on “weld on” plates and extrusions.

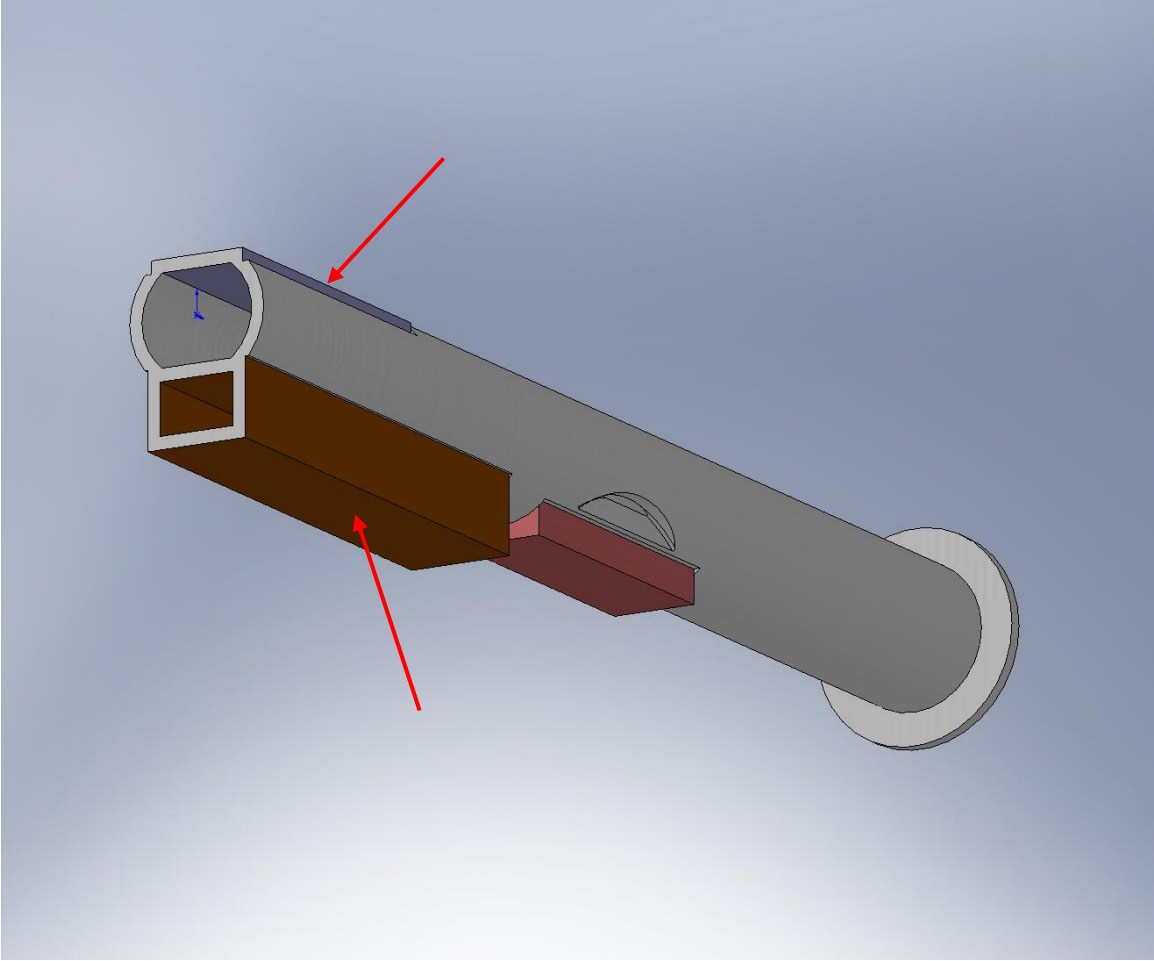


Figure 25. The plate on the top is 1/2"-thick steel and is included to allow clearance beneath the HAM chamber door flange. The rectangular tube welded to the bottom also has 1/2" wall thickness. This extrusion is added strictly for increased stiffness.

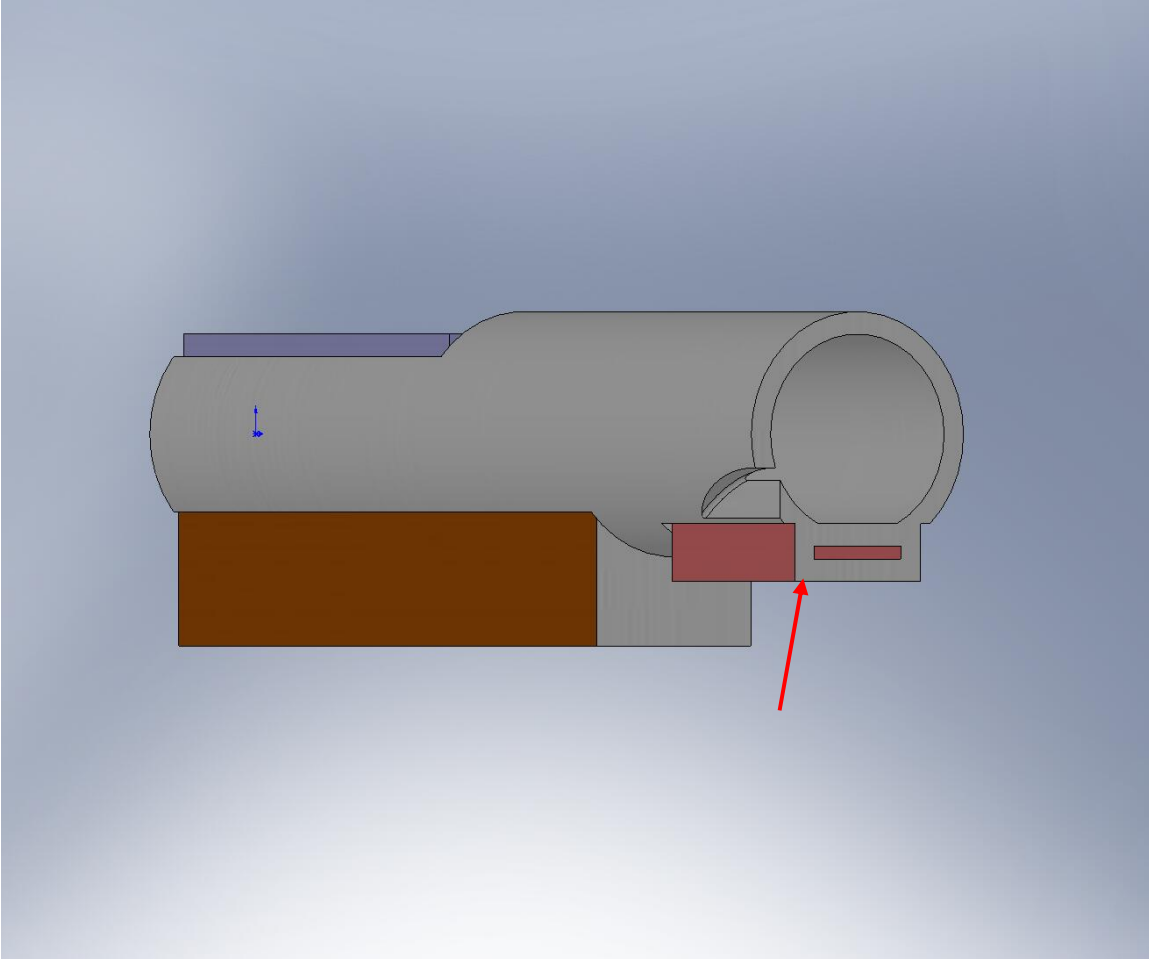


Figure 26. Cross-section view of Crossbeam, showing mid-plane of Support Tube Clamp interface. This interface is created by a welded-on steel extrusion, with 1/2" wall thickness. Full details of the interface have yet to be defined. Note also the scallop cut in the tube, which is described above, in Figure 6.

*Model Geometry: Spherical Clamp*

A new concept is proposed for clamping the Support Tubes to the Crossbeams, based on a ball joint. To more directly provide for tip/tilt adjustment of the Support Tube relative to the Crossbeam – a function now provided by the Spherical Bearing shown (simplified) in Figure 14 – we propose sliding a Spherical Sleeve over the end of the Support Tube. This Sleeve would fit moderately tightly over the cylindrical Tube end. The outside of the Sleeve would have two spherical faces, sharing a common radius and center, but separated by a flat section in the middle of the Sleeve – this would force contact toward the edges of the Sleeve, resulting in a more predictable moment stiffness. The Clamp (Figure 27) would have four spherical pads, again with common radius and center, and with the same radius as the spherical surfaces on the Spherical Sleeve. There would be slots for bolting the Clamp to the Crossbeam, allowing some adjustment along the axis of the Crossbeam before the mounting screws are tightened. This concept relies on a spring-loaded preloading mechanism, not described in this report. This preloader could be fairly simple and would provide a predictable, high force preload to the ball joint. In the FEA

described below for the two new concepts, we assume sufficient preload at these Clamps to prevent any slip between the mating components.

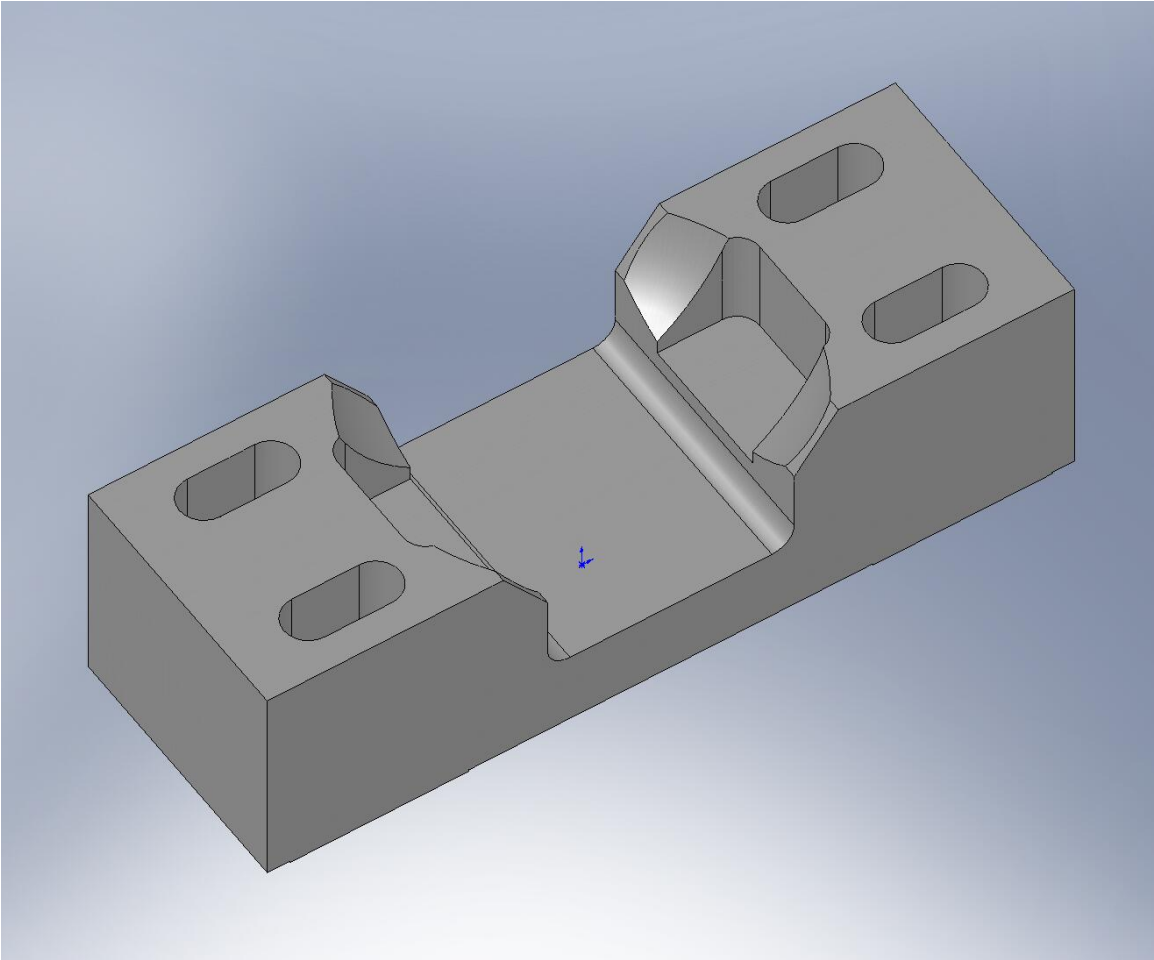


Figure 27. New concept for Support Tube Clamp. Four spherical pads form the seat for a matching Spherical Sleeve, which is shown in Figure 28.

*Model Geometry: Spherical Sleeve*

The FEA model for the Spherical Sleeve is shown in Figure 28. We would likely want to add some flexural hinges to the Sleeve to allow for small mismatches in radii of the Support Tube end and the Sleeve's inner bore, but this should not effect the system's stiffness and would only complicate the mesh. We recess the center of the Sleeve's inner bore, so the FEA model does not bond the Sleeve to the Support Tube over the entire surface. Since the preload from the Spherical Clamp acts on the Sleeve toward the outer edges of the Sleeve, there should be very little stiffness in this middle section.

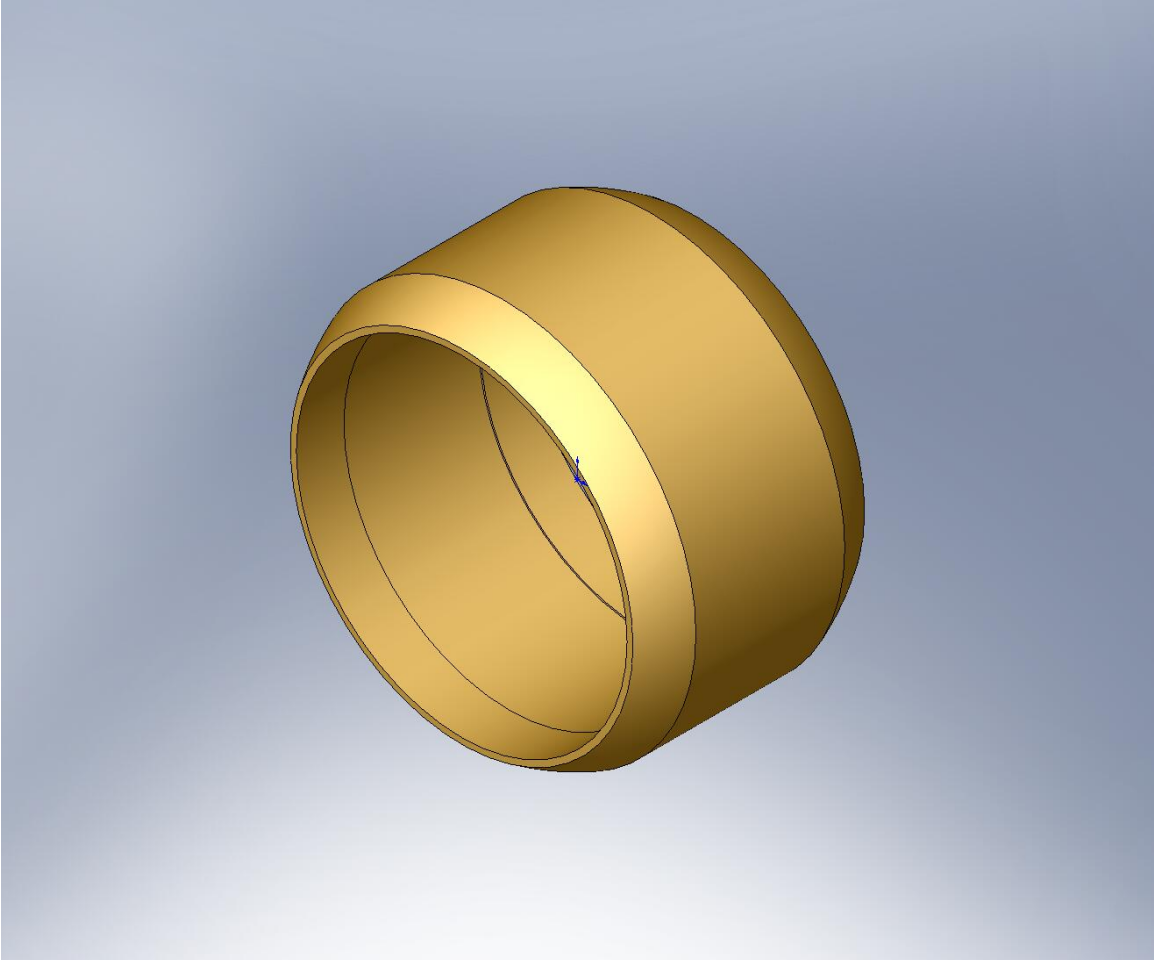


Figure 28. Spherical Sleeve couples the end of the Support Tube to the new, spherical Support Tube Clamp.

*Model Geometry: Support Tube “Nub”*

We assume the interface between the Support Tube end and the Spherical Sleeve is only stiff where the preload is high – in line with the four spherical pads in the Clamp. So, the Support Tube model is modified, to leave raised pads on the outside of the Tube end, which line up with the Clamp pads. Two additional pads are included where the spring-loaded preloader would compress the Sleeve/Tube/Clamp interface, though the preloader itself is not included in the FEA model.

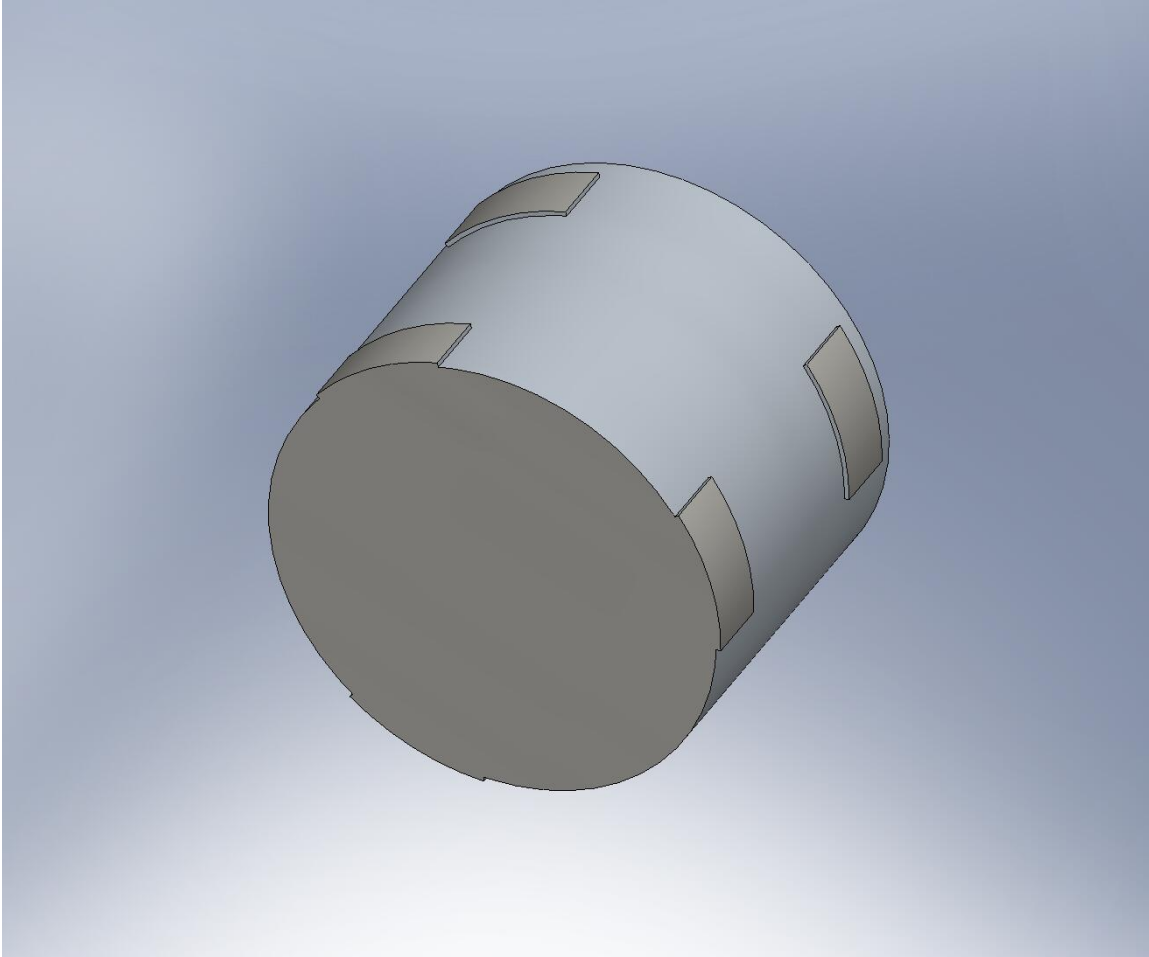


Figure 29. End of the Support Tube that interfaces with the Spherical Clamp, modified for FEA. The six raised pads around the cylinder roughly coincide with mating pads on the Spherical Clamp (and on the preloader, which is not modeled in the FEA).

#### Mesh Details

As noted above for the existing Crossbeam FEA (Figure 17), we set up the mesh such that the densest regions are in the Support Tube Clamp. This is shown in Figure 30.



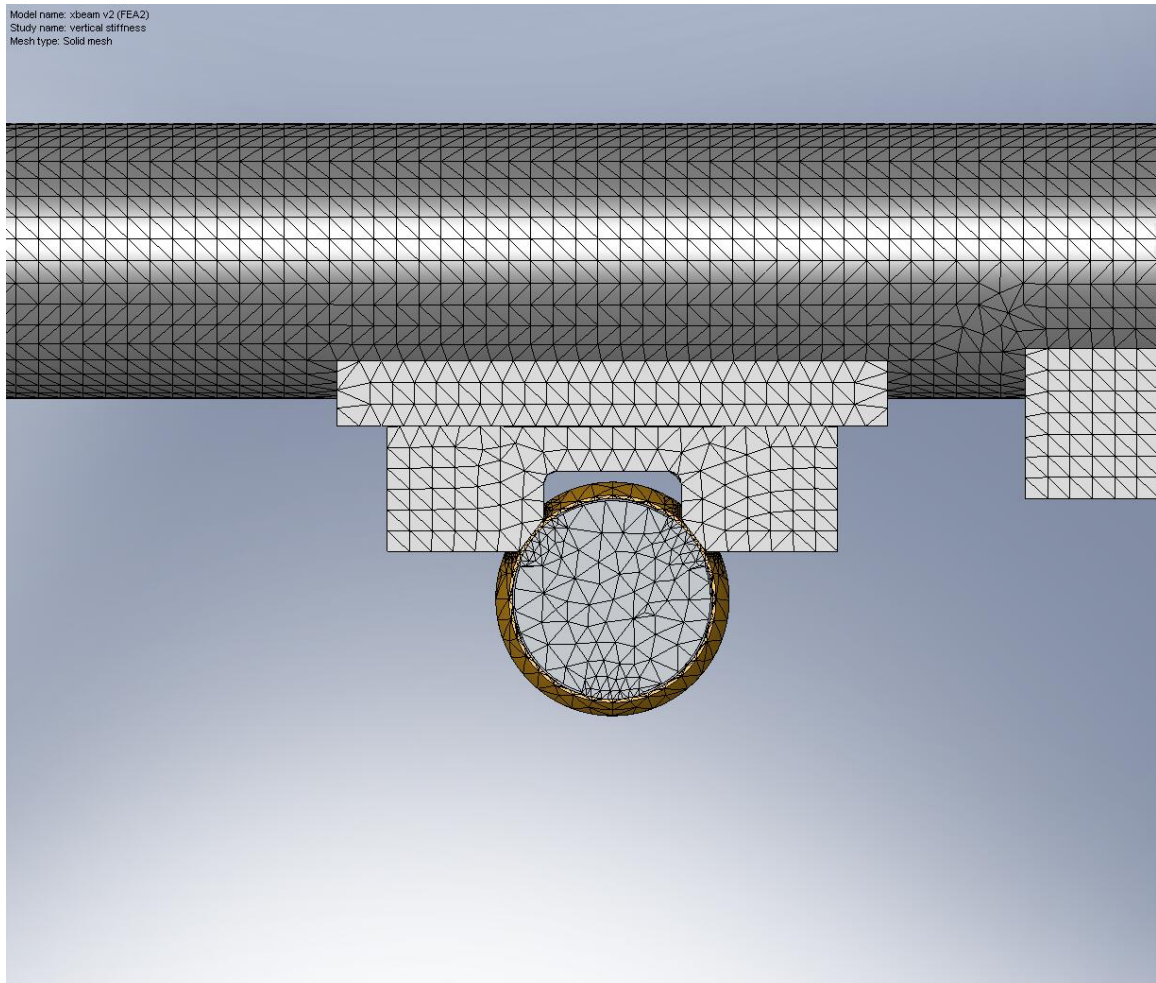


Figure 30. The mesh is densest around the Support Tube's Spherical Clamp and Sleeve.

The full meshed assembly is shown in Figure 31, and has the following properties:

- mesh controls – 1) 4 spherical pads in Spherical Clamp: 0.075"; 2) 2 inner bearing surfaces on Spherical Sleeve: 0.125"
- element size=0.45"
- total nodes=173,769
- total elements=102,907
- % elements with aspect ratio < 3=95.6
- % elements with aspect ratio > 10=0.05
- % distorted elements=0

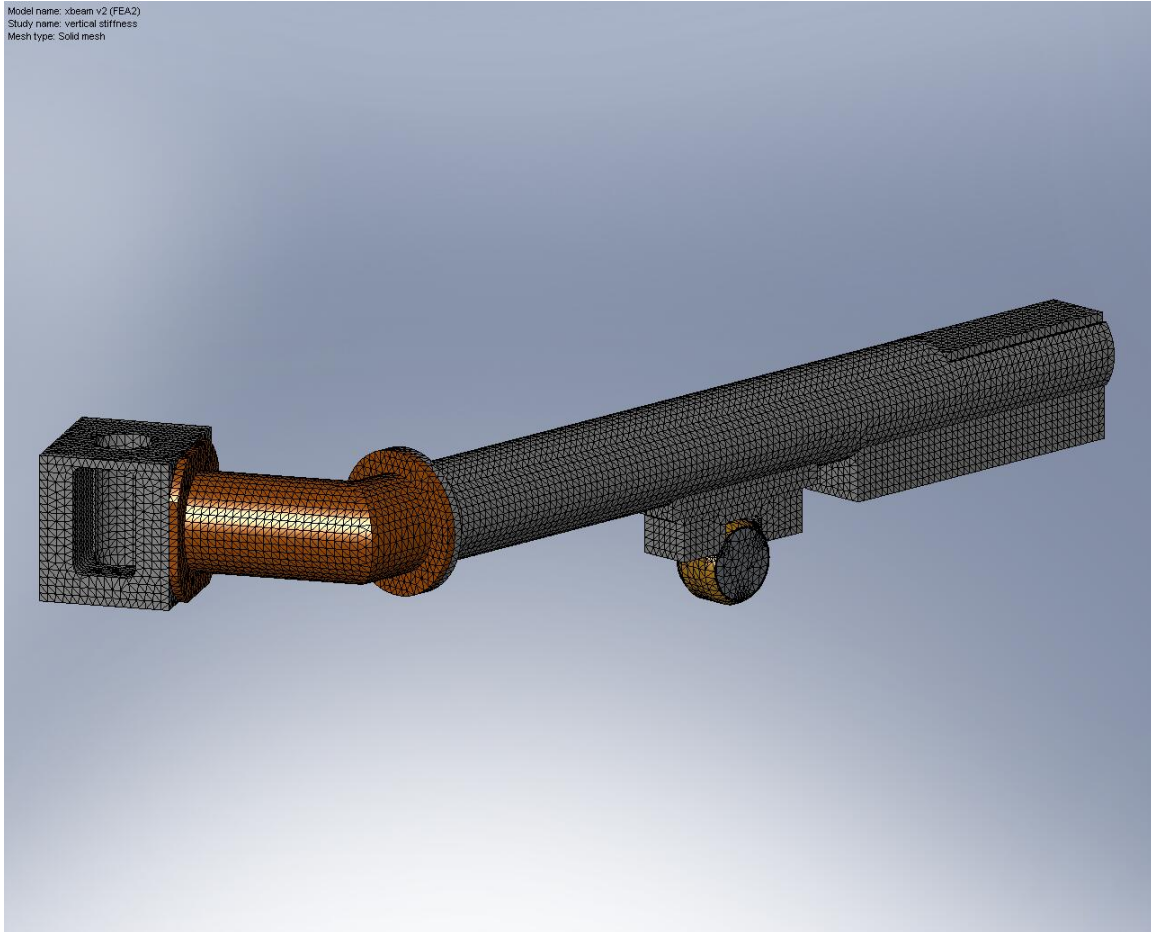


Figure 31. Meshed model for Low Crossbeam static FEA.

### Materials

The components of this FEA model are assigned the following material properties:

- *HEPI Boot*: Plain Carbon Steel –  $E_x=210$  GPa,  $\nu=.28$ ,  $G_{xy}=79$  GPa
- *Connector Tube*: Plain Carbon Steel – ...
- *Crossbeam*: Plain Carbon Steel – ...
- *Spherical Clamp*: AISI 304 –  $E_x=190$  GPa,  $\nu=.29$ ,  $G_{xy}=75$  GPa
- *Spherical Sleeve*: Aluminum 6061-T6 –  $E_x=69$  GPa,  $\nu=.33$ ,  $G_{xy}=26$  GPa
- *Support Tube*: AISI 304 – ...

Note we have not made final decisions on materials to be used for the new Clamp and Sleeve. Considerations other than stiffness (such as surface wear) would need to be analyzed more carefully before making final selections. We have simply picked 304 Stainless Steel and 6061-T6 Aluminum because they are common materials that should allow for reasonable predictions of the overall system stiffness.

### Boundary Conditions

#### *Study #1: vertical stiffness*

The force and constraints defined above for Study #1 of the existing Crossbeam system are reused for the Low Crossbeam concept, as shown in Figure 32.

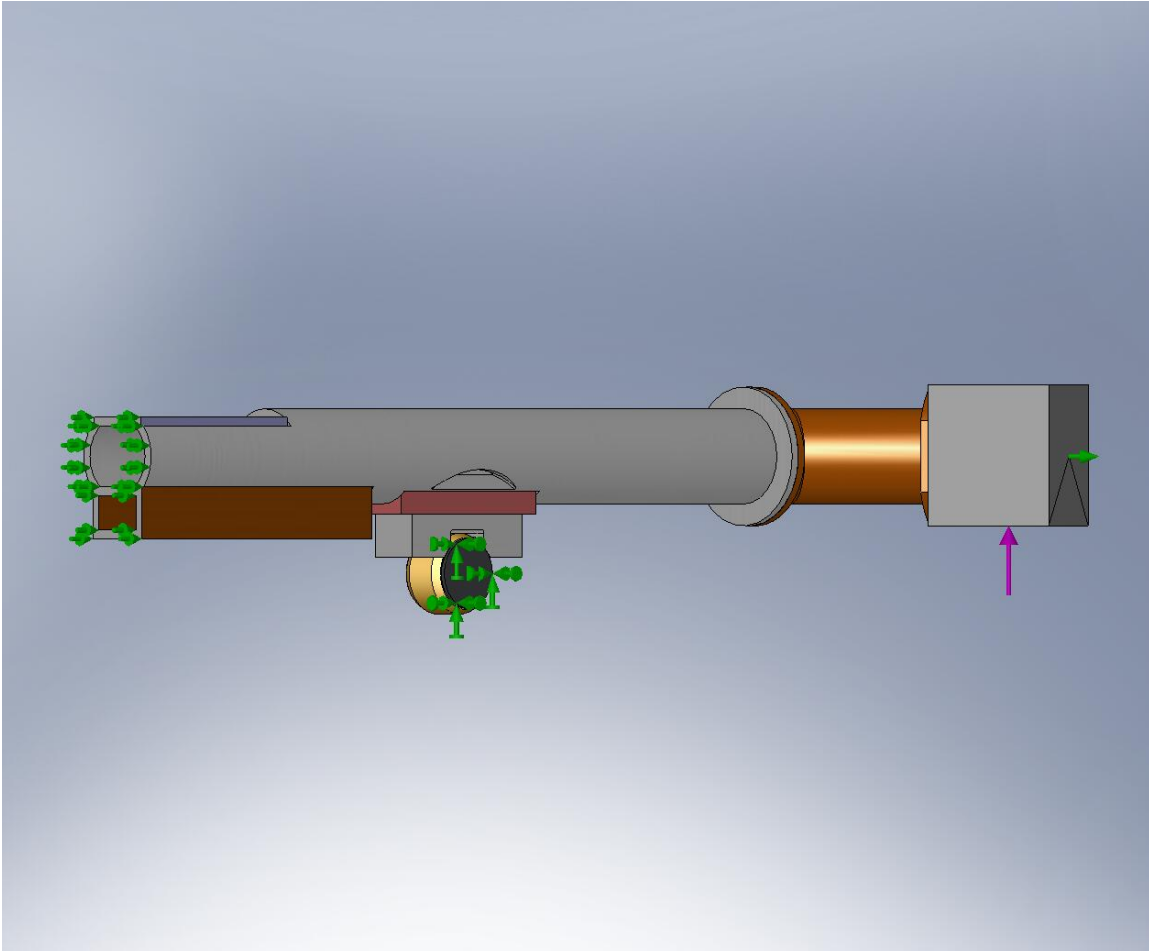


Figure 32. Green arrows show the constraints, while the purple arrow shows the applied force. Here, we examine the vertical stiffness of the Low Crossbeam design.

*Study #2: horizontal stiffness*

The force and constraints defined above for Study #2 of the existing Crossbeam system are reused for the Low Crossbeam concept, as shown in Figure 33.

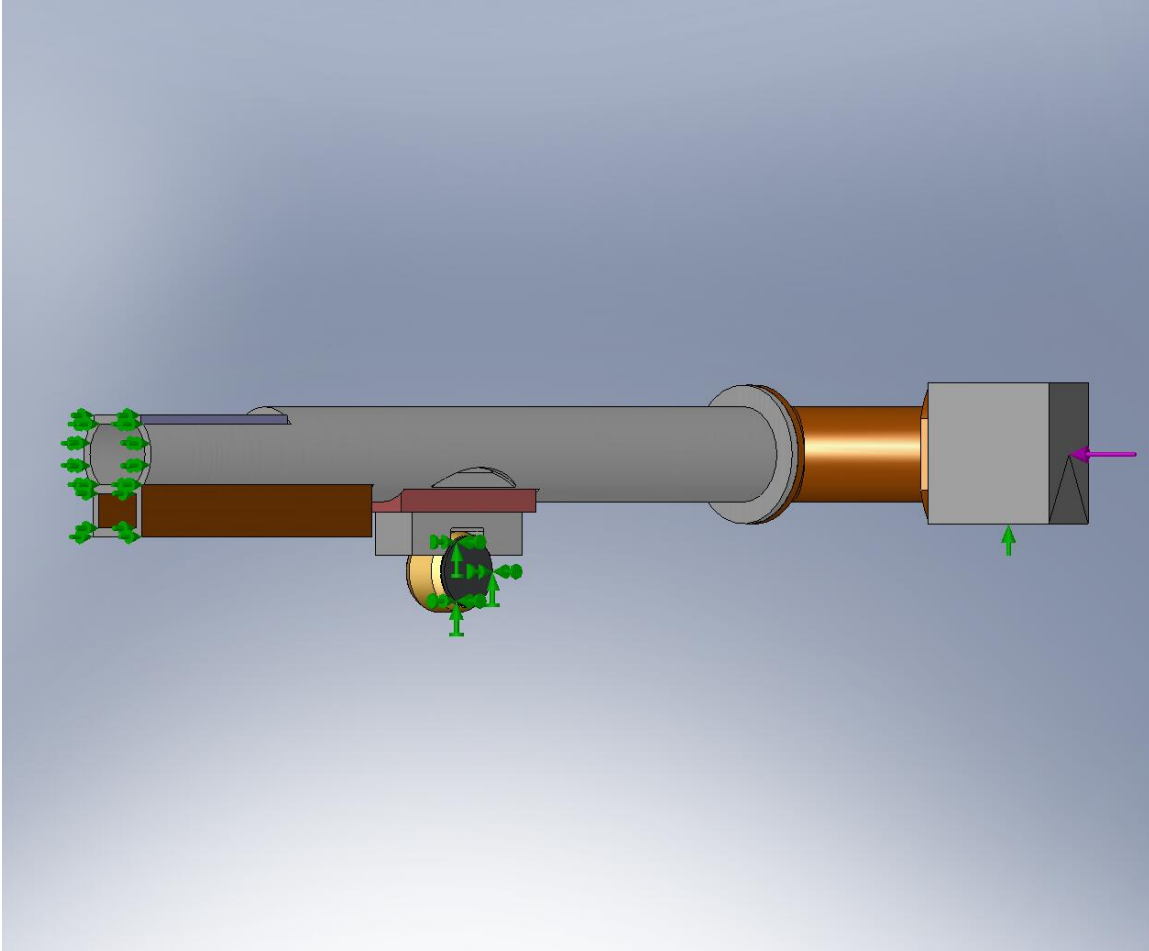


Figure 33. Here, we examine the horizontal stiffness of the Low Crossbeam concept.

*FEA Results*

*Study #1: vertical stiffness*

For a 1,000 N vertical force, the FEA solver predicts a vertical displacement of 221  $\mu\text{m}$  at the point of actuation. So, we have:

$$\mathbf{K}_{\text{low x-beam,vert-}\delta}=4.5 \text{ N}/\mu\text{m},$$

where  $\mathbf{K}_{\text{low x-beam,vert-}\delta}$  is the effective stiffness of the Low Crossbeam assembly as seen by the Vertical Actuator on HEPI.

In addition to the vertical deflection, we measure a rotation in the sensitive direction of the Horizontal L4-C of 413  $\mu\text{rad}$ . This corresponds to a parasitic rotational stiffness of:

$$\mathbf{K}_{\text{low x-beam,vert-}\theta}=2.4 \text{ N}/\mu\text{rad}$$

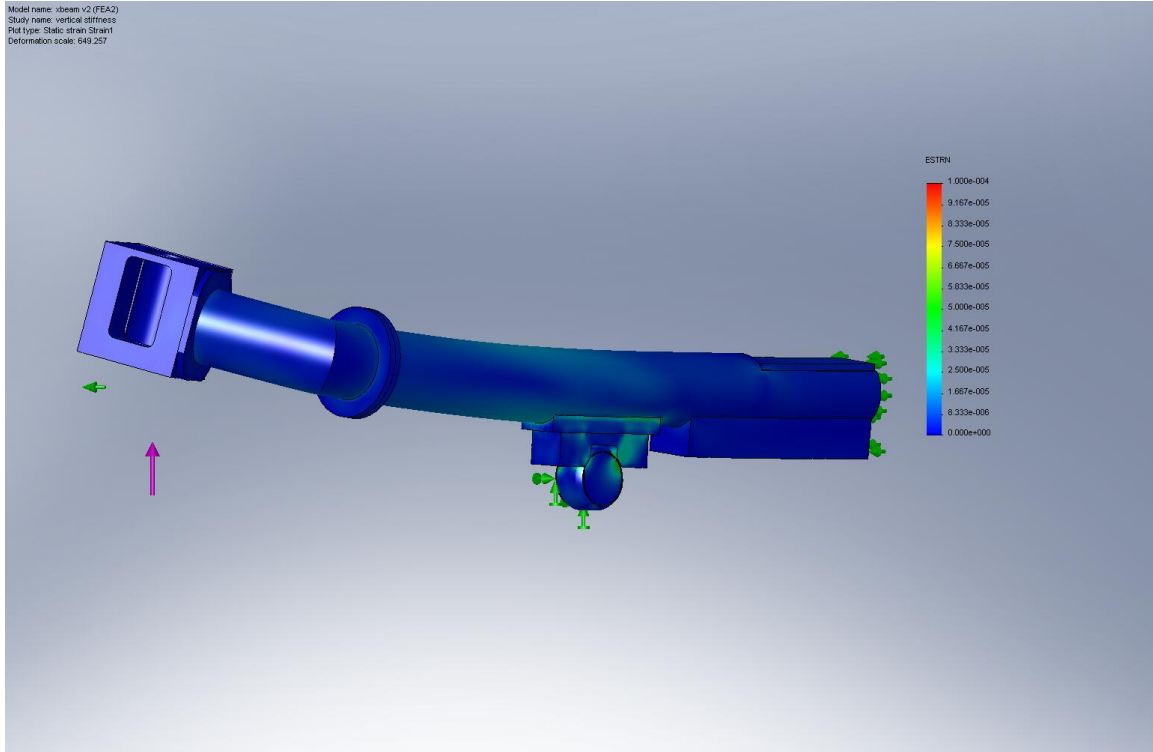


Figure 34. Strain plot for Low Crossbeam, with 1,000 N applied from HEPI's Vertical Actuator. Areas in red correspond to strain  $\geq 10^{-4}$ . Deformation is exaggerated, by a factor of 649x.

*Study #2: horizontal stiffness*

For a 1,000 N horizontal force, the FEA solver predicts a horizontal displacement of 100  $\mu\text{m}$  at the point of actuation. So, we have:

$$\mathbf{K}_{\text{low x-beam,horz-}\delta} = 10.0 \text{ N}/\mu\text{m},$$

where  $\mathbf{K}_{\text{low x-beam,horz-}\delta}$  is the effective stiffness of the Low Crossbeam assembly as seen by the Horizontal Actuator on HEPI.

We also measure a rotation in the sensitive direction of the Horizontal L4-C of 27  $\mu\text{rad}$ . This corresponds to a parasitic rotational stiffness of:

$$\mathbf{K}_{\text{low x-beam,horz-}\theta} = 37.0 \text{ N}/\mu\text{rad}$$

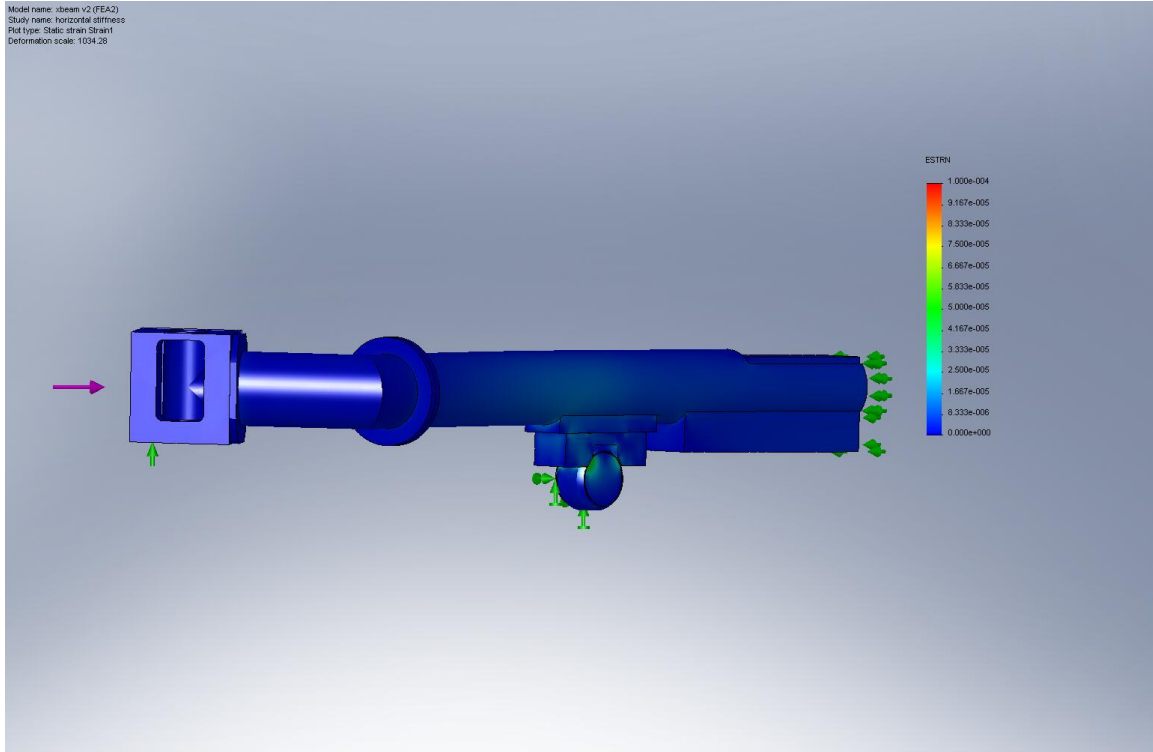


Figure 35. COSMOS strain plot, for horizontal force applied to Low Crossbeam assembly. Red areas have strain  $\geq 10^{-4}$ . Deformation is exaggerated, by a factor of 1,034x.

### Static Analysis – Model #3: High Crossbeam Assembly Concept

#### Model Geometry

The models of the HEPI Boot (Figure 11), Spherical Clamp (Figure 27), Spherical Sleeve (Figure 28), and Support Tube “nub” (Figure 29) are all identical to those used in the Low Crossbeam FEA model.

#### *Model Geometry: Connect Tube Adapter*

It may be necessary to bolt a plate between the HEPI Boot and the top-mounted Connector Tube (Figure 36), to convert the interface from the Boot’s bolt pattern to the Tube’s bolt pattern. At this time, we have modeled a simple, thin (.29” tall) plate bonded to the top of the Boot. This detail would need to be developed further, if the High Crossbeam design were selected. For this analysis, however, the addition of the plate should have very little effect.



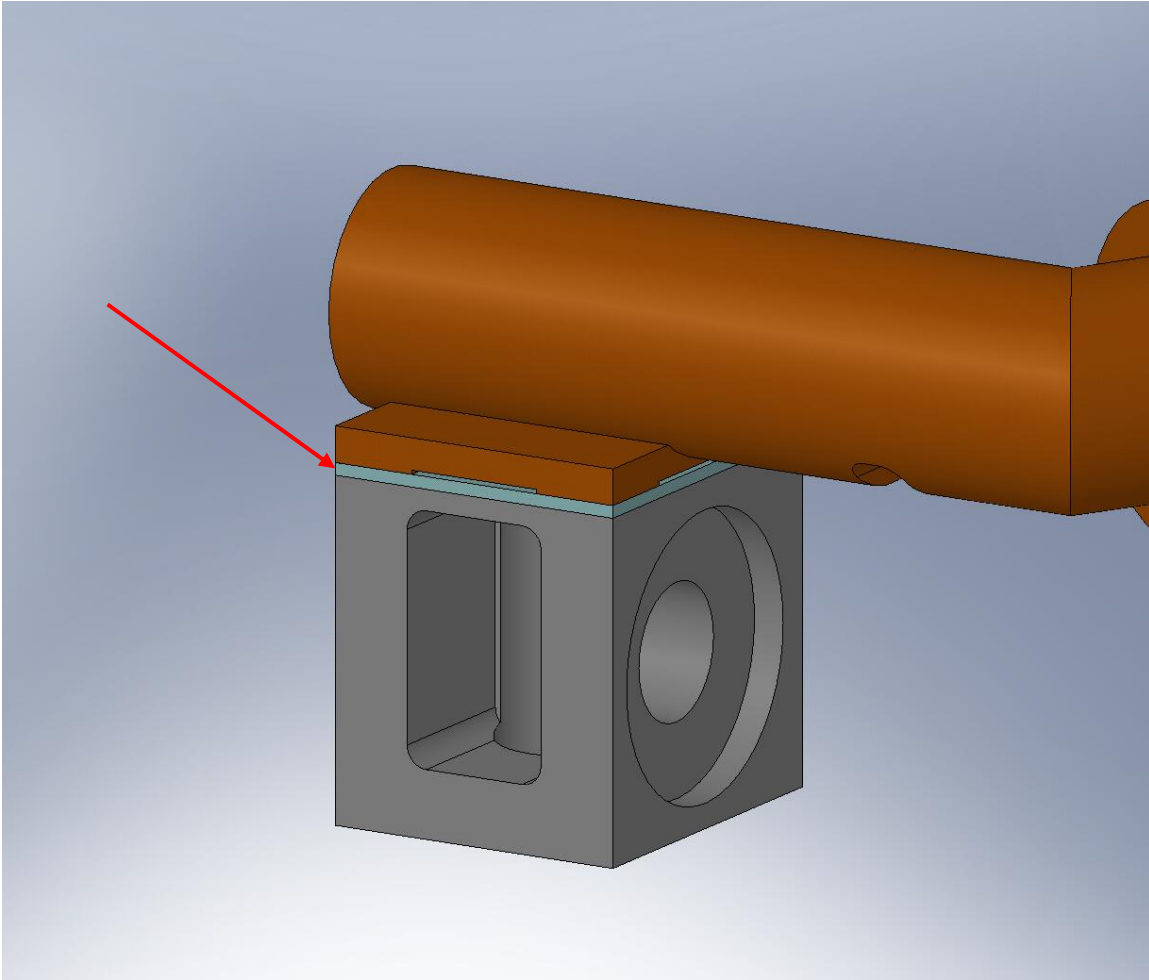


Figure 36. The blue plate represents an adapter from one bolt pattern to another. It would likely need to be thicker than is shown here, to allow enough thread engagement for the Connector Tube's mounting bolts. It is possible that this component would not be needed at all, if the desired bolt pattern could be machined directly into the Boot.

*Model Geometry: Connector Tube*

The Connector Tube used to couple the High Crossbeam to the HEPI Boot is very similar to the one proposed for the Low Crossbeam (see Figure 23). The diameter and wall thickness are the same, as well as the round mating flange. On the HEPI end, the Tube extends over the HEPI Boot and bolts on via a welded plate. See Figure 37. For the FEA, we use four raised pads on the bottom of the interface plate to force contact only around the mounting bolts. To simplify the mesh, we again leave out the actual bolt holes. The back end of the Tube is sealed with a 1/2"-thick welded cap. As mentioned above (Figure 8), we also cut some material from the underside of the Tube, around where the HEPI Housing would extend. See Figure 38. This detail would need to be reconsidered, if the High Crossbeam design were selected.

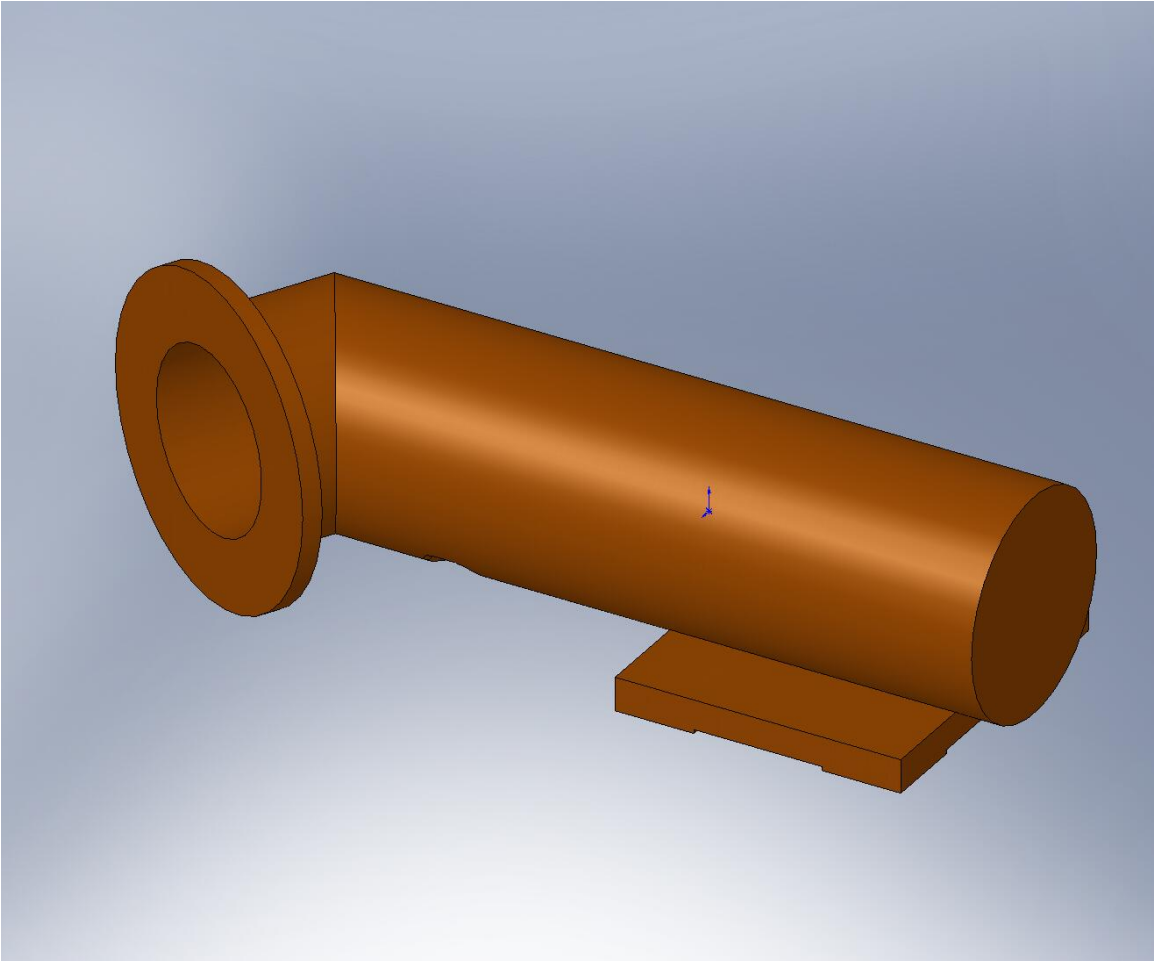


Figure 37. Connector Tube proposed for the High Crossbeam concept. It is mostly similar to the Low Crossbeam design, except for the mounting plate detail and the notch shown in Figure 38.

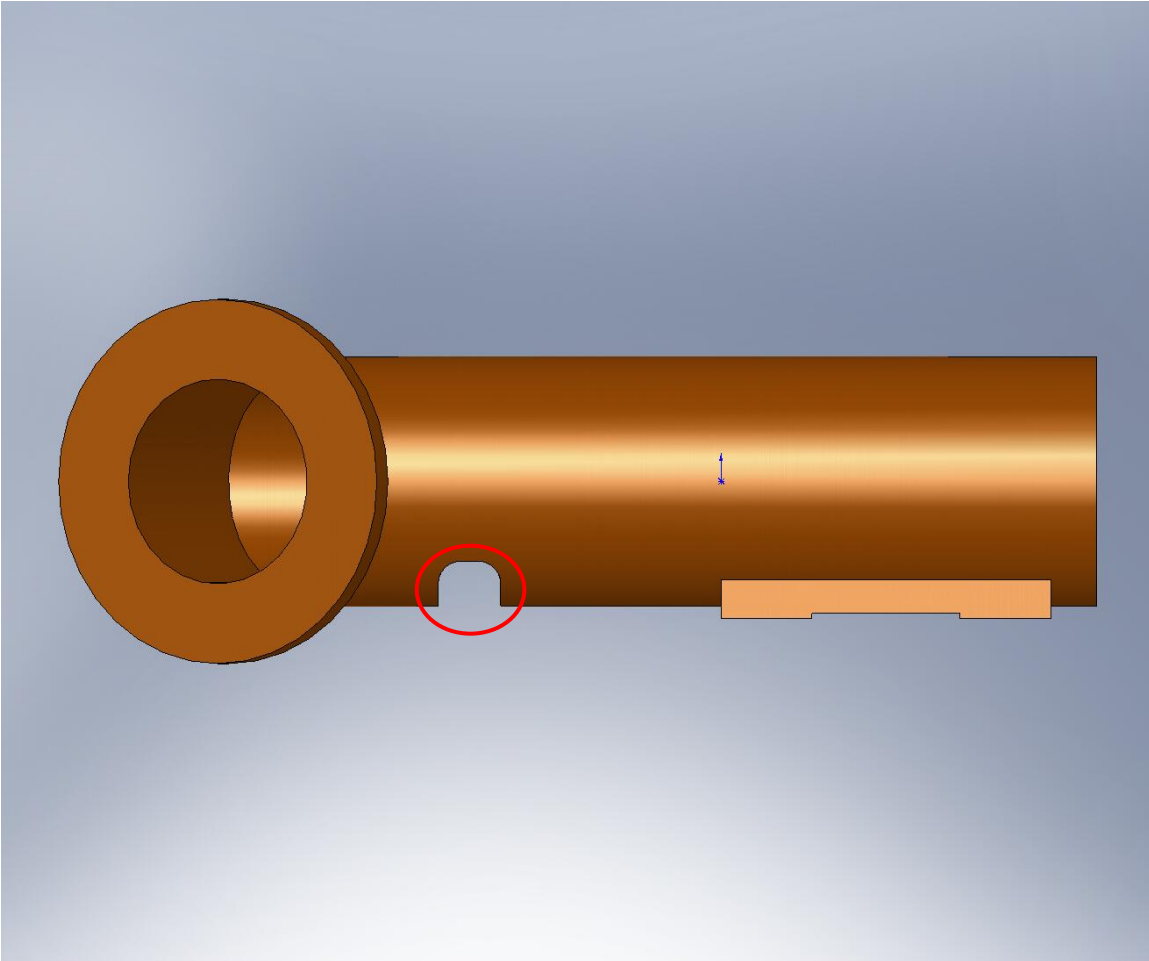


Figure 38. The highlighted notch is added to the Connector Tube to allow clearance around the existing HEPI Housing.

*Model Geometry: Crossbeam*

The High Crossbeam tube is identical to the one described above for the Low Crossbeam, except for a cylindrical notch cut into the tube near each end, to avoid interfering with the HEPI Offload Springs. See Figure 39. This is another detail of the High Crossbeam design that would require careful thought, taking into account machinability of the tube and variability in the HEPI installations' true dimensions.

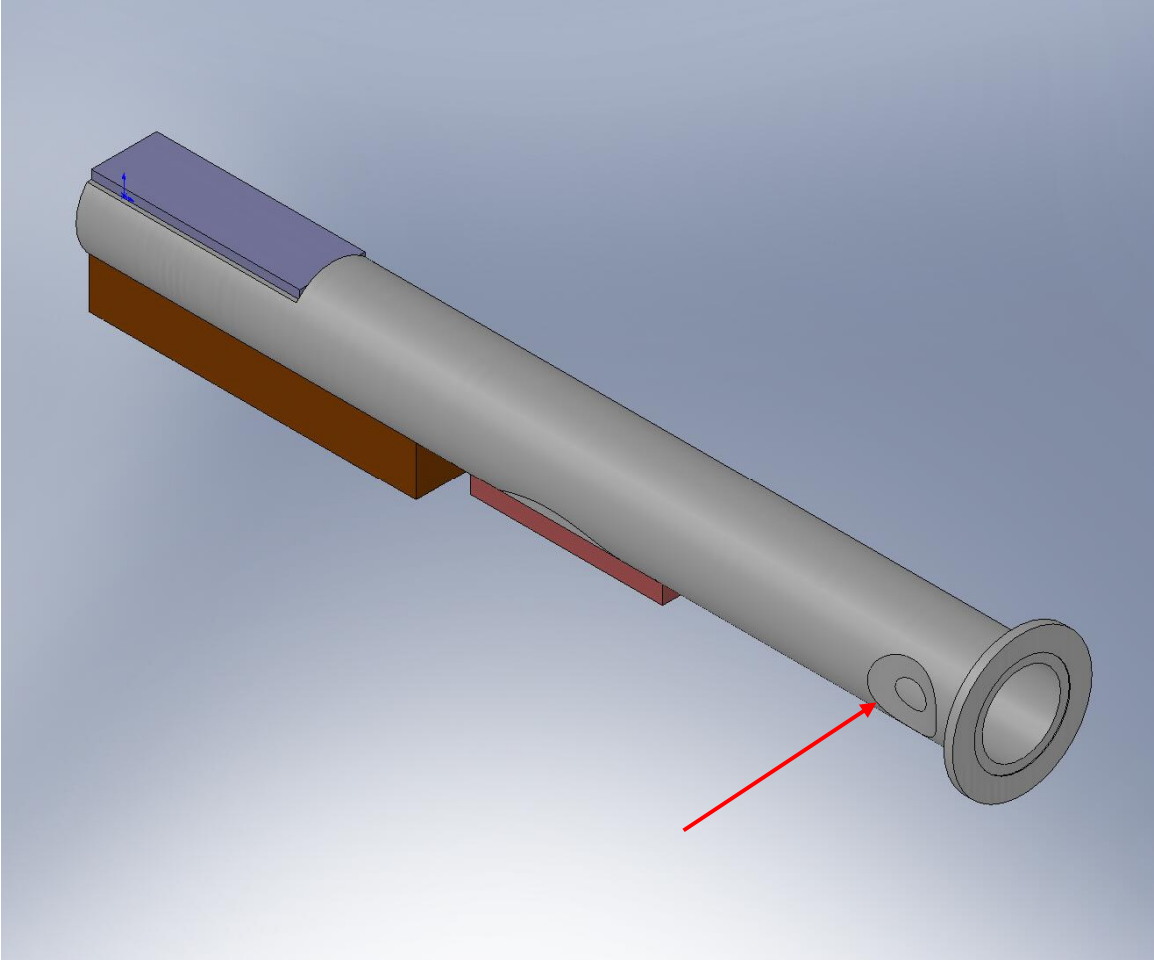


Figure 39. Note the cylindrical notch toward the end of the Crossbeam tube. This detail is added to provide clearance around the HEPI's front Offload Spring.

Mesh Details

Again, the mesh is densest around the Support Tube Clamp. See Figure 40.

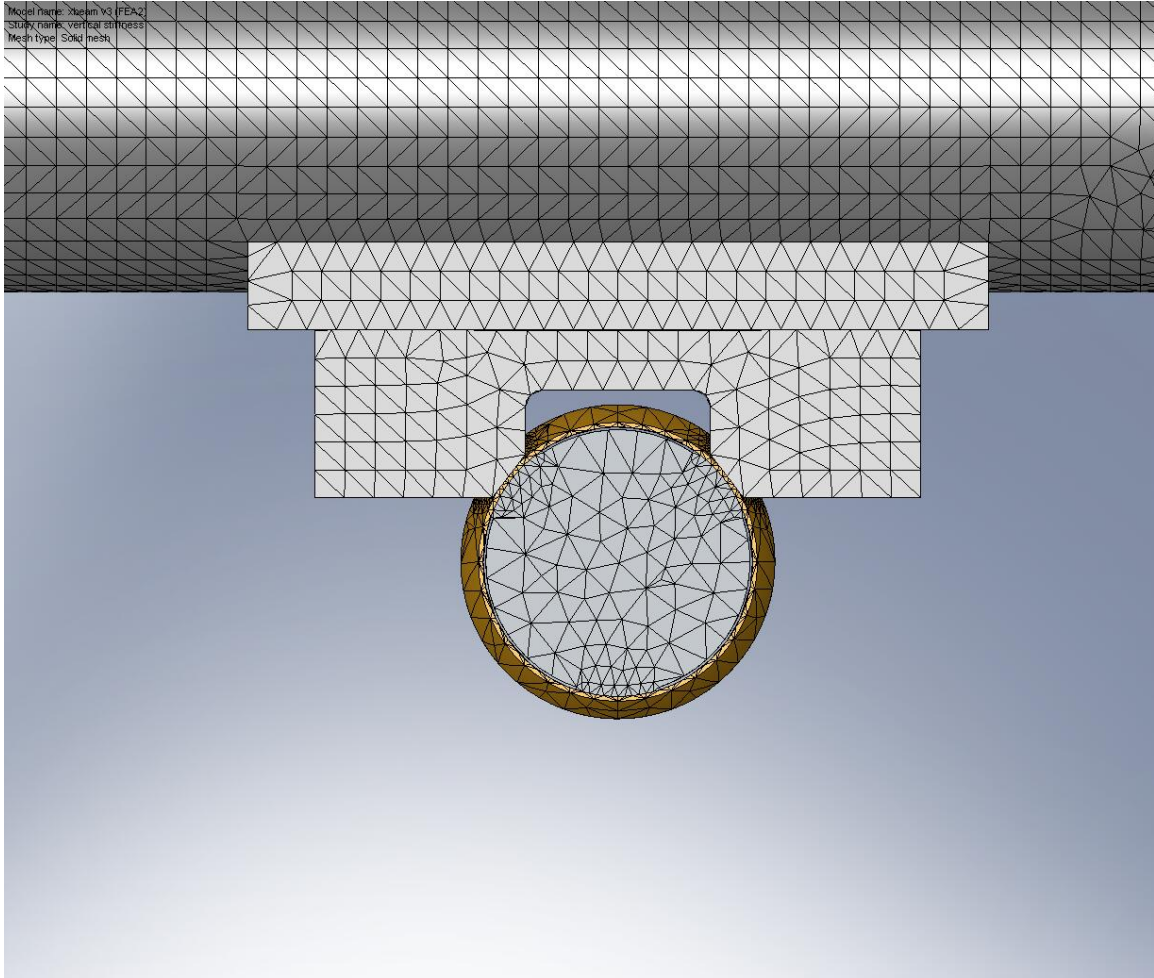


Figure 40. Mesh is densest around the four pads in the Spherical Clamp, through the Spherical Sleeve, and penetrating into the Support Tube.

The meshed assembly is shown in Figure 41, and has the following properties:

- mesh controls – 1) 4 spherical pads in Spherical Clamp: 0.075"; 2) 2 inner bearing surfaces on Spherical Sleeve: 0.125"
- element size=0.45"
- total nodes=188,021
- total elements=111,057
- % elements with aspect ratio < 3=95.5
- % elements with aspect ratio > 10=.06
- % distorted elements=0

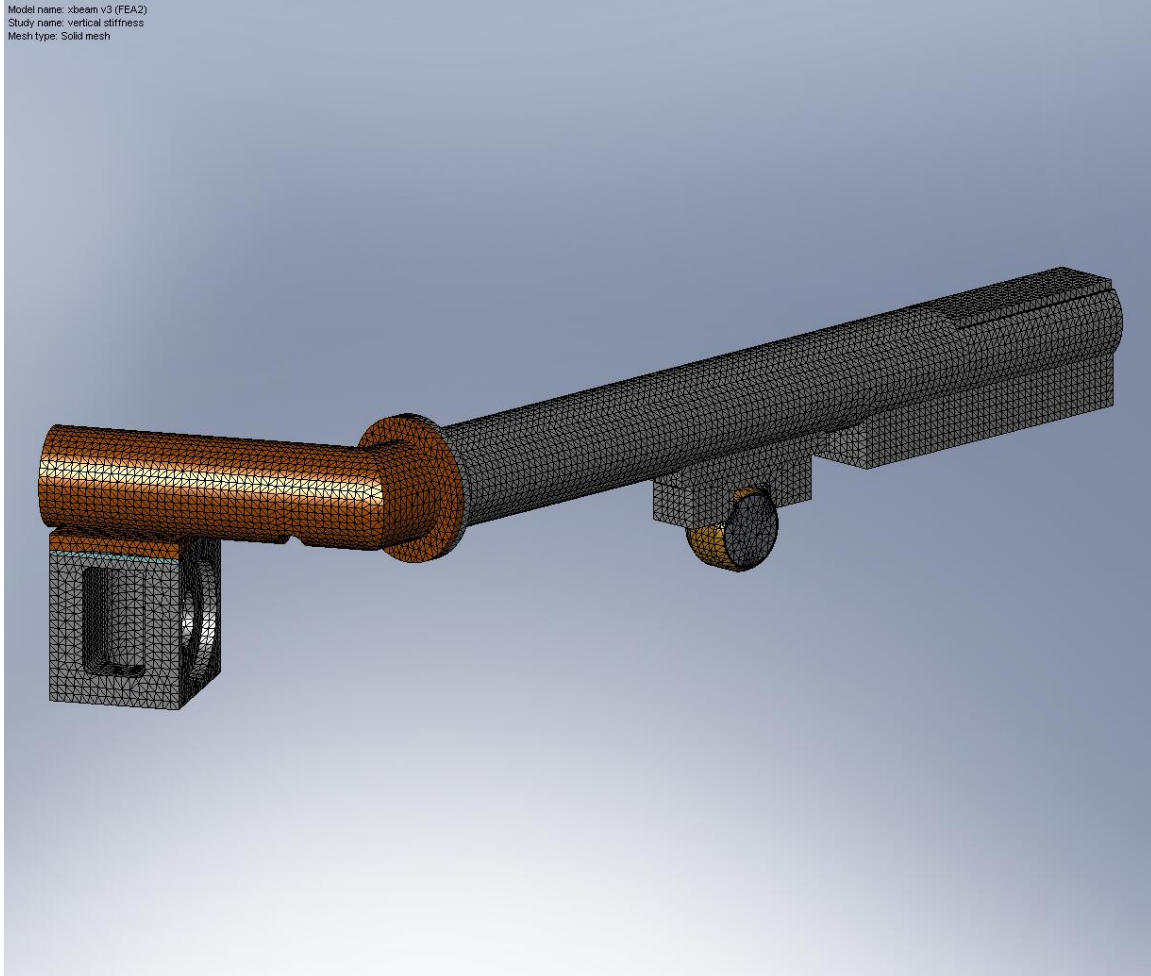


Figure 41. The meshed model used for static analysis of the High Crossbeam concept.

### Materials

The components of this FEA model are assigned the following material properties:

- *HEPI Boot*: Plain Carbon Steel –  $E_x=210$  GPa,  $\nu=.28$ ,  $G_{xy}=79$  GPa
- *Connector Tube Adapter*: Plain Carbon Steel – ...
- *Connector Tube*: Plain Carbon Steel – ...
- *Crossbeam*: Plain Carbon Steel – ...
- *Spherical Clamp*: AISI 304 –  $E_x=190$  GPa,  $\nu=.29$ ,  $G_{xy}=75$  GPa
- *Spherical Sleeve*: Aluminum 6061-T6 –  $E_x=69$  GPa,  $\nu=.33$ ,  $G_{xy}=26$  GPa
- *Support Tube*: AISI 304 – ...

### Boundary Conditions

*Study #1: vertical stiffness*

The force and constraints for Study #1 are shown in Figure 42. The vertical force is 1,000 N.



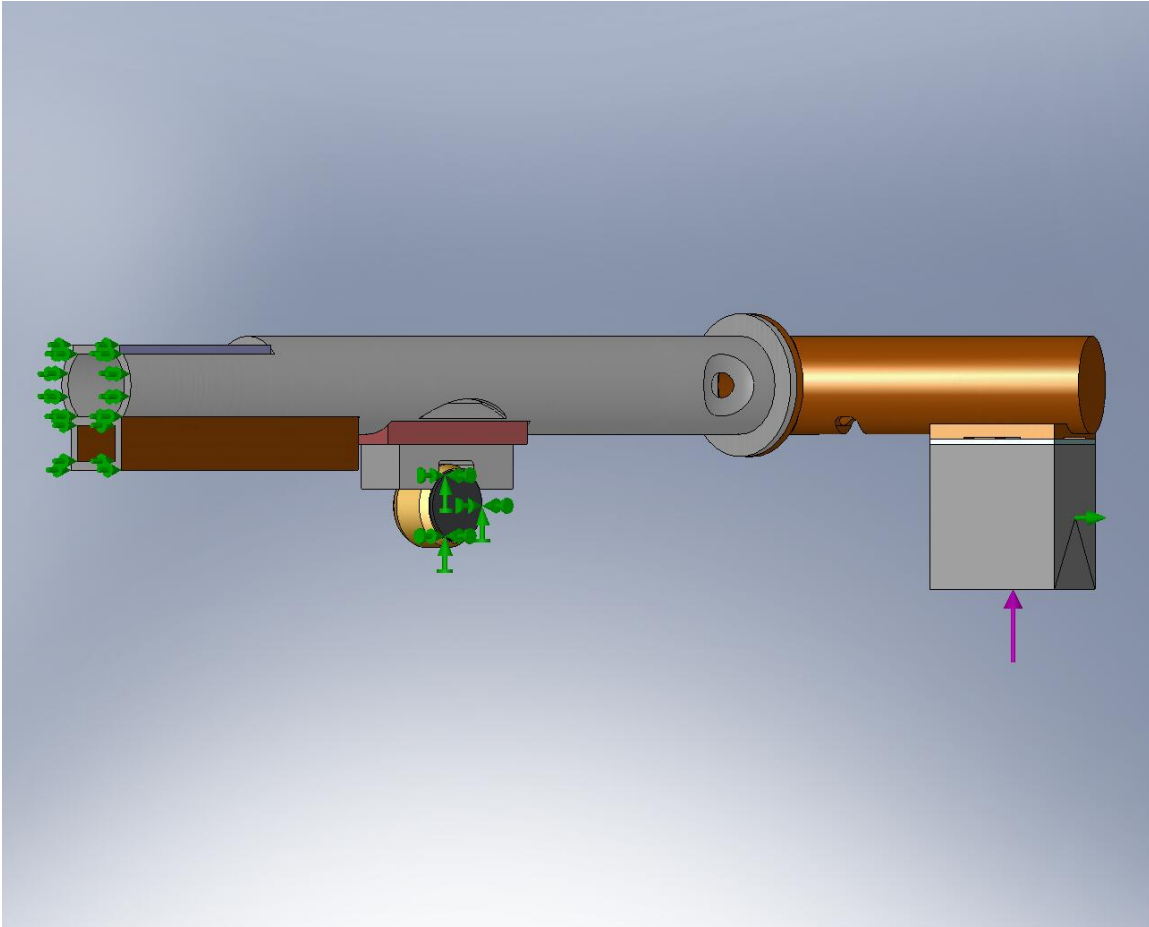


Figure 42. Green arrows show the constraints, while the purple arrow shows the applied force. Here, we examine the vertical stiffness of the High Crossbeam design.

*Study #2: horizontal stiffness*

The force and constraints for Study #2 are shown in Figure 43. The horizontal force is 1,000 N.

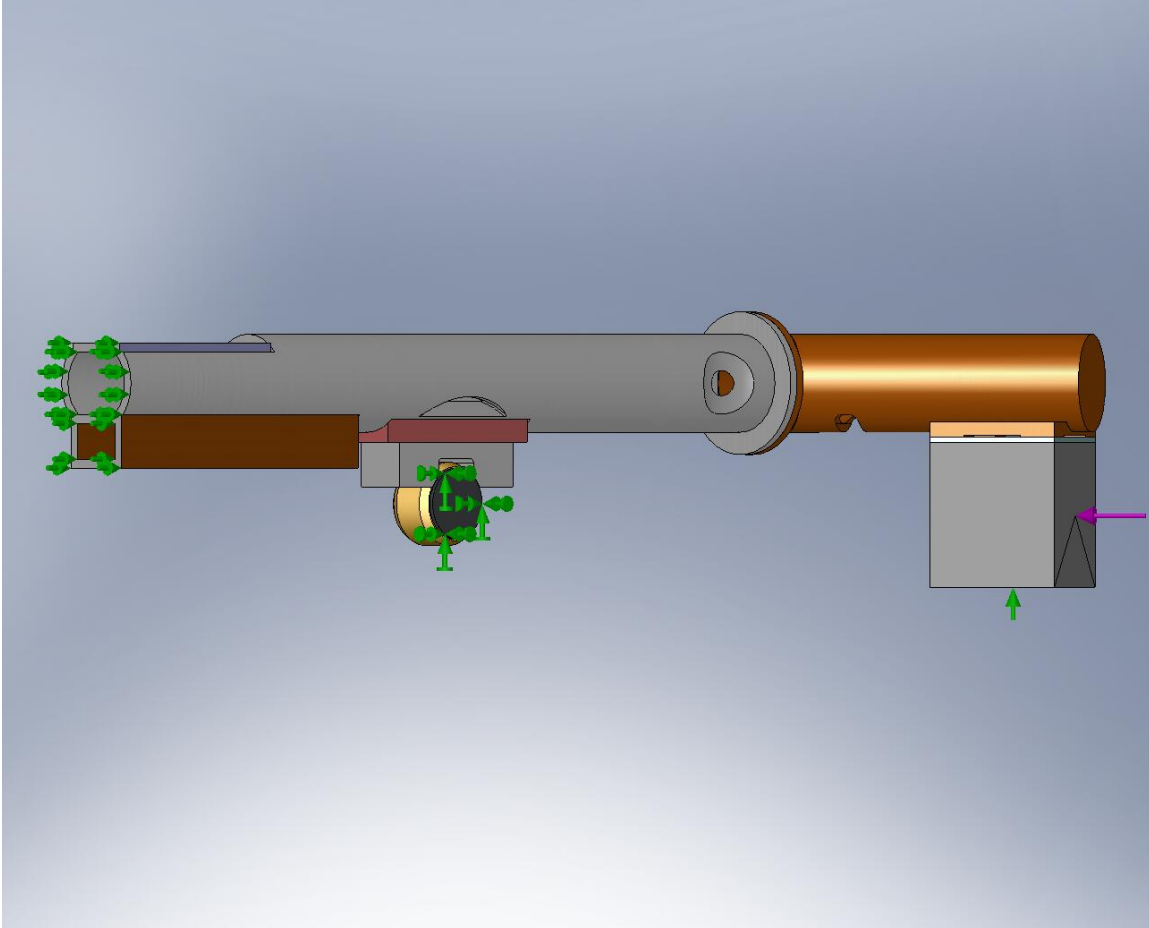


Figure 43. Here, we examine the horizontal stiffness of the High Crossbeam concept.

### FEA Results

#### *Study #1: vertical stiffness*

For a 1,000 N vertical force, the FEA solver predicts a vertical displacement of 196  $\mu\text{m}$  at the point of actuation. So, we have:

$$\mathbf{K}_{\text{high x-beam,vert-}\delta} = 5.1 \text{ N}/\mu\text{m},$$

where  $\mathbf{K}_{\text{high x-beam,vert-}\delta}$  is the effective stiffness of the High Crossbeam assembly as seen by the Vertical Actuator on HEPI.

In addition to the vertical deflection, we measure a rotation in the sensitive direction of the Horizontal L4-C of 342  $\mu\text{rad}$ . This corresponds to a parasitic rotational stiffness of:

$$\mathbf{K}_{\text{high x-beam,vert-}\theta} = 2.9 \text{ N}/\mu\text{rad}$$

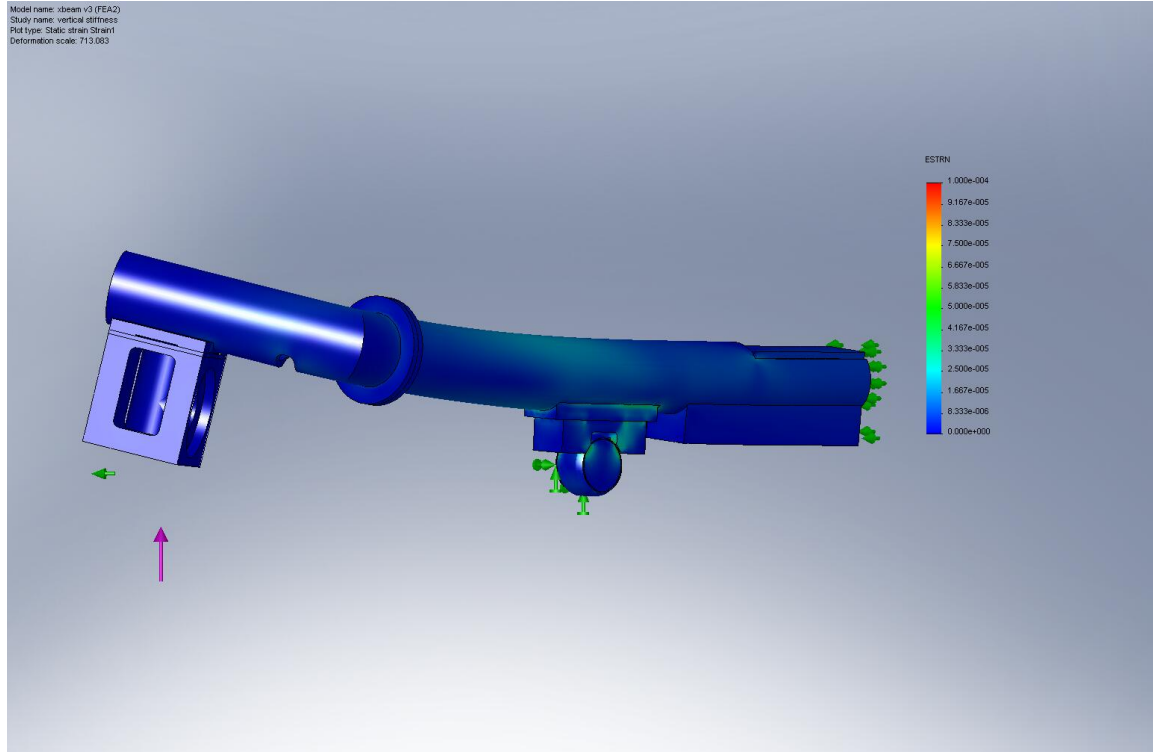


Figure 44. Strain plot for High Crossbeam, with 1,000 N applied from HEPI's Vertical Actuator. Areas in red correspond to strain  $\geq 10^{-4}$ . Deformation is exaggerated, by a factor of 713x.

*Study #2: horizontal stiffness*

For a 1,000 N horizontal force, the FEA solver predicts a horizontal displacement of 107  $\mu\text{m}$  at the point of actuation. So, we have:

$$\mathbf{K}_{\text{high x-beam,horz-}\delta} = 9.3 \text{ N}/\mu\text{m},$$

where  $\mathbf{K}_{\text{high x-beam,horz-}\delta}$  is the effective stiffness of the High Crossbeam assembly as seen by the Horizontal Actuator on HEPI.

We also measure a rotation in the sensitive direction of the Horizontal L4-C of 58  $\mu\text{rad}$ . This corresponds to a parasitic rotational stiffness of:

$$\mathbf{K}_{\text{high x-beam,horz-}\theta} = 17.2 \text{ N}/\mu\text{rad}$$

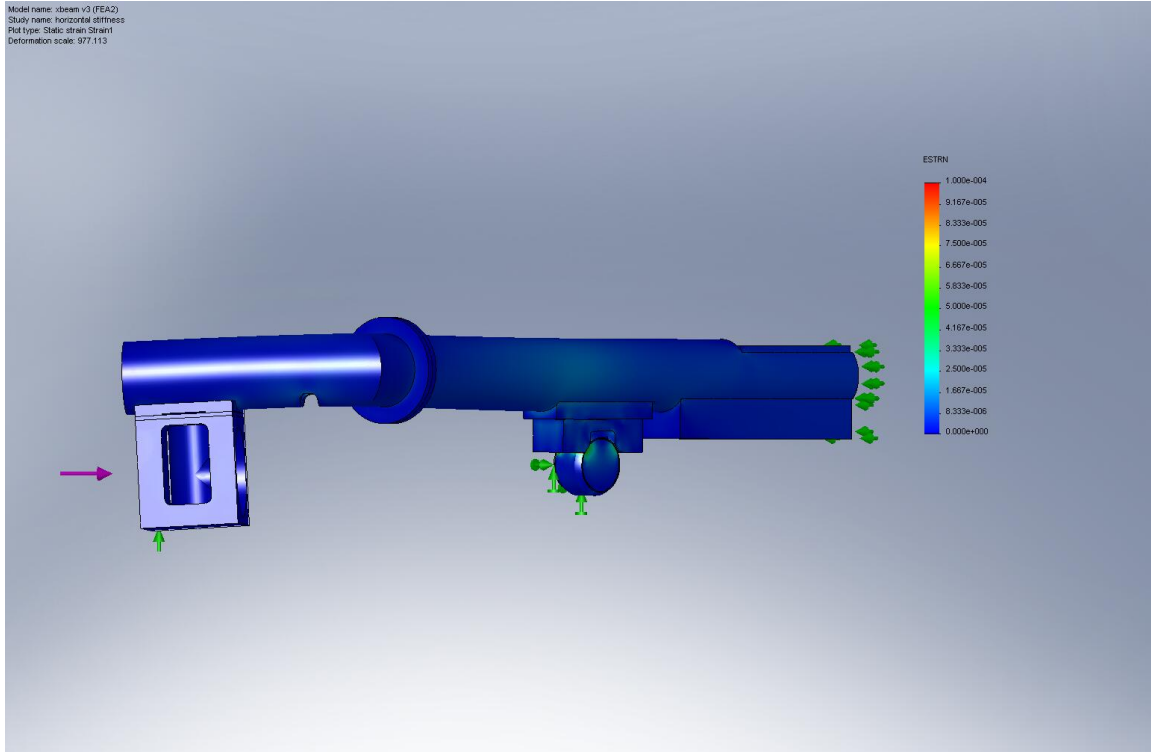


Figure 45. COSMOS strain plot, for horizontal force applied to High Crossbeam assembly. Red areas have strain  $\geq 10^{-4}$ . Deformation is exaggerated, by a factor of 977x.

### Static Analysis – Summary

Table 1 lists all the stiffnesses described above.  $K_{\text{vert-}\delta}$  is the assembly's stiffness as seen by the HEPI Vertical Actuator. E.g., to produce a vertical translation at the HEPI Boot of  $1 \mu\text{m}$ , the Vertical Actuator would need to exert 5.1 N force for the High Crossbeam concept (given the other boundary conditions described above). Similarly,  $K_{\text{vert-}\theta}$  is the assembly's parasitic stiffness from a vertical force to a rotation in the Horizontal L4-C's sensitive direction (tilt/horizontal coupling degree-of-freedom).

	$K_{\text{vert-}\delta}$ (N/ $\mu\text{m}$ )	$K_{\text{horz-}\delta}$ (N/ $\mu\text{m}$ )	$K_{\text{vert-}\theta}$ (N/ $\mu\text{rad}$ )	$K_{\text{horz-}\theta}$ (N/ $\mu\text{rad}$ )
<b>Existing Design</b>	2.5	2.6	1.4	9.6
<b>Low Crossbeam</b>	4.5	10.0	2.4	37.0
<b>High Crossbeam</b>	5.1	9.3	2.9	17.2

Table 1. Stiffness values calculated for the existing Crossbeam design and the two new concepts. Green shaded boxes indicate the largest value for a given measure of stiffness.

Clearly, both the Low and High Crossbeam concepts are significantly stiffer than the existing Crossbeam design. This is especially true when considering the tilt/horizontal coupling stiffnesses (last two columns). It is somewhat surprising that the High Crossbeam concept is actually stiffer than the Low Crossbeam concept, as seen by the HEPI Vertical Actuator. It appears this is caused by the vertical offset from the Horizontal Actuator constraint to the axis of the Connector Tube – when the HEPI Boot translates up, it is prevented from translating along the Actuator axis at the point of actuation. So, the Boot rotates about the point of actuation, which forces the Connector

Tube to push the Crossbeam out further than it would for the same amount of rotation in the Low Crossbeam design. This leverage adds resistance to translation/rotation of the Boot, resulting in a higher effective stiffness relative to the Low Crossbeam design.

The most significant difference between the static performance of the Low and High Crossbeams is in their parasitic stiffness from horizontal force to Horizontal L4-C tilt. The Low Crossbeam is more than twice as stiff in this degree-of-freedom. This should translate to a significantly lower tilt/horizontal coupling zero frequency for the Low Crossbeam design (by approximately  $\sqrt{2}$ ).

### **Modal Analysis – Model #1: Existing Crossbeam Assembly**

We next attempt to predict the low-frequency resonant modes of the three competing designs, starting with the existing Crossbeam assembly. For this exercise, we must build a more complete model of the Support Structure, including two Crossbeams, four sets of Clamps, two Support Tubes, and a representative payload. For the payload, we use a simple rectangular solid, with roughly the same length and width as the HAM ISI Stage 0 Base (LIGO P/N D071001), but thicker. We set the thickness so the resulting mass (using the density of Aluminum 6061-T6) is 991 kg, corresponding to the approximate mass of the full Stage 0 Assembly (D071410). Note that we assume the lowest natural frequencies for the Support Structures will all be significantly higher than the rigid-body modes of the ISI Stage 1 on Stage 0, allowing us to neglect the Stage 1 mass from these frequency analyses.

#### Model Geometry

The FEA model used for the modal analysis of the existing Crossbeam design is shown in Figure 46. The basic geometry of the HEPI Shim Stack, Crossbeam, Spherical Bearing, and Support Tube Clamp are unchanged from the model described above for the static analysis. However, the method of constraining the HEPI Boots is slightly different, in that the constraints are applied over a small square face, instead of at a point (Figure 47). The basic idea is the same as used above, where the Actuators are treated as infinitely stiff in the direction of actuation. However, by constraining over an area, we add some moment stiffness, which may or may not be close to the real moment stiffness of the Actuators (from the Tripod and blade flexures). We have not attempted to quantify the moment stiffness due to this constraint, nor have we tried to find any measured values for the real Actuator stiffness.

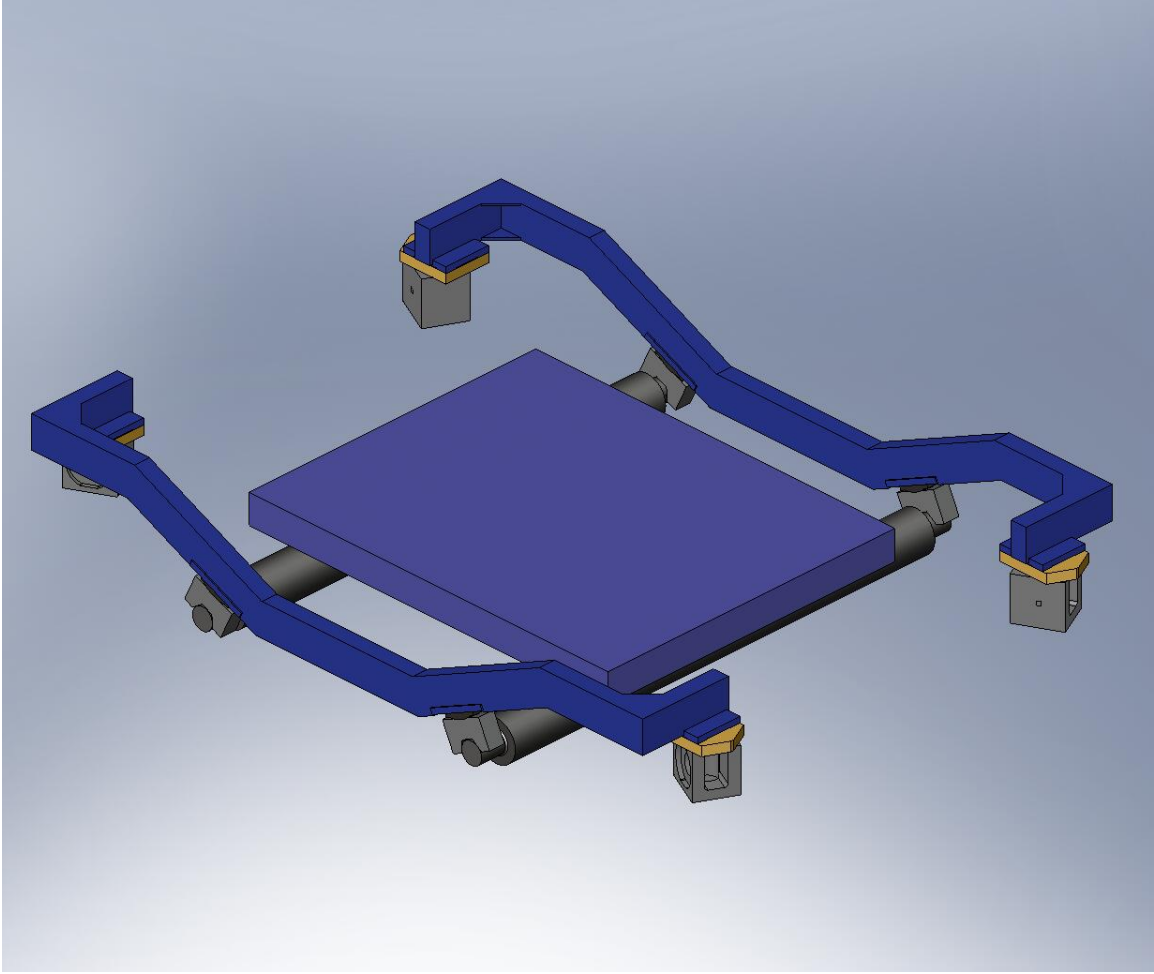


Figure 46. Full Support Structure assembly, for the existing Crossbeam design.



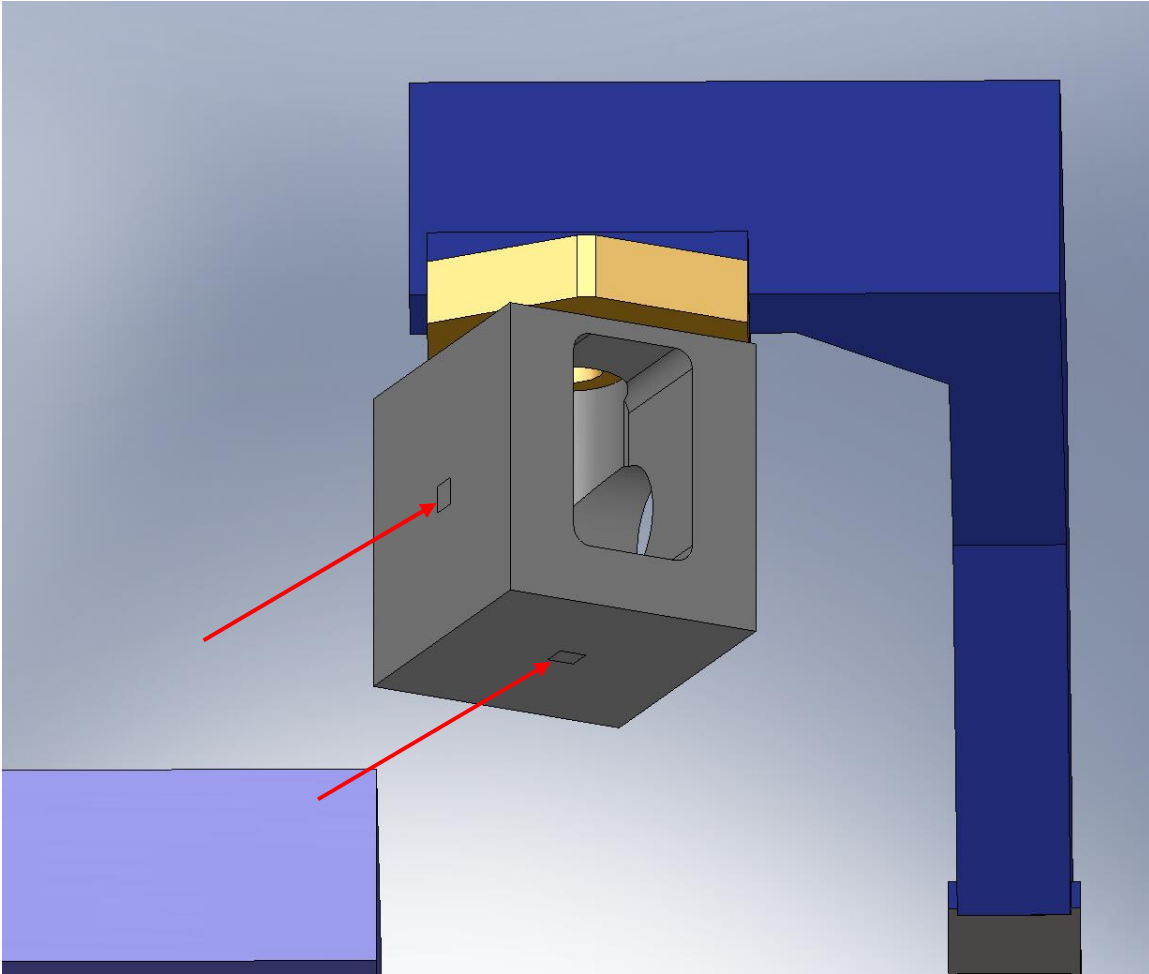


Figure 47. The square “Split Line” features shown here were added to the HEPI Boot model, to provide areas for the Actuator constraints.

Another significant feature of the finite element model is the full geometry of the Support Tubes. As shown in Figure 48, we model the Stage 0 payload as being bonded to all of the mounting bosses on the top of the Tubes. To simplify the mesh, we remove all mounting holes and gasket features.

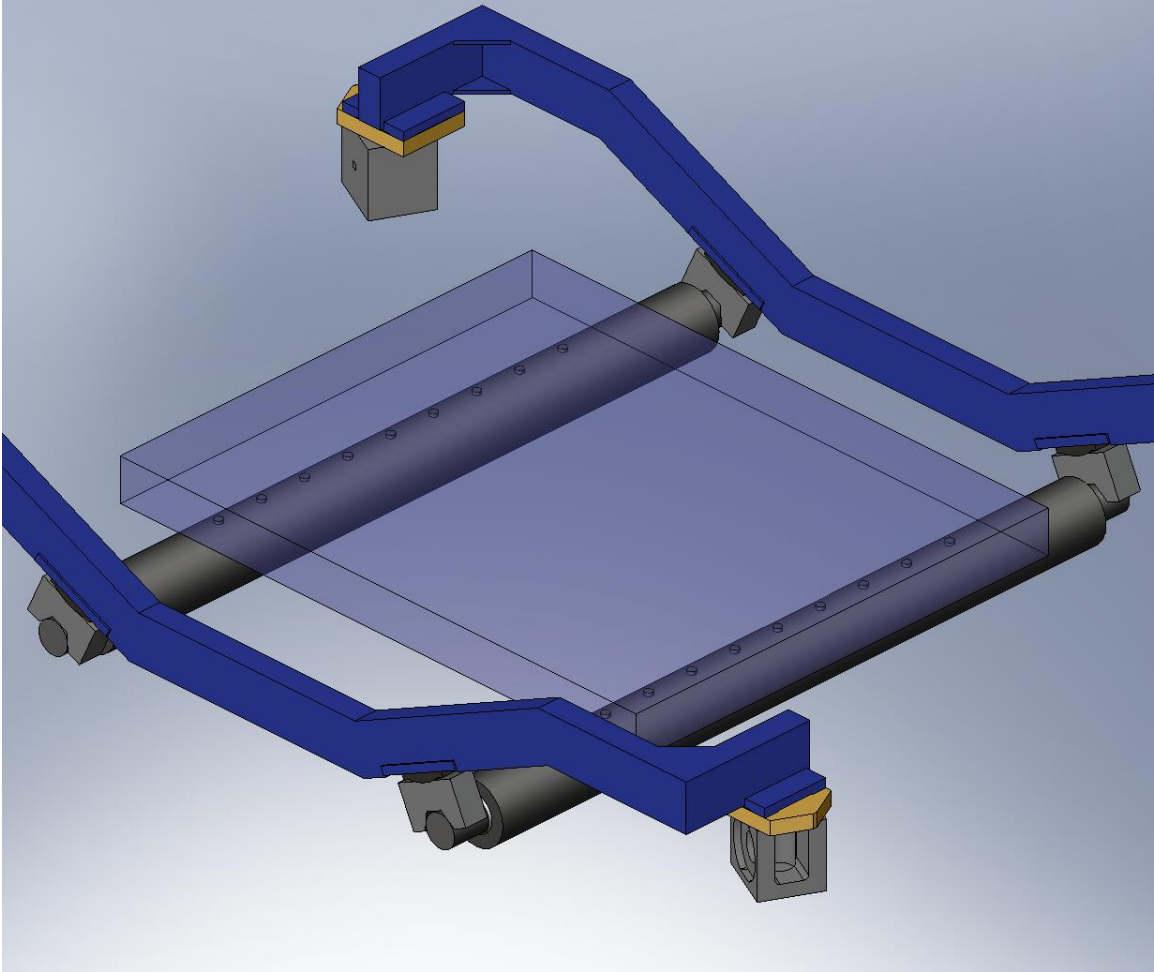


Figure 48. The (transparent) Stage 0 dummy payload contacts nine circular bosses on the top of each Support Tube. Note that in reality, each Support Tube has 11 bosses, but the outer two do not touch the Stage 0 Base. Also, the middle three bosses are inaccessible on one side of the Base, so they are not bolted to the ISI. We do not expect a significant error in the predicted system performance due to this deviation, however.

#### Mesh Details

We define denser mesh regions around the Support Tube Clamps, and a less dense mesh within the Stage 0 dummy payload. The meshed model is shown in Figure 49.

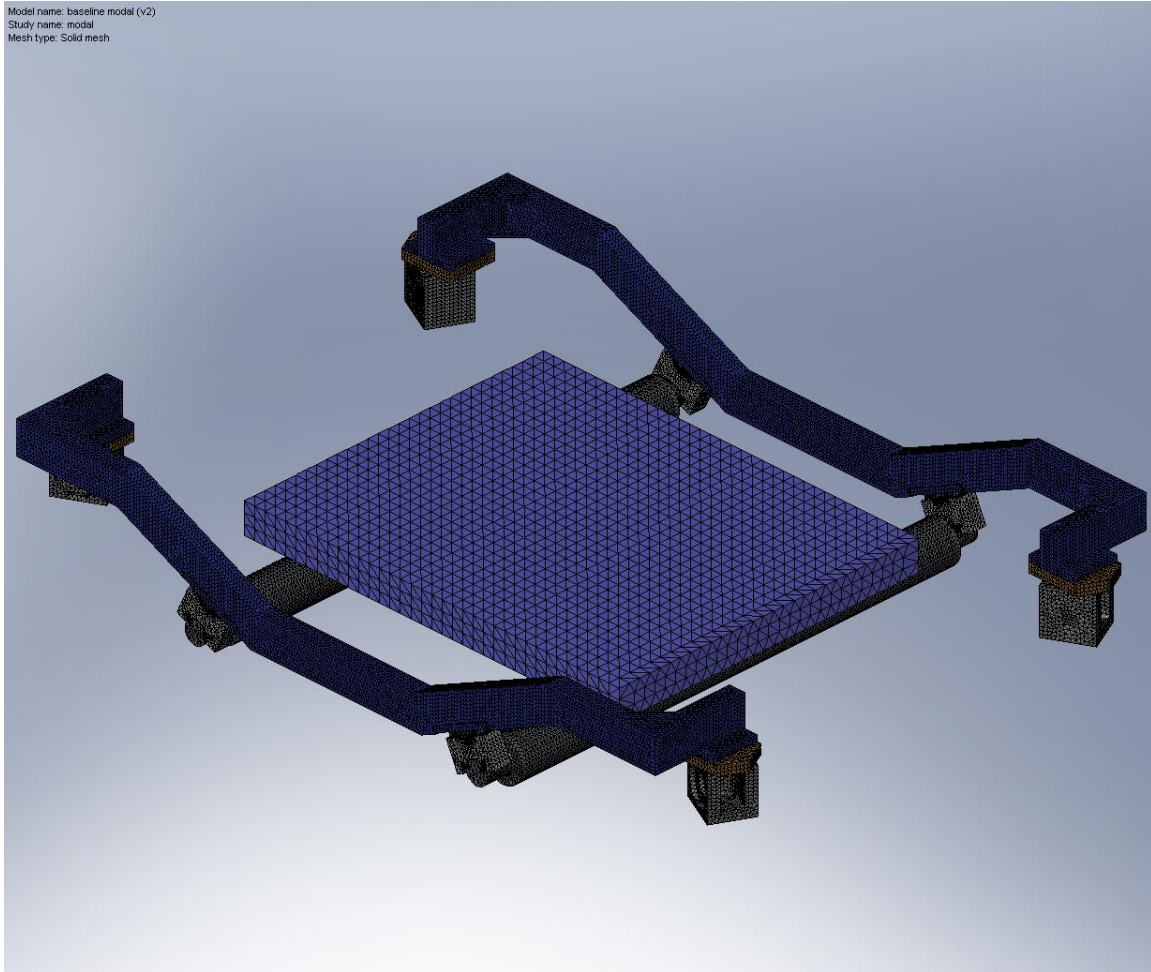


Figure 49. Meshed model for modal analysis of existing Crossbeam design.

Details of the mesh are as follows:

- mesh controls – 1) 8 flats on Support Tubes' ends: 0.075"; 2) 4 spherical surfaces on Spherical Bearings: 0.150"; 3) all bodies except Stage 0 dummy mass: 0.60"
- element size=2.0"
- total nodes=648,734
- total elements=377,988
- % elements with aspect ratio < 3=95.5
- % elements with aspect ratio > 10=0.02
- % distorted elements=0

### Materials

The components of this FEA model are assigned the following material properties:

- 4x *HEPI Boot*: Plain Carbon Steel –  $E_x=210$  GPa,  $\nu=.28$ ,  $G_{xy}=79$  GPa
- 4x *HEPI Shim Stack*: Plain Carbon Steel – ...
- 2x *Crossbeam*: Plain Carbon Steel – ...
- 4x *Clamp Spherical Bearing*: Plain Carbon Steel – ...

- *4x Clamp Mounting Base*: Aluminum AA356.0-F –  $E_x=72$  GPa,  $\nu=.33$ ,  $G_{xy}=27$  GPa
- *2x Support Tube*: AISI 304 –  $E_x=190$  GPa,  $\nu=.29$ ,  $G_{xy}=75$  GPa
- *1x Stage 0 Dummy Mass*: Aluminum 6061-T6 –  $E_x=69$  GPa,  $\nu=.33$ ,  $G_{xy}=26$  GPa

### Boundary Conditions

As mentioned above, we constrain this model over small square faces on the HEPI Boots, where the (4) Vertical and (4) Horizontal HEPI Actuators would attach. The nodes on these surfaces cannot translate along their respective actuation directions, but they are free to slide in-plane. This implies some finite moment stiffness from the Actuators, which we do not attempt to quantify in this study.

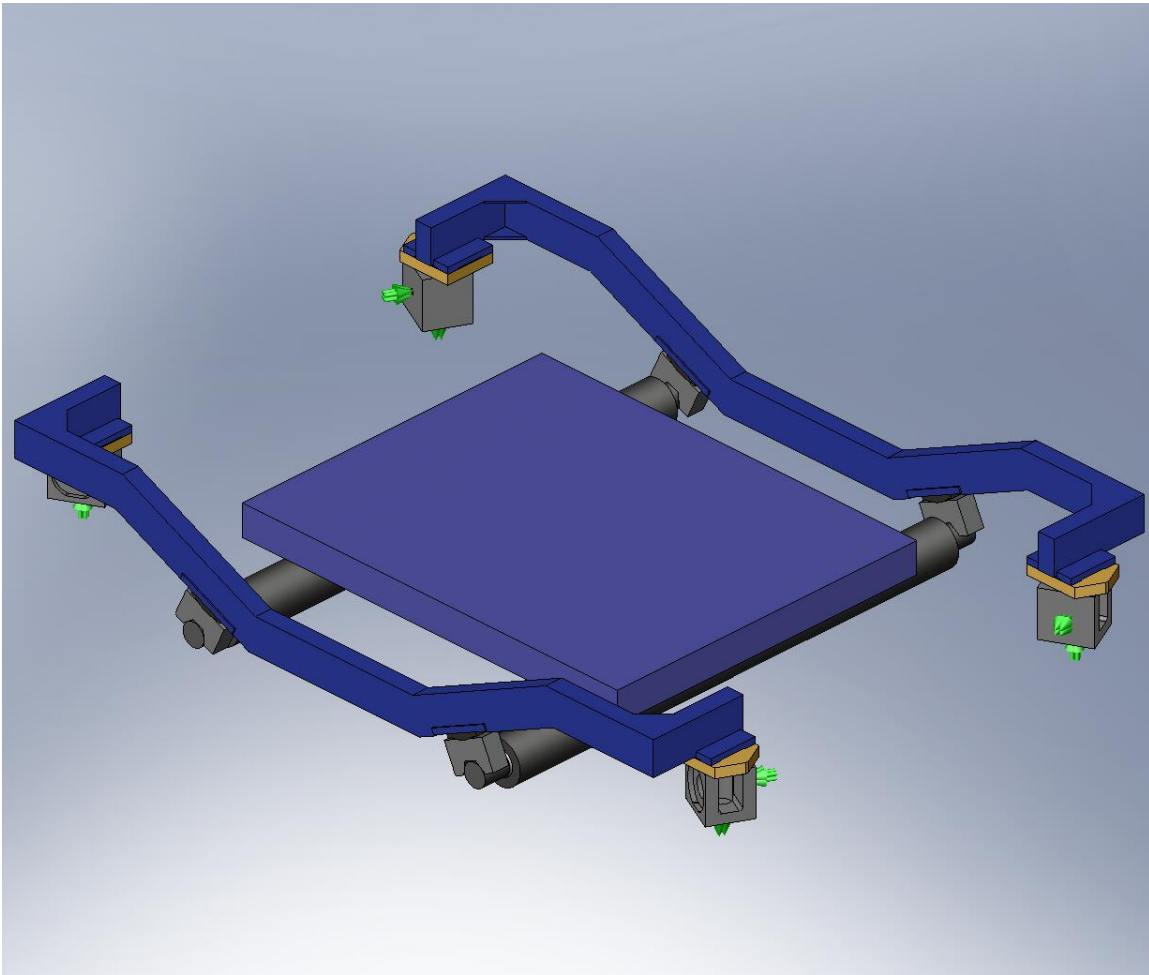


Figure 50. Constraints applied to existing Crossbeam modal study. The green arrows indicate nodes that cannot translate in the indicated direction.

### FEA Results

COSMOS calculates the first four modes for this structure, using the “FFEPlus” solver. The frequencies are:

$$f_1 = 6.1 \text{ Hz}$$

$$f_2 = 14.0 \text{ Hz}$$

$$f_3 = 15.0 \text{ Hz}$$

$$f_4 = 22.5 \text{ Hz}$$

In the discussion that follows, we refer to a coordinate system in which:  
 $X$  is parallel to the Crossbeam's long axis,  
 $Y$  is parallel to the Support Tube axis, and  
 $Z$  is vertical.

The  $f_1 = 6.1 \text{ Hz}$  mode is an  $X$ -translation mode. A snapshot of the modeshape is shown in Figure 51:

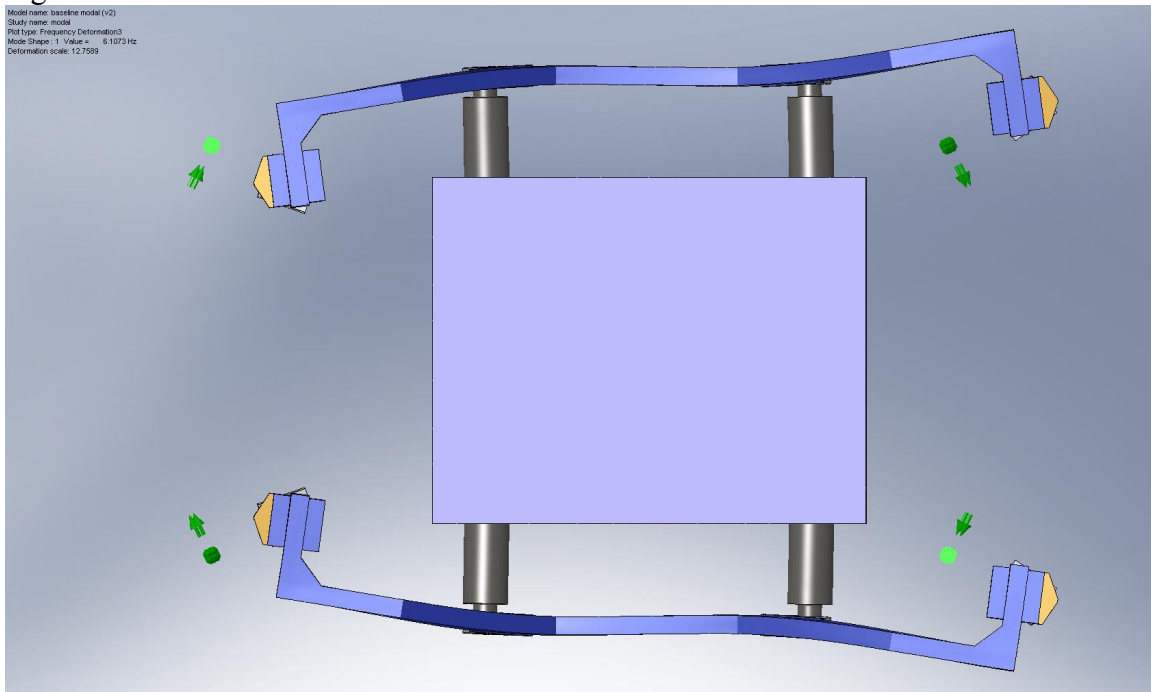


Figure 51. The lowest mode of the existing Crossbeam structure is primarily a translation in  $X$ .

The  $f_2 = 14.0$  Hz mode is a Y-translation mode, as shown in Figure 52:

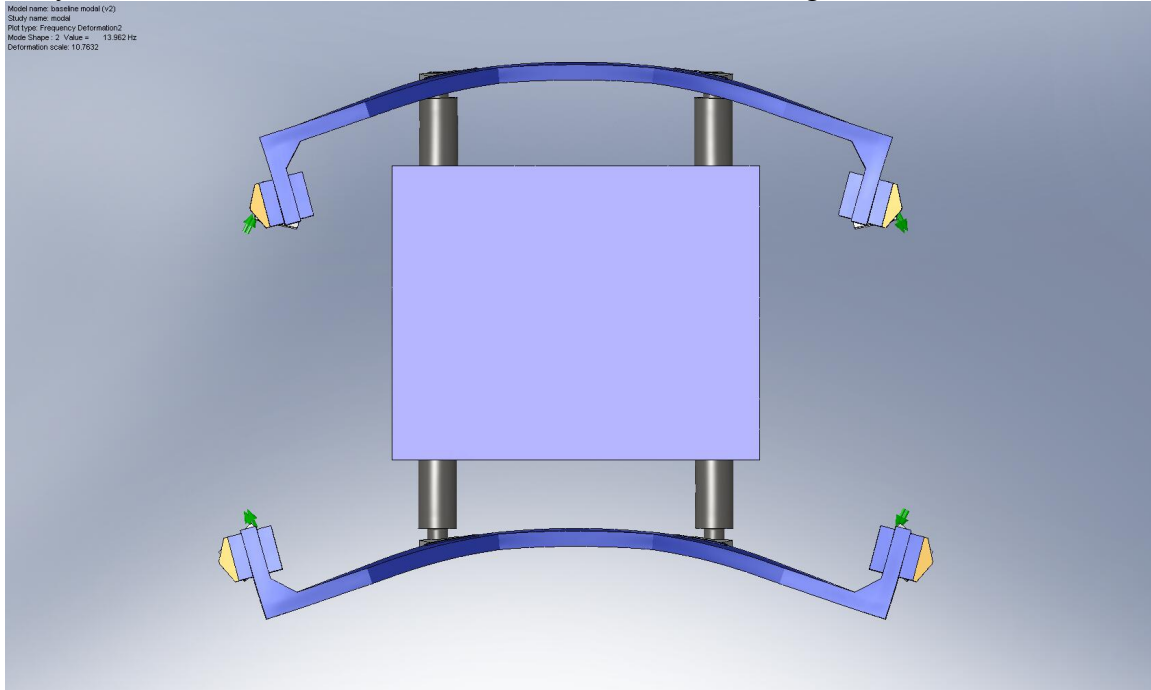


Figure 52. The  $f_2$  mode of the existing Crossbeam structure is primarily a translation in Y.

The  $f_3 = 15.0$  Hz mode is a Z-translation mode, as shown in Figure 53:

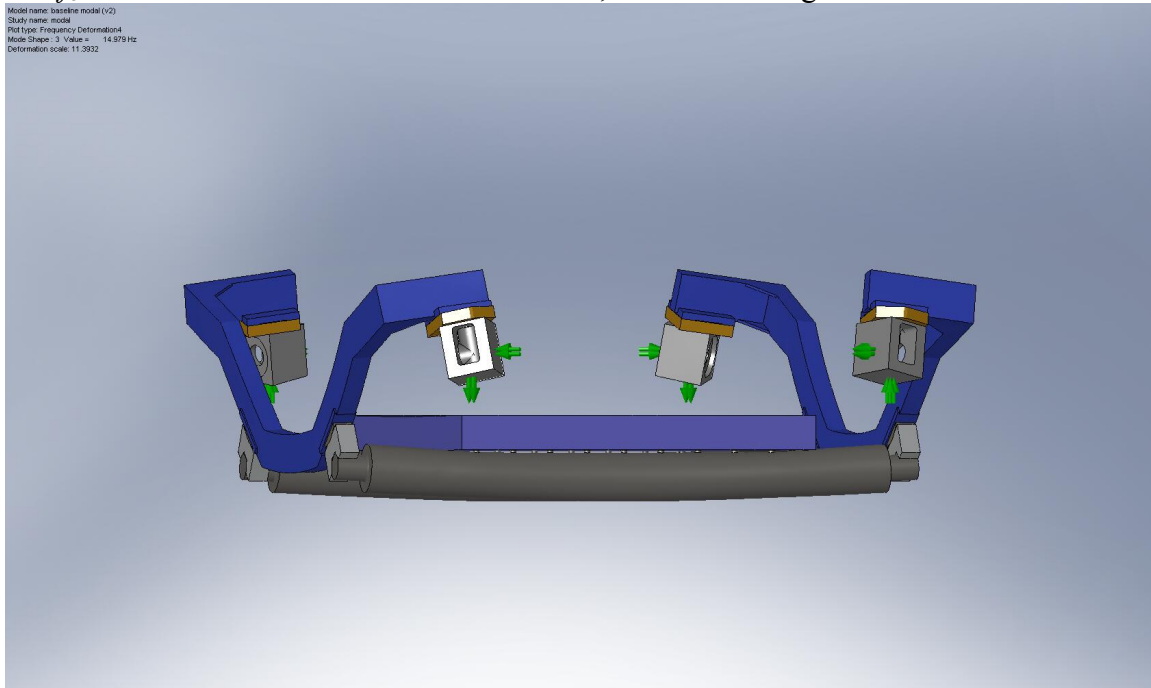


Figure 53. The  $f_3$  mode of the existing Crossbeam structure is primarily a translation in Z.

Finally, the  $f_4 = 22.5$  Hz mode is an Rz-rotation mode. A snapshot of this modeshape is shown in Figure 54:

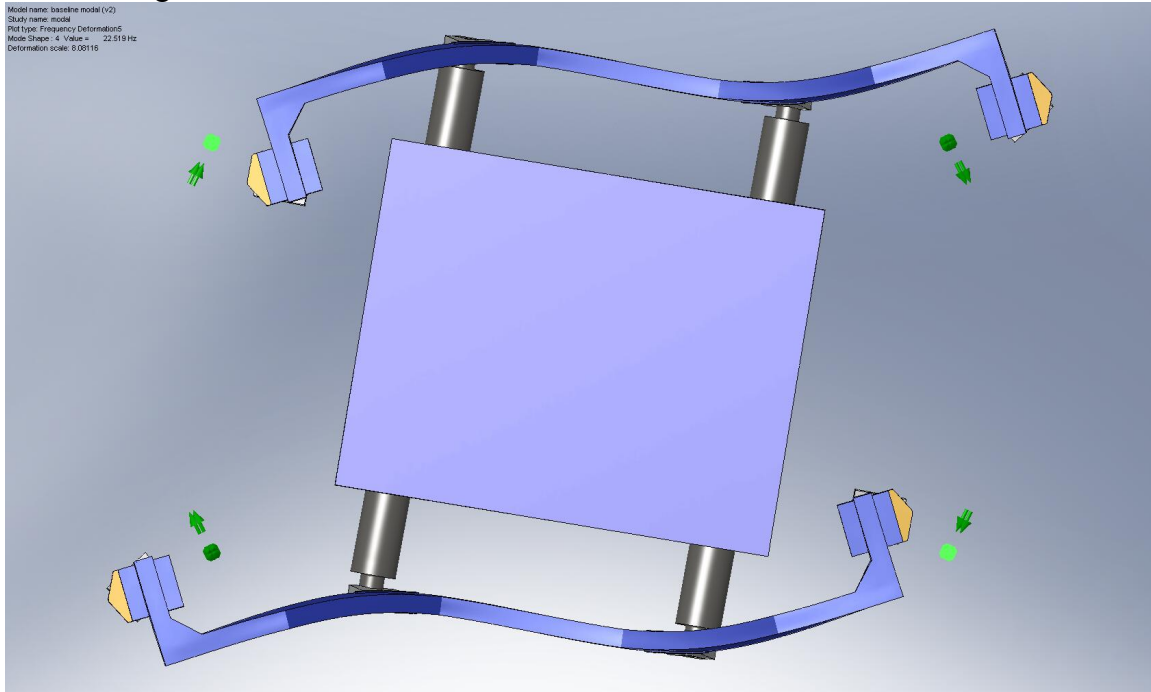


Figure 54. The  $f_4$  mode of the existing Crossbeam structure is primarily a rotation about the vertical (Z) axis.

### **Modal Analysis – Model #2: Low Crossbeam Concept Assembly**

The study setup is the same as described above for the existing Crossbeam design, but this time we use the Low Crossbeam part geometries. Considerations for the HEPI Boot, Support Tubes, and Stage 0 dummy mass are identical to what was used for that study. So, we skip the “Model Geometry” section and proceed directly to a description of the meshed model:

#### Mesh Details

When defining the mesh, we use the same basic principle described above for the existing design: higher density near the Clamps, lower density in the dummy payload.



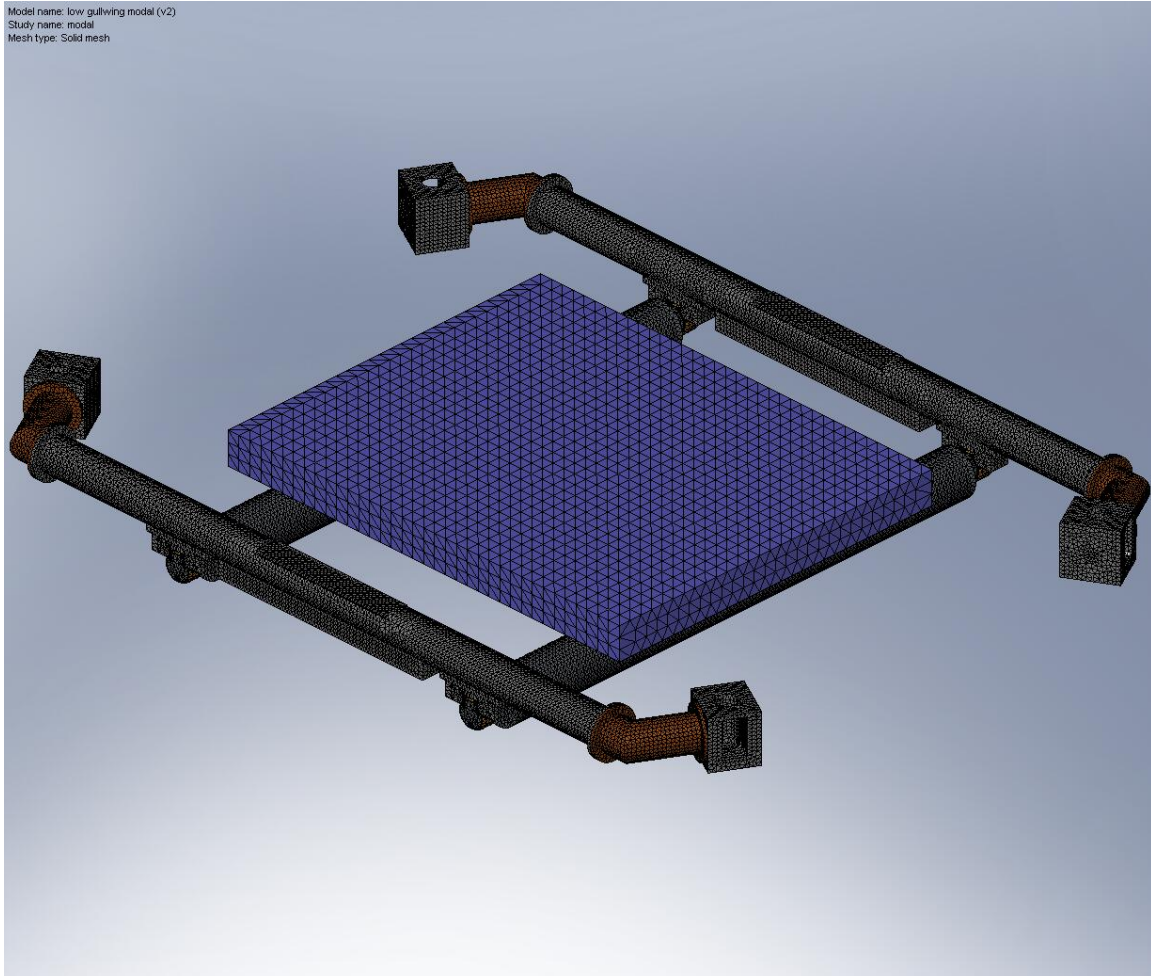


Figure 55. Meshed model for modal analysis of Low Crossbeam concept.

Details of the mesh are as follows:

- mesh controls – 1) 16 spherical pads in Spherical Clamps: 0.075"; 2) 8 inner bearing surfaces on Spherical Sleeve: 0.15"; 3) all bodies except Stage 0 dummy mass: 0.60"
- element size=2.0"
- total nodes=577,428
- total elements=326,837
- % elements with aspect ratio < 3=91.1
- % elements with aspect ratio > 10=0.32
- % distorted elements=0

### Materials

The components for this FEA model are assigned the following material properties:

- *4x HEPI Boot*: Plain Carbon Steel –  $E_x=210$  GPa,  $\nu=.28$ ,  $G_{xy}=79$  GPa
- *4x Connector Tube*: Plain Carbon Steel – ...
- *2x Crossbeam*: Plain Carbon Steel – ...
- *4x Spherical Clamp*: AISI 304 –  $E_x=190$  GPa,  $\nu=.29$ ,  $G_{xy}=75$  GPa
- *4x Spherical Sleeve*: Aluminum 6061-T6 –  $E_x=69$  GPa,  $\nu=.33$ ,  $G_{xy}=26$  GPa

- 2x Support Tube: AISI 304 – ...
- 1x Stage 0 Dummy Mass: Aluminum 6061-T6 – ...

### Boundary Conditions

Boundary conditions are identical to those described above for the existing Crossbeam modal analysis.

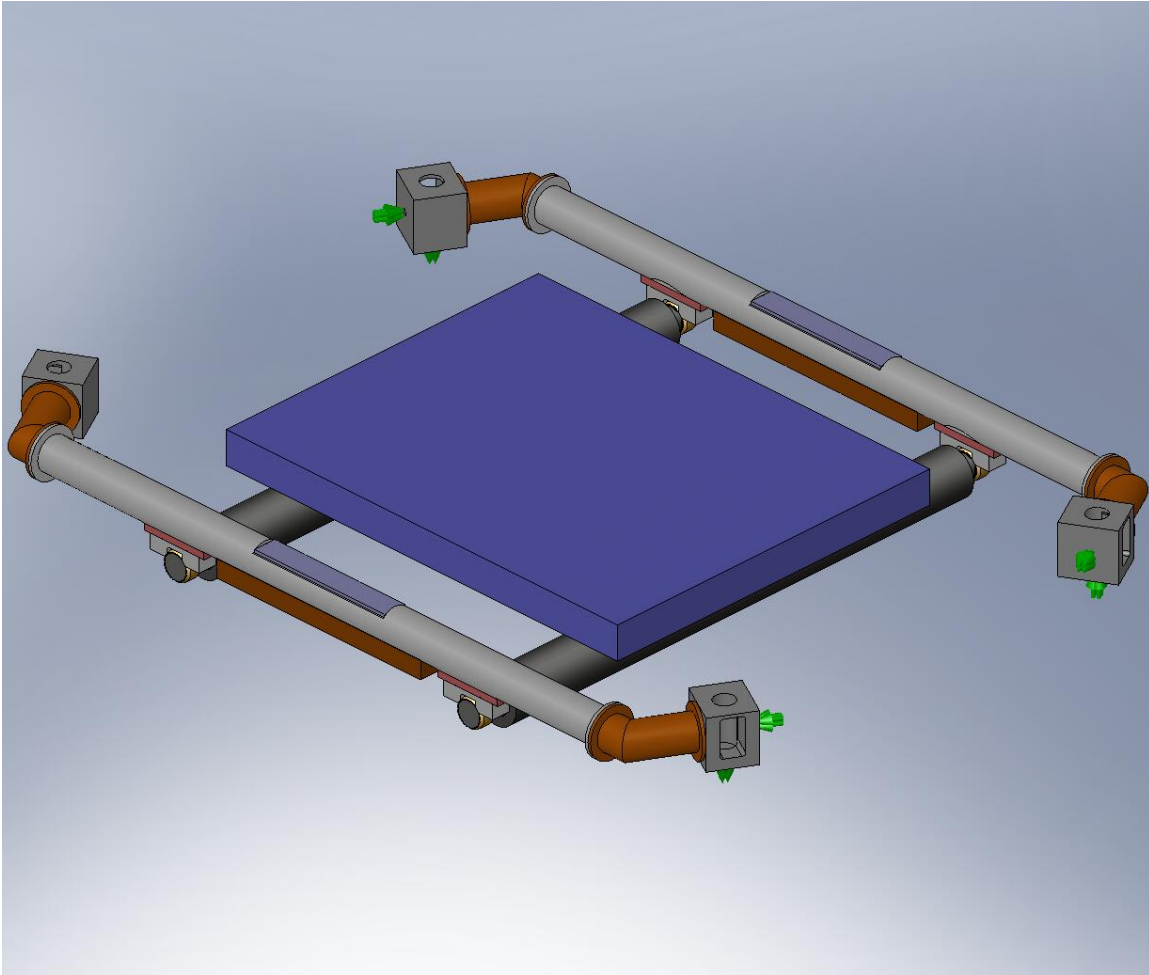


Figure 56. The Actuator attachment “patches” on the HEPI Boots are prevented from translating in the direction of the Actuators’ axes.

### FEA Results

COSMOS calculates the first four modes for this structure, with the following resonant frequencies:

$$f_1 = 11.8 \text{ Hz}$$

$$f_2 = 16.9 \text{ Hz}$$

$$f_3 = 23.7 \text{ Hz}$$

$$f_4 = 28.7 \text{ Hz}$$

The  $f_1 = 11.8$  Hz mode is an X-translation mode. A snapshot of the modeshape is shown in Figure 57:

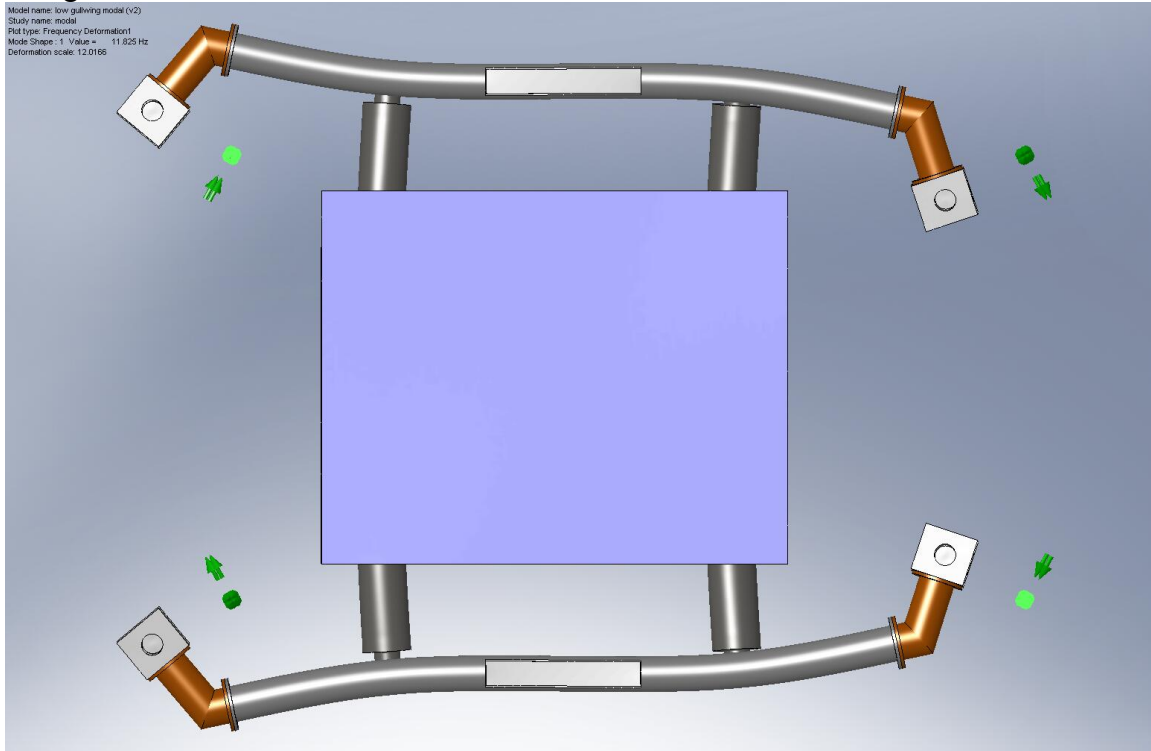


Figure 57. The lowest mode of the existing Crossbeam structure is primarily a translation in X.

The  $f_2 = 16.9$  Hz mode is a Z-translation mode, as shown in Figure 58:

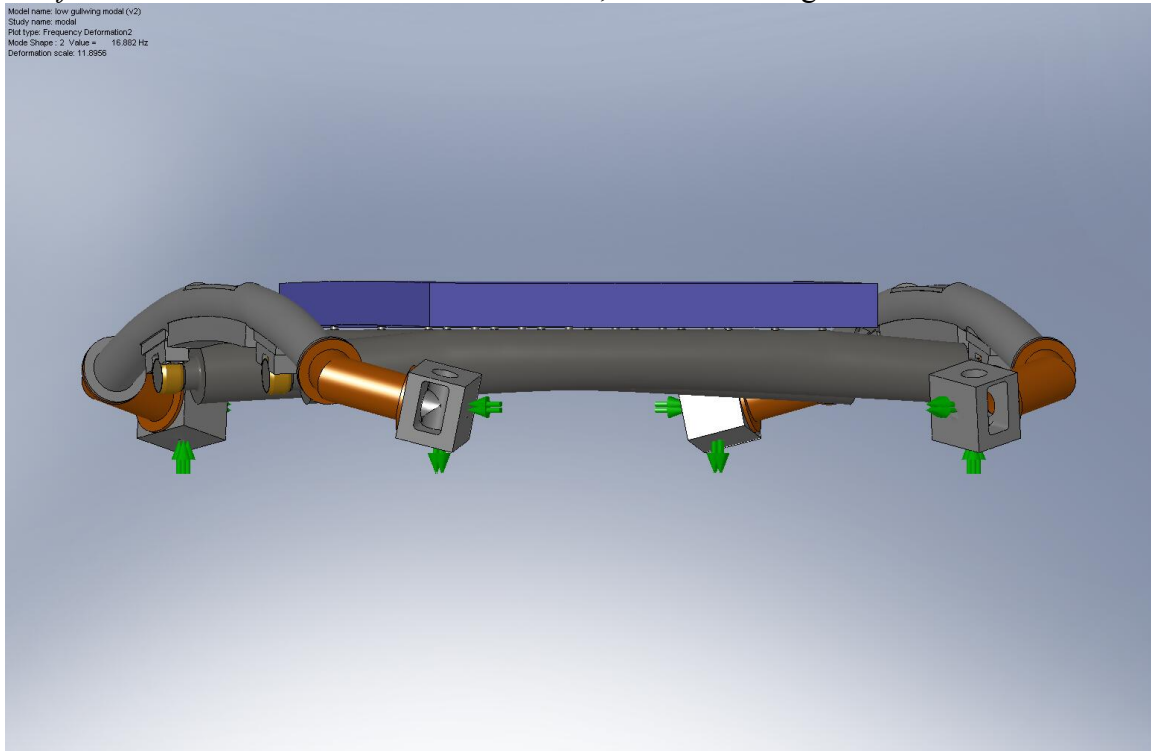


Figure 58. The  $f_2$  mode of the Low Crossbeam structure is primarily a vertical translation.

The  $f_3 = 23.7$  Hz mode is a Y-translation mode, as shown in Figure 59:

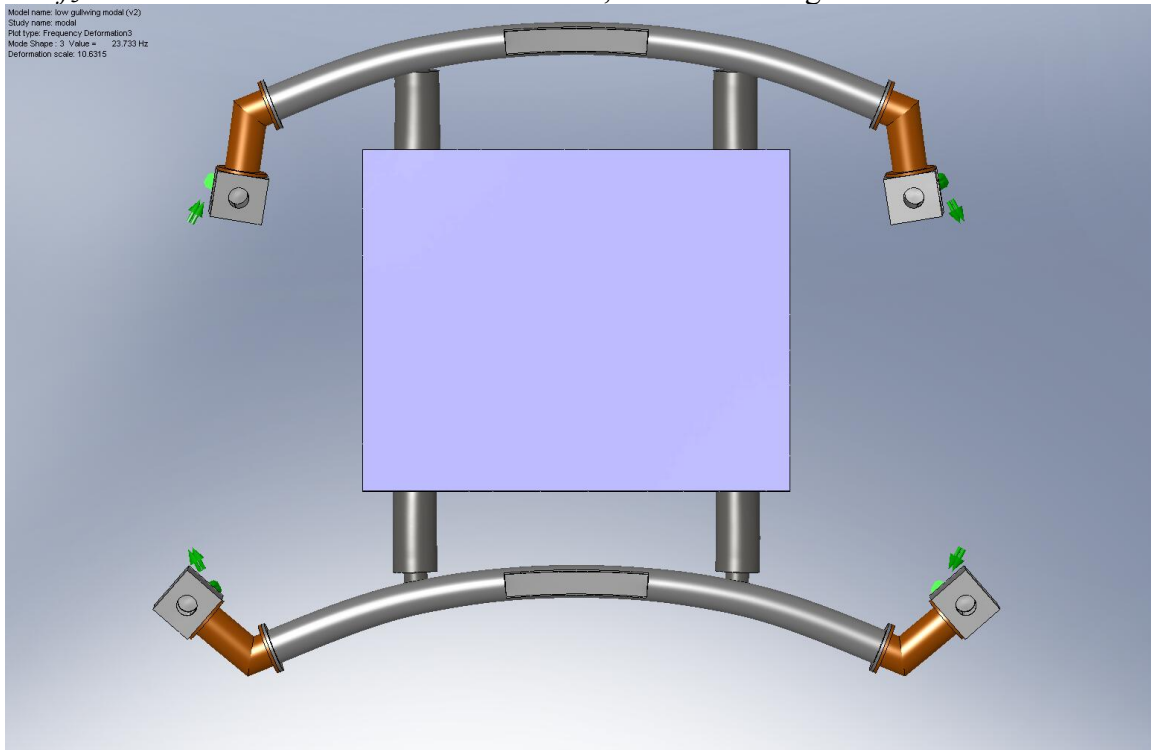


Figure 59. The  $f_3$  mode of the Low Crossbeam structure is primarily a translation in Y.

The  $f_4 = 28.7$  Hz mode is an Rx-rotation mode, as shown in Figure 60:

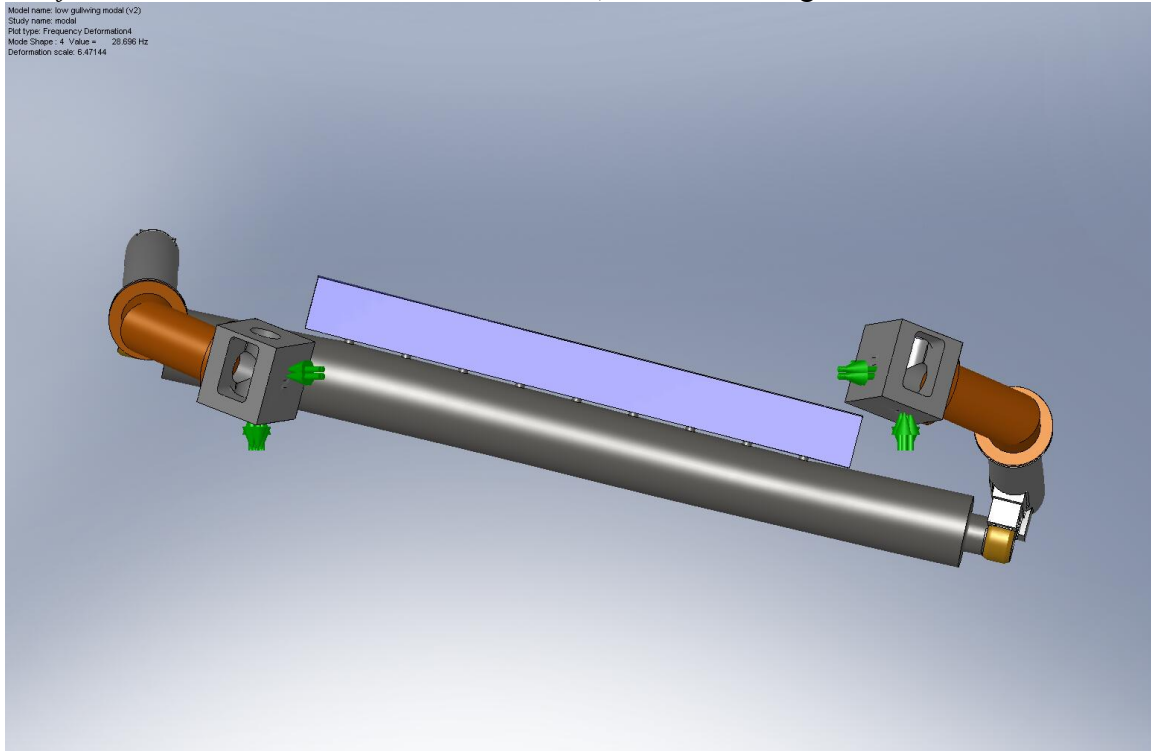


Figure 60. The  $f_4$  mode of the Low Crossbeam structure is primarily a rotation about the X axis.

### Modal Analysis – Model #3: High Crossbeam Concept Assembly

Finally, we examine the frequency behavior of the proposed High Crossbeam concept. Again, the model geometry is almost identical to what is already described above, so we turn directly to the mesh description.

#### Mesh Details

Again, we defined the mesh with higher density around the Clamps and lower density in the Stage 0 dummy mass.

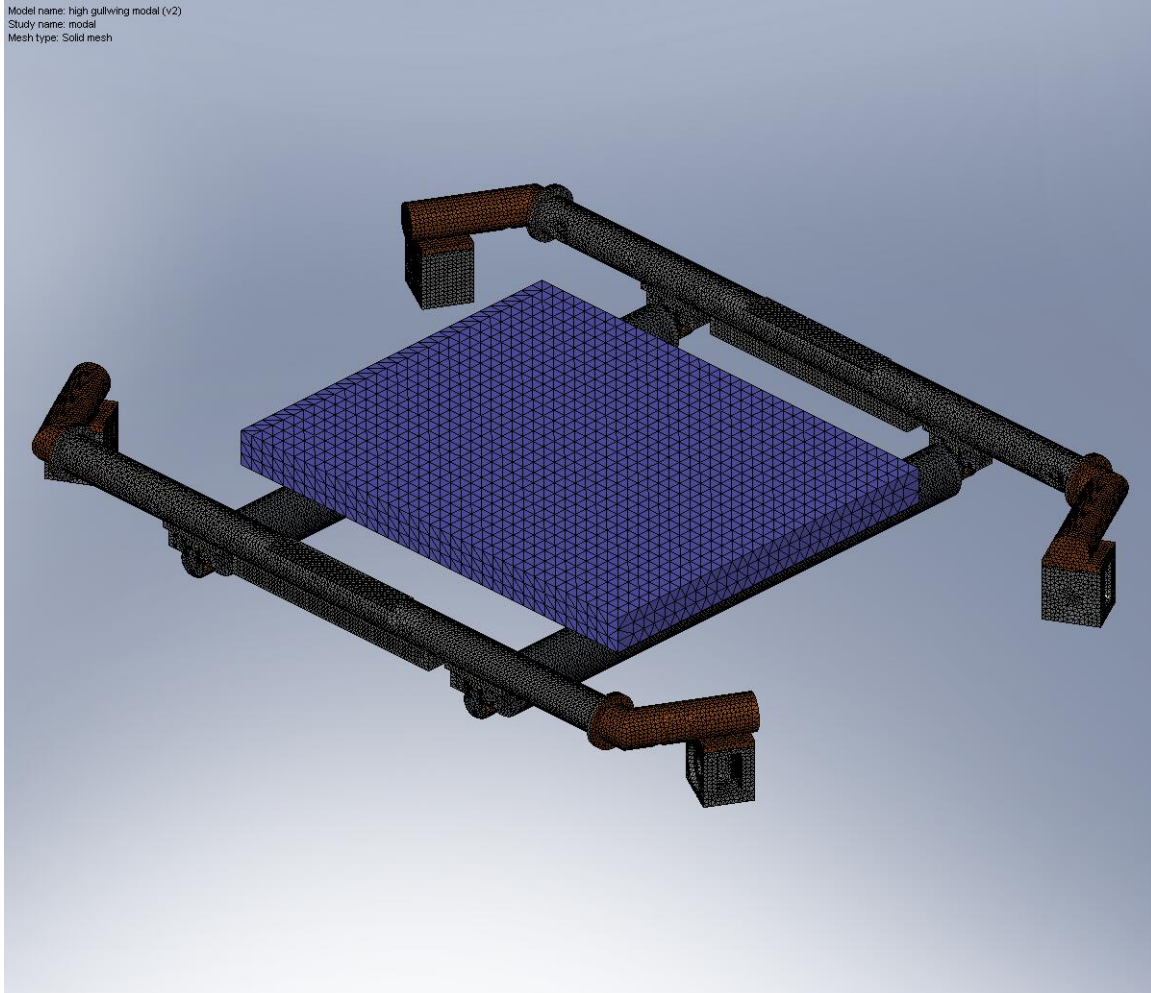


Figure 61. Meshed finite element model of the High Crossbeam assembly.

Details of the mesh are as follows:

- mesh controls – 1) 16 spherical pads in Spherical Clamps: 0.075"; 2) 8 inner bearing surfaces on Spherical Sleeve: 0.15"; 3) all bodies except Stage 0 dummy mass: 0.60"
- element size=2.0"
- total nodes=612,309
- total elements=346,704
- % elements with aspect ratio < 3=91.4
- % elements with aspect ratio > 10=0.30
- % distorted elements=0

### Materials

The components of this FEA model are assigned the following material properties:

- 4x *HEPI Boot*: Plain Carbon Steel –  $E_x=210$  GPa,  $\nu=.28$ ,  $G_{xy}=79$  GPa
- 4x *Connector Tube Adapter*: Plain Carbon Steel – ...
- 4x *Connector Tube*: Plain Carbon Steel – ...
- 2x *Crossbeam*: Plain Carbon Steel – ...
- 4x *Spherical Clamp*: AISI 304 –  $E_x=190$  GPa,  $\nu=.29$ ,  $G_{xy}=75$  GPa



- *4x Spherical Sleeve*: Aluminum 6061-T6 –  $E_x=69$  GPa,  $\nu=.33$ ,  $G_{xy}=26$  GPa
- *2x Support Tube*: AISI 304 – ...
- *1x Stage 0 Dummy Mass*: Aluminum 6061-T6 – ...

### Boundary Conditions

Boundary conditions are identical to those described above, for both the existing Crossbeam and the Low Crossbeam modal analyses.

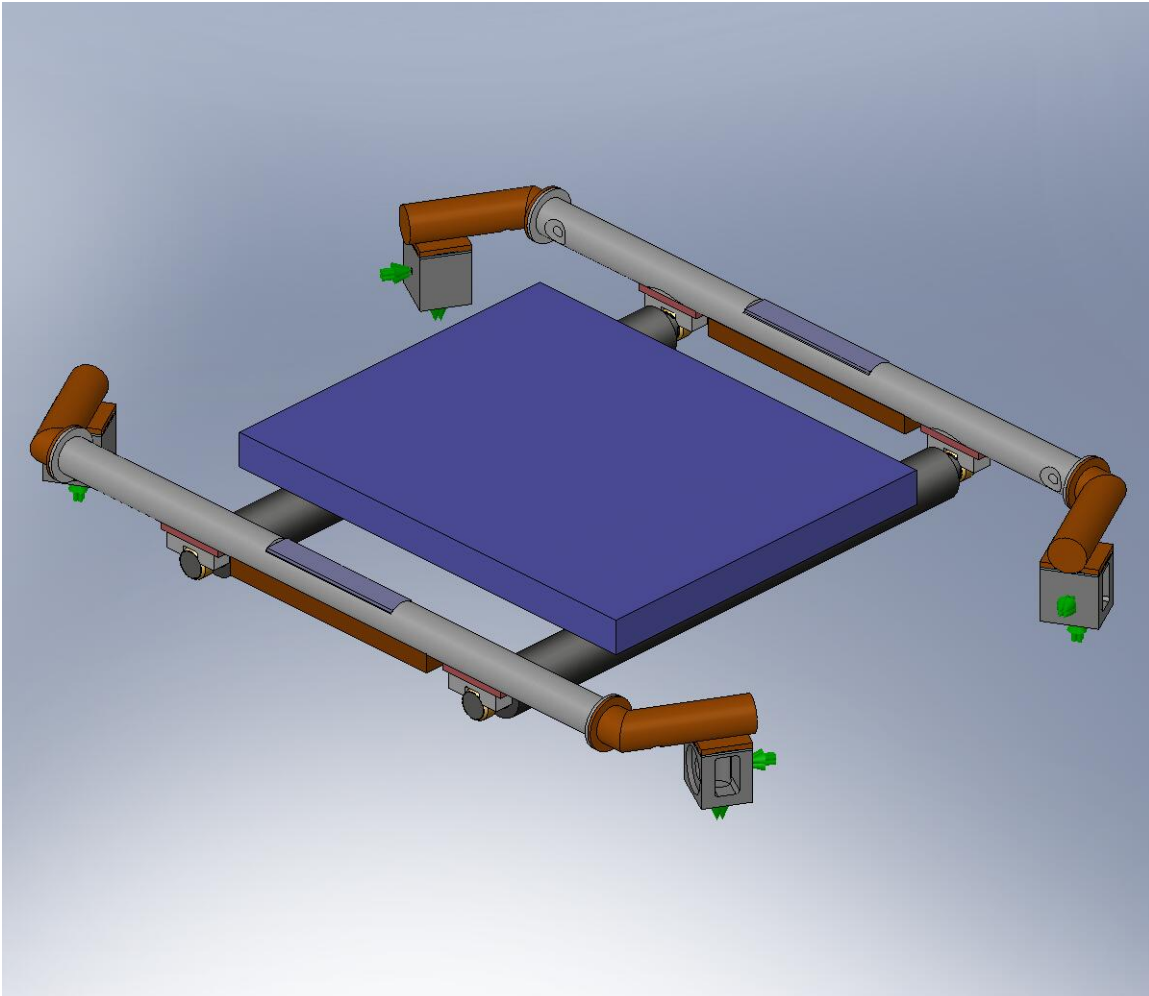


Figure 62. The High Crossbeam modal analysis shares the same constraints as described above for both the existing Crossbeam design and the Low Crossbeam concept.

### FEA Results

COSMOS calculates the first four modes for this structure, with the following resonant frequencies:

$$\begin{aligned}
 f_1 &= 11.2 \text{ Hz} \\
 f_2 &= 17.0 \text{ Hz} \\
 f_3 &= 20.8 \text{ Hz} \\
 f_4 &= 30.9 \text{ Hz}
 \end{aligned}$$



The  $f_1 = 11.2$  Hz mode is an X-translation mode. A snapshot of the modeshape is shown in Figure 63:

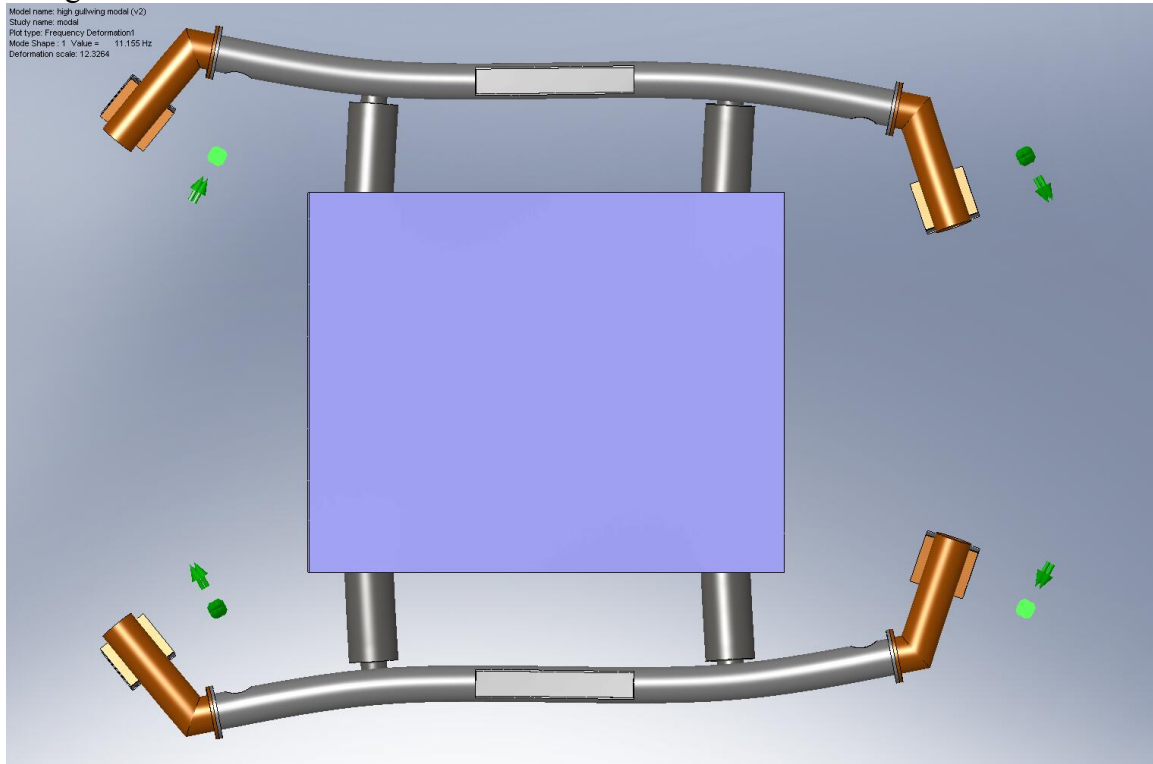


Figure 63. The lowest mode of the High Crossbeam structure is primarily a translation in X.

The  $f_2 = 17.0$  Hz mode is a Z-translation mode, as shown in Figure 64:

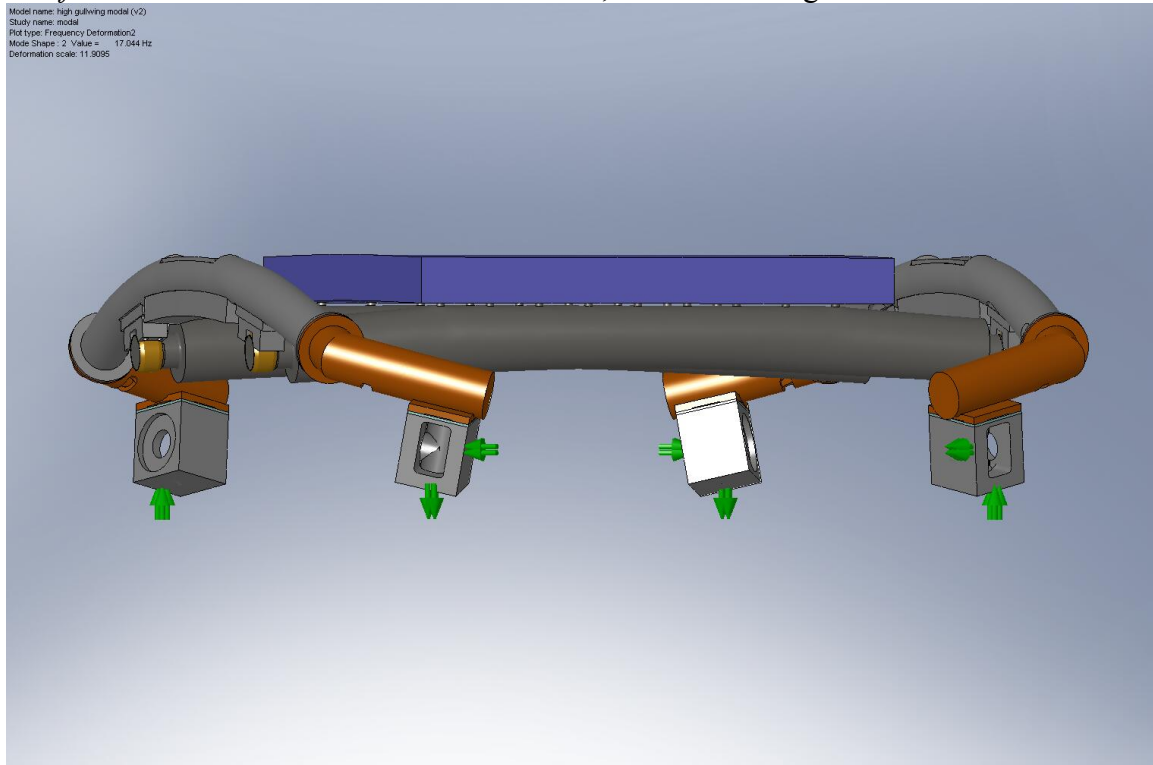


Figure 64. The  $f_2$  mode of the High Crossbeam concept is primarily a vertical translation.

The  $f_3 = 20.8$  Hz mode is a Y-translation mode, as shown in Figure 65:

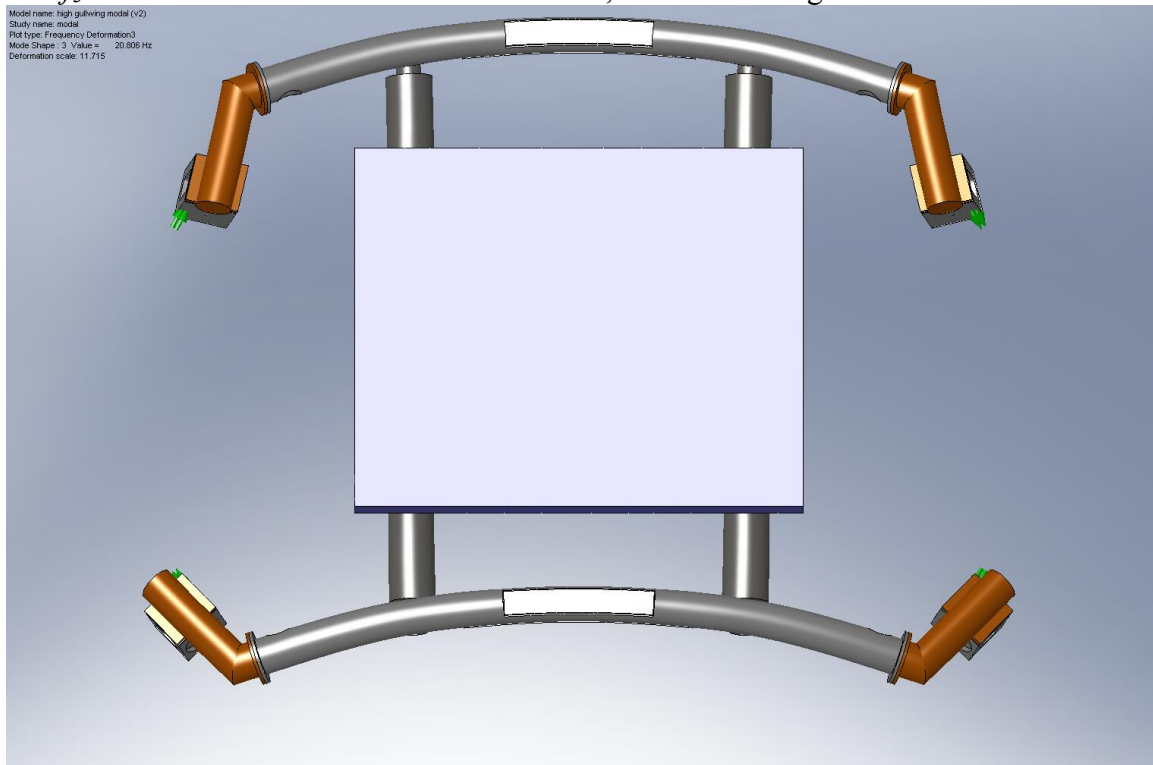


Figure 65. The  $f_3$  mode of the High Crossbeam structure is primarily a translation in Y.

The  $f_4 = 30.9$  Hz mode is an Rx-rotation mode, as shown in Figure 66:

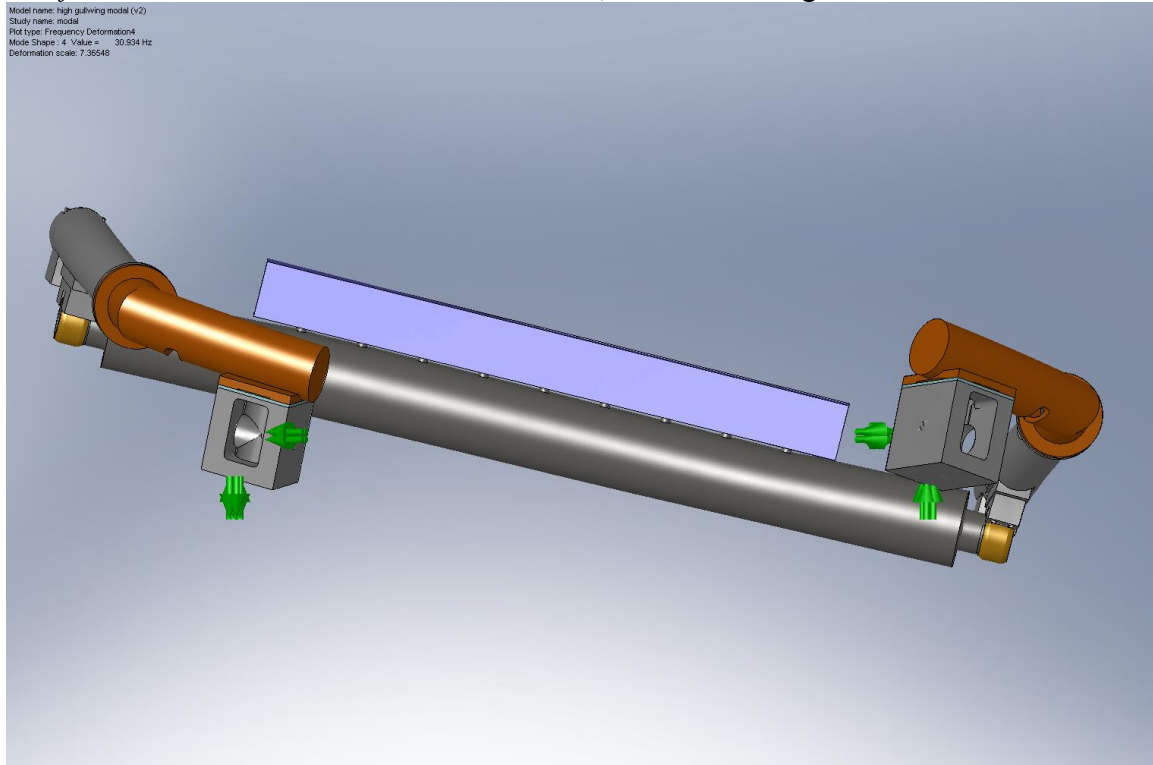


Figure 66. The  $f_4$  mode of the High Crossbeam structure is primarily a rotation about the X axis.

### Modal Analysis – Summary

Table 2 lists all the predicted eigenfrequencies described in the preceding analysis, divided into basic modeshapes:  $X$  refers to translations along the X-axis,  $R_x$  refers to rotations about the X-axis, etc. We include lower bounds in the entries for the modes that were not computed (e.g., the  $R_x$  mode for the existing Crossbeam design).

	$X$ (Hz)	$Z$ (Hz)	$Y$ (Hz)	$R_x$ (Hz)	$R_z$ (Hz)
<b>Existing Design</b>	6.1	15.0	14.0	>22.5	22.5
<b>Low Crossbeam</b>	11.8	16.9	23.7	28.7	>28.7
<b>High Crossbeam</b>	11.2	17.0	20.8	30.9	>30.9

Table 2. Predicted natural frequencies for the existing Crossbeam design and the two new Crossbeam concepts, as calculated in COSMOS. The green boxes highlight the design with the best (i.e., highest) frequency for the given modeshape.

Both the Low and High Crossbeams provide a significant increase in the lowest mode frequency, for oscillations of the Stage 0 mass in the X-direction. The effective stiffness of the round Crossbeams in this degree-of-freedom is clearly much higher than we expect from the existing rectangular Gullwing arrangement. However, we see that the improvement in the Z-direction is expected to be fairly small. This makes sense, since the Gullwings are stiffest in bending in this mode, as the height of the cross-section (6") is much greater than the width (3").

The Low Crossbeam concept provides a significant improvement over the High Crossbeam in the Y-mode. We believe this results from the vertical offset in the High Crossbeam design between the Horizontal Actuators (the stiff coupling from the Support Structure to ground) and the Connector Tube/Crossbeam. The resulting lengthening of the force loop, relative to the Low Crossbeam design, simply reduces the effective stiffness in this degree-of-freedom.

### **Final Summary**

Both the Low Crossbeam and High Crossbeam designs offer substantial benefit over the existing Gullwing design, considering both:

- 1) static stiffness, which corresponds to tilt/horizontal coupling behavior at low frequency, and
- 2) modal vibrations, which limit isolation performance at higher frequencies.

Refer to Table 1 and Table 2 for quantitative characterizations of the new concepts, in comparison to the existing design. Though the performance difference between the concepts is relatively small, I recommend choosing the Low Crossbeam design to achieve the best system performance. For this decision, I believe the most critical result is the parasitic stiffness from a horizontal push on the HEPI Boot to a pitch rotation of the Horizontal L4-C. This is given by  $K_{\text{horz-}\theta}$  in Table 1. The parasitic stiffness for the Low Crossbeam design is 37.0 N/ $\mu\text{rad}$ , compared to 17.2 N/ $\mu\text{rad}$  for the High Crossbeam design. Using a simple analysis, this 2x difference in stiffness could result in an approximately  $\sqrt{2}$  reduction in the tilt/horizontal coupling zero frequency.

There remain some important design details yet to be determined, if we are to develop the Low Crossbeam concept for installation within Advanced LIGO. Some of these issues are addressed above. Most notably, we would need to 1) bolt a Crossbeam Connector Tube to the side of each HEPI Boot, while still accommodating two L4-C accelerometers inside/on the Boot; and 2) remove the HEPI Piers and replace with shorter versions at LIGO Livingston. Issue #1 should be a relatively simple design problem, while issue #2 may introduce significant planning challenges.

## Appendix A: Modal Analysis of Existing Crossbeam Geometry, with “Super-Stiff” Materials

In addition to the modal analysis of the existing Crossbeam system described above, we also checked the effect of replacing the critical structural elements with much stiffer versions of the same elements. The quickest approach is simply increasing the moduli of elasticity ( $E_x$  and  $G_{xy}$ ) by a large factor. By using stiffer materials for only one structural element at a time, we can determine which element is the “weakest link” in the structural chain, in terms of stiffness. If the natural frequencies predicted for the structure are greatly increased by using a much stiffer material, it is likely we can significantly improve the system’s effective stiffness by redesigning the element for greater stiffness (by shortening the force loop, increasing the moment of inertia, etc.).

We start by increasing the moduli of elasticity for the Support Tubes by a factor of 1,000x. The eigenfrequencies calculated by COSMOS are:

$$\begin{aligned} f_1 &= 6.6 \text{ Hz} \\ f_2 &= 14.8 \text{ Hz} \\ f_3 &= 16.3 \text{ Hz} \\ f_4 &= 23.5 \text{ Hz} \end{aligned}$$

The modeshapes are almost identical to those shown in Figure 51, Figure 52, Figure 53, and Figure 54. For example, the  $f_3$  (Z-translation) mode for the “super-stiff” Support Tubes is shown in Figure 67:

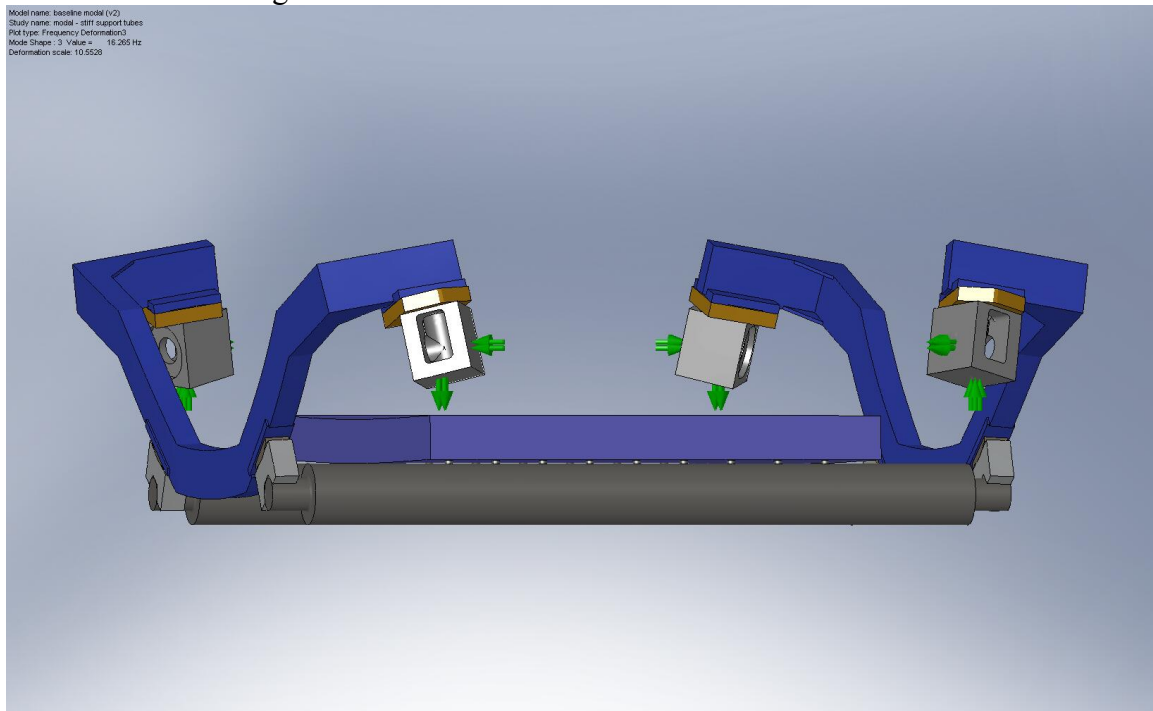


Figure 67. The  $f_3$  mode of the existing Crossbeam geometry, using a “super-stiff” material for the Support Tubes.

The modal frequencies do increase slightly over the baseline values, but not enough to motivate a major redesign of the Support Tubes.

Next, we run a modal analysis with “super-stiff” Support Tube Clamps (both the Spherical Bearings and the Vee-block Clamps). The predicted eigenfrequencies are:

$$\begin{aligned} f_1 &= 6.4 \text{ Hz} \\ f_2 &= 15.3 \text{ Hz} \\ f_3 &= 15.8 \text{ Hz} \\ f_4 &= 24.4 \text{ Hz} \end{aligned}$$

Again, we see a slight improvement over the values listed in Table 2, but not enough to suggest major increases in the natural frequencies can be obtained by simply redesigning the Clamps (though, I still believe we can produce more robust Clamps based on the ball joint design described above...).

Finally, we run the modal analysis for “super-stiff” Gullwings. The resulting eigenfrequencies are much higher than what we calculate for the real material behavior:

$$\begin{aligned} f_1 &= 24.5 \text{ Hz} \\ f_2 &= 36.1 \text{ Hz} \\ f_3 &= 46.5 \text{ Hz} \\ f_4 &= 49.3 \text{ Hz} \end{aligned}$$

The modeshapes change dramatically, as shown below:

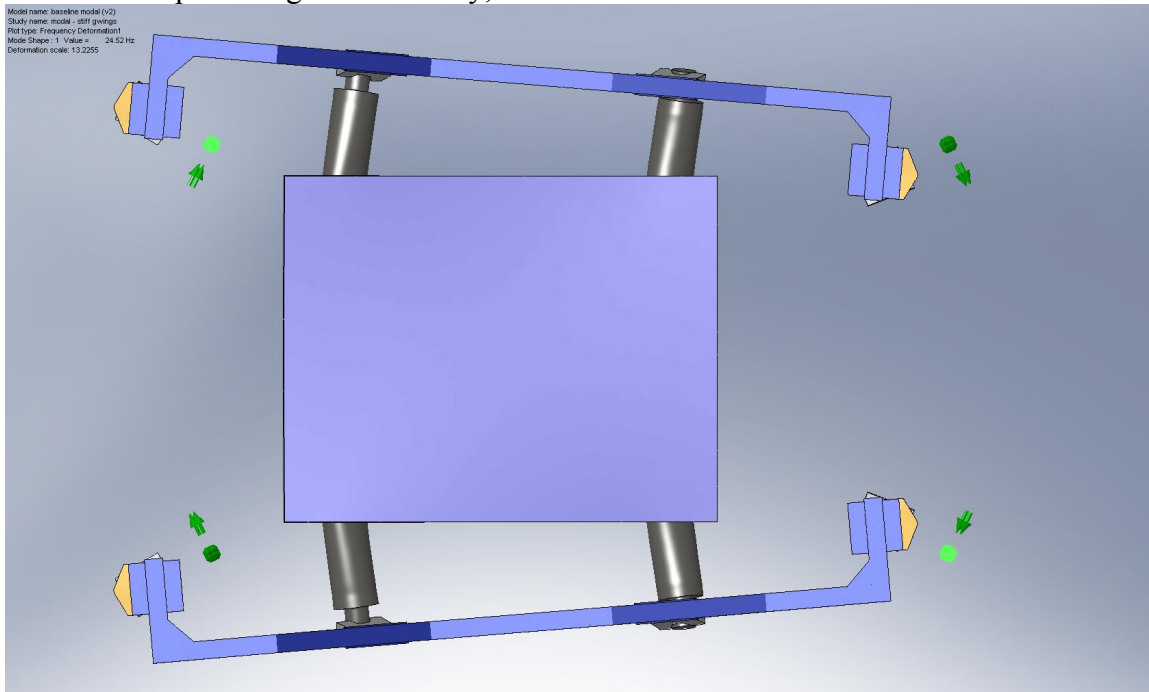


Figure 68. The  $f_1$  mode of the existing Crossbeam geometry, using “super-stiff” Gullwings. We see a variation on the X-translation modeshape described in the analyses above.

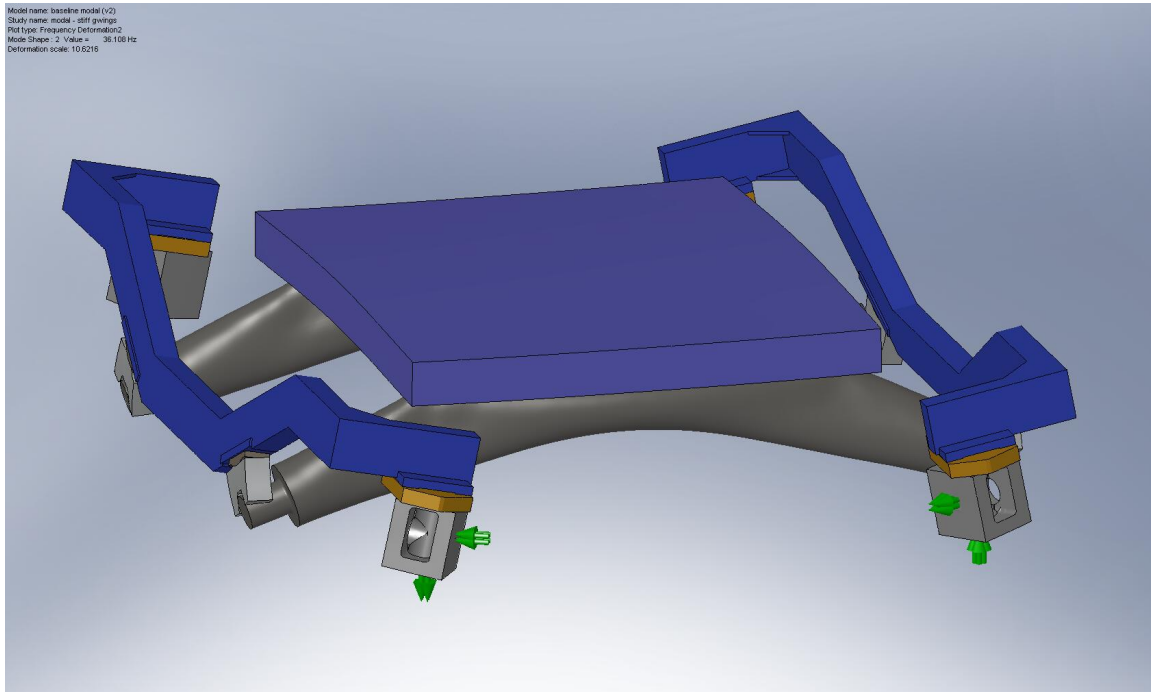


Figure 69. The  $f_2$  mode of the existing Crossbeam geometry, using “super-stiff” Gullwings. This is a Z-translation mode, where the Support Tubes bend in an abnormal way.

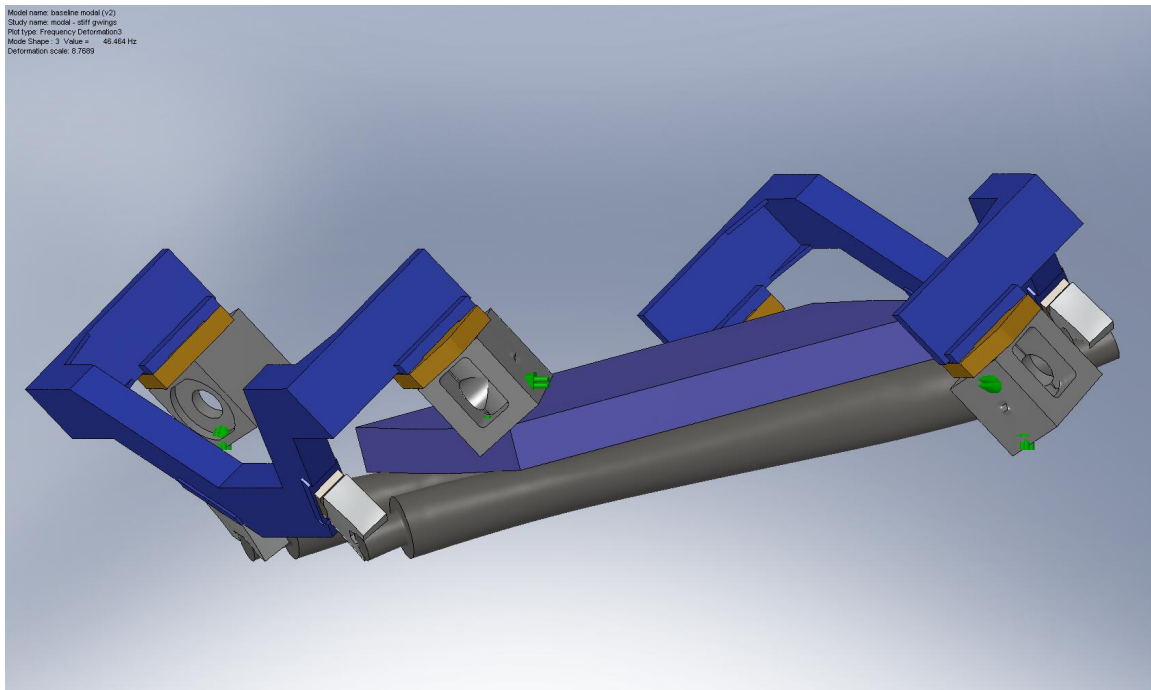


Figure 70. The  $f_3$  mode of the existing Crossbeam geometry, using “super-stiff” Gullwings.



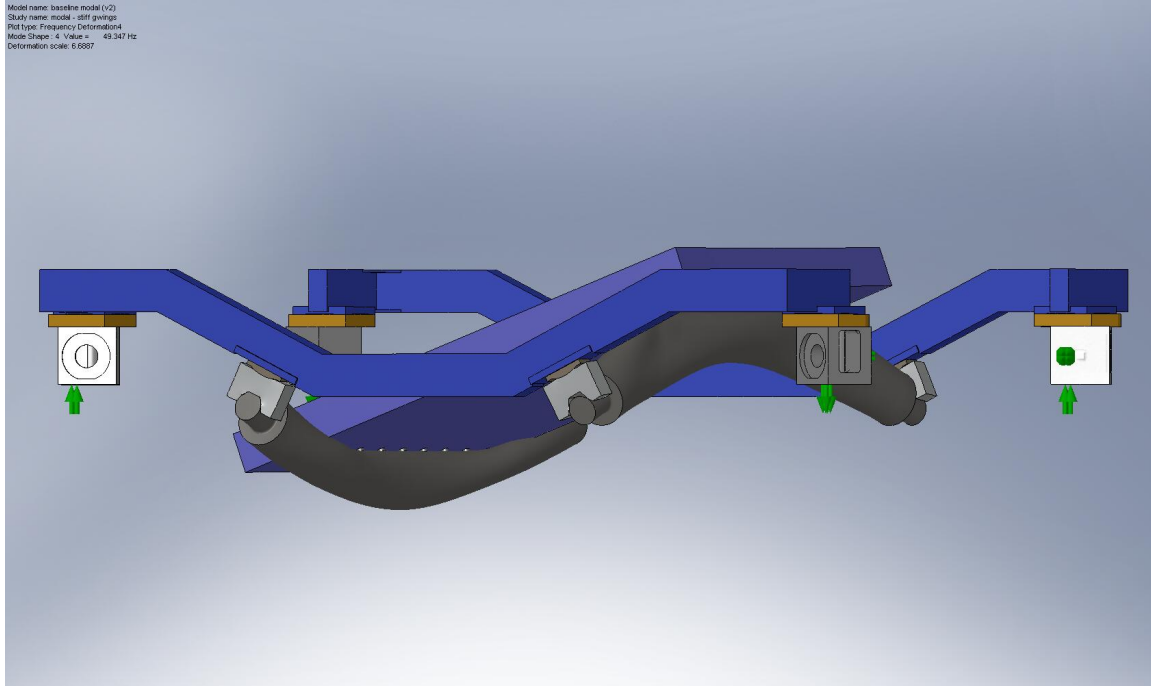


Figure 71. The  $f_4$  mode of the existing Crossbeam geometry, using “super-stiff” Gullwings.

This analysis provides strong support for our decision to redesign the Crossbeams. It is clear the current design can be made much stiffer. By significantly increasing the Crossbeam stiffness, we can expect significantly higher Support Structure eigenfrequencies (as well as a lower tilt/horizontal coupling zero frequency, as mentioned in the main section).

*It is important to recognize, however, that we have not included the HEPI systems in this model. If the compliance of the HEPI structure is of the same order as the compliance of the Gullwings, it may limit the performance benefit that can be attained by simply switching to stiffer Crossbeams. We plan further work, to extend the FEA to include the HEPI structures (including the Piers, if applicable).*

## Appendix B: Comparison to Previous Structural Analysis

In 2005, Laurent Ruet studied the dynamics of the HAM Support Structure at LASTI. He posted a report to the MIT iLog describing his FEA model of the system. The post is dated Friday, August 26, 2005.

Laurent used ALGOR to run the analysis and set up his model slightly differently from the models described above. Also, it is unclear what payload mass was used for his model. However, the basic results are interesting, as they should be roughly comparable to the existing Crossbeam modal analysis described above.

His results are copied here:

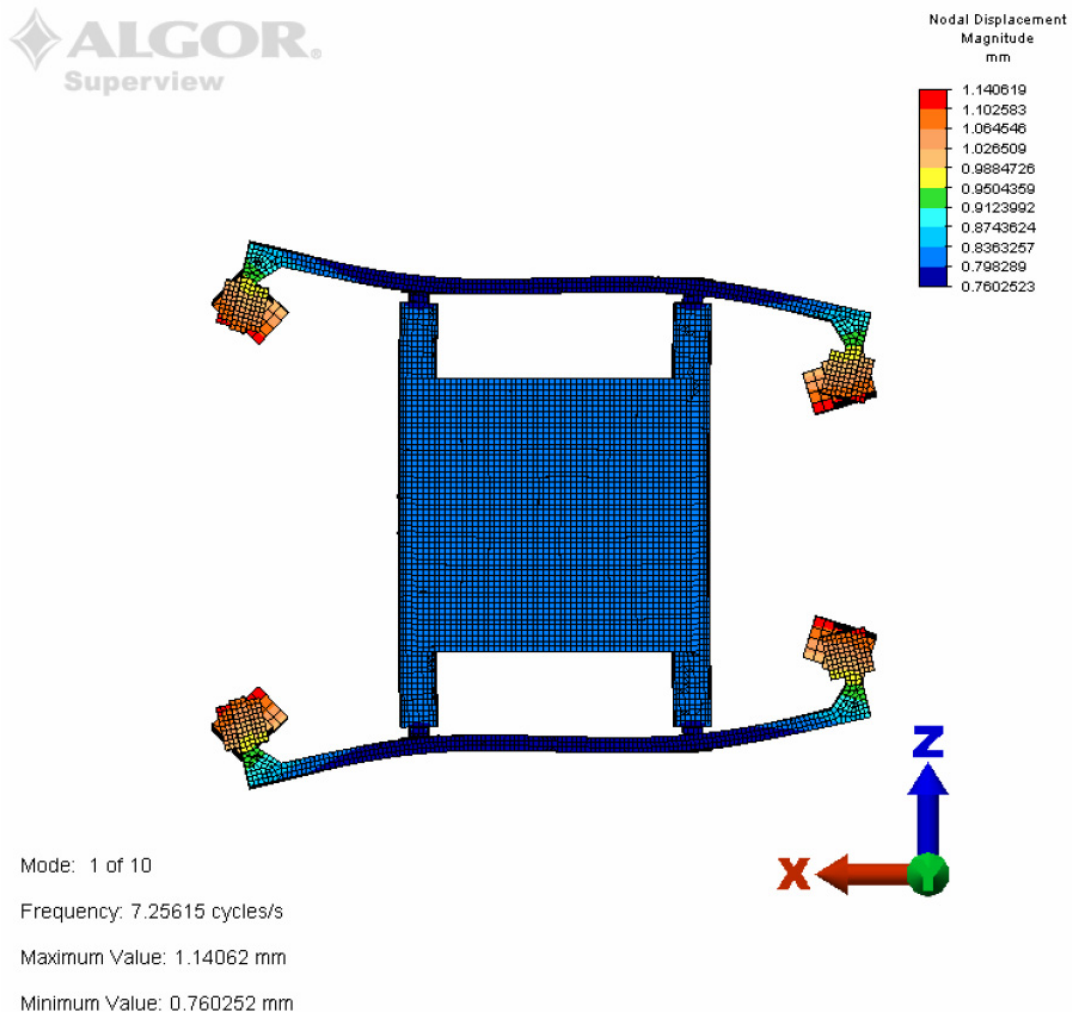


Figure 72. Laurent predicted a 7.3 Hz eigenfrequency for this modeshape, compared to 6.1 Hz predicted above.

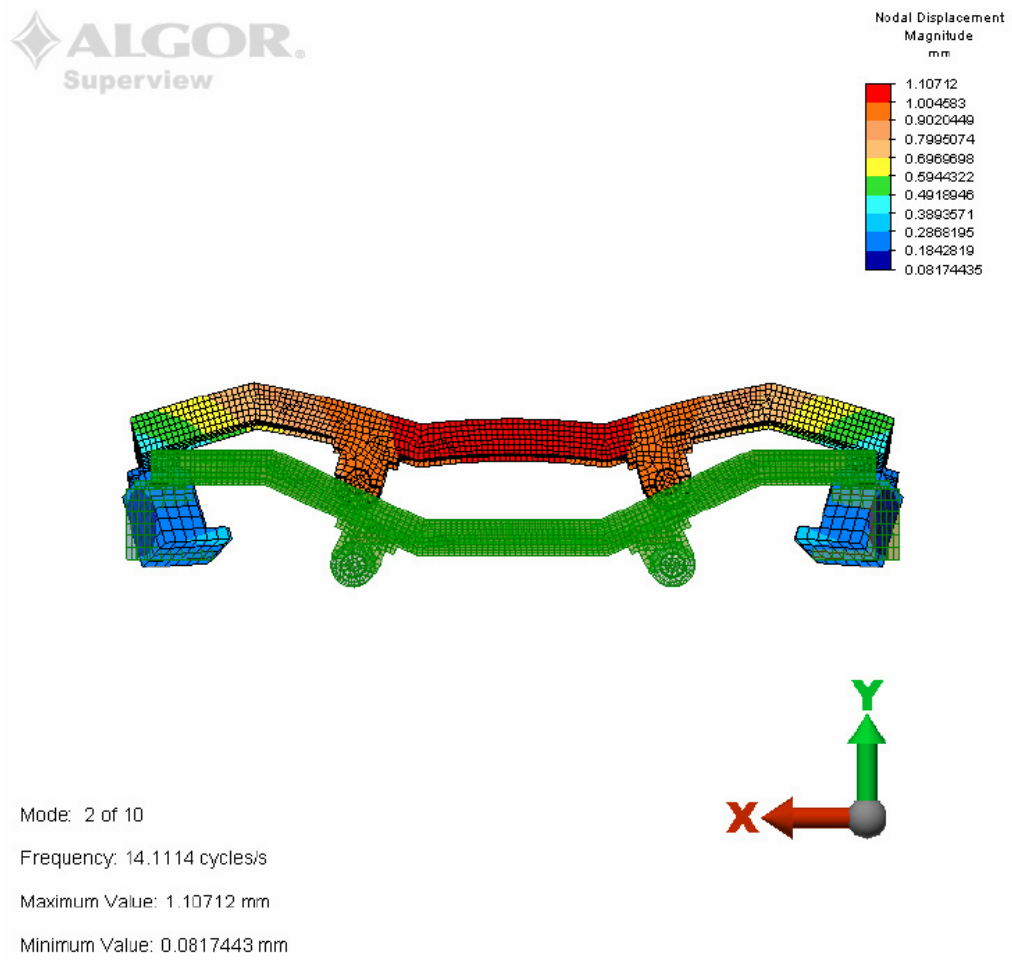


Figure 73. Laurent's FEA predicts 14.1 Hz for the vertical vibration modal frequency. We predict 15.0 Hz for this mode, above.

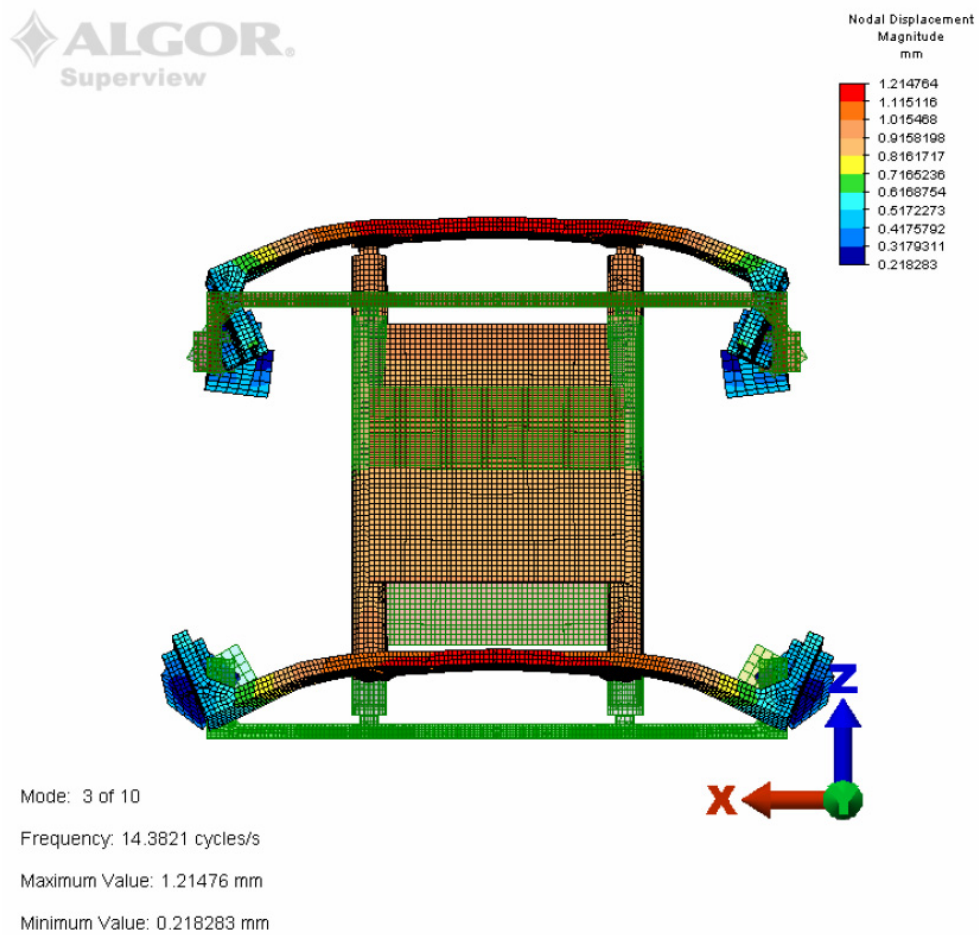


Figure 74. Finally, the ALGOR model predicted a 14.4 Hz mode with this shape. The same shape is predicted in our COSMOS model at 14.0 Hz.

The agreement is exceptionally good, considering the many differences between the two models. This provides some additional evidence that the modal analysis described in this report is reasonable.